

QUANTIFICATION OF BRADYKINESIA IN PARKINSON'S DISEASE BY  
USING FACIAL IMAGES AND EMG RECORDINGS

A THESIS SUBMITTED TO  
THE GRADUATE SCHOOL OF INFORMATICS OF  
THE MIDDLE EAST TECHNICAL UNIVERSITY  
BY

SABRİ CAN ÖLÇEK

IN PARTIAL FULFILLMENT OF THE REQUIREMENTS FOR THE DEGREE  
OF DOCTOR OF PHILOSOPHY  
IN  
MEDICAL INFORMATICS

APRIL 2023



Approval of the thesis:

QUANTIFICATION OF BRADYKINESIA IN PARKINSON'S DISEASE BY USING  
FACIAL IMAGES AND EMG RECORDINGS

Submitted by SABRİ CAN ÖLÇEK in partial fulfillment of the requirements for the degree  
of **Doctor of Philosophy in Health Informatics Department, Middle East Technical  
University** by,

Prof. Dr. Banu Günel Kılıç  
Dean, **Graduate School of Informatics**

---

Assoc. Prof. Dr. Yeşim Aydın Son  
Head of Department, **Health Informatics**

---

Assoc. Prof. Dr. Yeşim Aydın Son  
Supervisor, **Health Informatics, METU**

---

Assoc. Prof. Dr. Didem Gökçay  
Co-Supervisor, **Department of Artificial  
Intelligence and Data Engineering, ITU**

---

**Examining Committee Members:**

Prof. Dr. Banu Günel Kılıç  
Information Systems, METU

---

Assoc. Prof. Dr. Yeşim Aydın Son  
Health Informatics, METU

---

Assoc. Prof. Yusuf Özgür Çakmak  
Department of Anatomy, University of Otago

---

Asst. Prof. Dr. Aykut Eken  
Biomedical Engineering, TOBB ETÜ

---

Asst. Prof. Dr. Burçak Otlı Sarıtaş  
Health Informatics, METU

---

**Date:**



**I hereby declare that all information in this document has been obtained and presented in accordance with academic rules and ethical conduct. I also declare that, as required by these rules and conduct, I have fully cited and referenced all material and results that are not original to this work.**

**Name, Last name: SABRİ CAN ÖLÇEK**

**Signature : \_\_\_\_\_**

## ABSTRACT

### QUANTIFICATION OF BRADYKINESIA IN PARKINSON'S DISEASE BY USING FACIAL IMAGES AND EMG RECORDINGS

Ölçek, Sabri Can

Ph.D, Department of Medical Informatics

Supervisor: Assoc. Prof. Dr. Yeşim Aydın Son

Co-Supervisor: Assoc. Prof. Dr. Didem Gökçay

April 2023, 94 pages

Parkinson's disease (PD) is a neurodegenerative disorder characterized by both motor and non-motor symptoms. The five-scale scoring system called Unified Parkinson's Disease Rating Scale (UPDRS) is the most common tool used in symptom assessment. UPDRS III is the subsection targeting the motor symptoms and is based on the observations of the clinicians. Since the clinical assessment method is based on the visual observation and a five scale scoring, it is highly likely that the scores of two physicians differ. In fact, during multiple studies, it is observed that the scores can be biased to the dominant symptom. Furthermore, this system requires the physicians to conduct the measurements themselves, which is quite time consuming. Thus, it is important to have a repeatable, quantifiable method not just to evaluate the patient's condition but to even detect the subtle changes. Beside Tremor, Bradykinesia is one of the main features of Parkinson's Disease which is especially used to determine stage of the disease. The bradykinesia with rigidity can seriously hinder the patient's movements as a result, the quality of their life. The assessment methods are mostly based on the rapid movements such as counting the number of touches made between thumb and index finger. There are many studies focusing on these tasks to measure bradykinesia by using various devices such as accelerometers, gyroscopes, and custom-built wearables. However, there is a lack of simple devices and methods that can be repeated even at home by the patient himself. In this study, we developed measurements based on a non-contact device called leap motion, using hand movements. In addition, a special hardware and software interface is developed to collect and process multi modal data by using facial images and EMG recordings. We also improved the data processing techniques to predict bradykinesia from facial movements in a better way.

Keywords: parkinson's disease, bradykinesia, emg, facial image, updrs

## ÖZ

### PARKİNSON HASTALIĞINDA BRADİKİNEZİNİN YÜZ GÖRÜNTÜLERİ VE EMG KAYITLARI KULLANILARAK SAYISALLAŞTIRILMASI

Ölçek, Sabri Can

Doktora, Sağlık Bilişimi Bölümü

Tez Yöneticisi: Doç. Dr. Yeşim Aydın Son

Tez Eş Danışmanı: Doç. Dr. Didem Gökçay

Nisan 2023, 94 sayfa

Parkinson hastalığı (PD), hem motor hem de motor olmayan semptomlarla karakterize edilen bir nörodejeneratif hastalıktır. Birleşik Parkinson Hastalığı Derecelendirme Ölçeği (UPDRS) adı verilen beşli puanlama sistemi, semptom değerlendirmesinde kullanılan en yaygın araçtır. UPDRS III motor semptomları hedefleyen alt bölümdür ve klinisyenlerin gözlemlerine dayanmaktadır. Klinik değerlendirme yöntemi, görsel gözleme ve dörtlü bir puanlamaya dayandığından, iki hekimin puanlaması arasında fark olma olasılığı yüksektir. Hatta yapılan birçok çalışmada bu özelliklerden dolayı puanların, baskın semptomu kayabileceği gözlemlenmiştir. Ayrıca bu sistem hekimlerin ciddi zaman alan ölçümleri bizzat kendilerinin yapmasını gerektirmektedir. Bu nedenle, sadece hastanın durumunu değerlendirmek için değil, aynı zamanda ince değişiklikleri bile tespit etmek için tekrarlanabilir, ölçülebilir bir yöntemle sahip olmak önemlidir. Tremor'un yanı sıra, özellikle hastalığın evresini belirlemek için kullanılan bradikinezi, Parkinson Hastalığı'nın ana özelliklerinden biridir. Rijidite ile bradikinezi, hastanın hareketlerini ve sonuç olarak, yaşam kalitelerini ciddi oranda engelleyebilmektedir. Değerlendirme yöntemleri çoğunlukla, başparmak ve işaret parmağı arasında yapılan dokunuşların sayılması gibi hızlı hareketlere dayanmaktadır. İvmeölçerler, jiroskoplar ve özel yapım giyilebilir cihazlar gibi çeşitli araçları kullanarak bradikineziyi ölçmek için bu görevlere odaklanan birçok çalışma bulunmaktadır. Ancak evde bile hastanın kendisi tarafından tekrarlanabilecek basit cihaz ve yöntemlerin eksikliği vardır. Bu çalışmada, leap motion adlı temassız cihaz ile el hareketlerini kullanan bir ölçüm geliştirdik. Ek olarak, çok modlu yüz görüntüleri ve EMG kayıtlarını toplamak ve işlemek için özel bir yazılım ve donanım arayüzü de geliştirilmiştir. Yüz hareketlerinden bradikineziyi tahmin eden veri işleme teknikleri de daha iyi bir şekilde iyileştirilmiştir.

Anahtar Sözcükler: parkinson hastalığı, bradykinesia, emg, yüz görüntüsü, updrs

To whom supported me  
in my toughest times...

## ACKNOWLEDGEMENTS

I would like to express my deepest gratitude to my supervisor, Assoc. Prof. Dr. Didem Gökçay. She has always been patient and supportive. Taught me a lot and made this work an adventurous journey.

Besides my supervisor, I would like to thank my co-advisor Assoc. Prof. Yusuf Özgür Çakmak without him this work would have never existed. He opened new doors to me and gave me chance to work on Parkinson's Disease which is one of the heartrending diseases. Being able to contribute to this world is much further than one PhD work.

I would also like to thank Assoc. Prof. Dr. Yeşim Aydın Son for administering my thesis submission process due to a legal obligation mandated by METU senate. Whenever I need an administrative question or guidance, she answered all of them patiently and helped me overcome many issues which could have been disaster. I am truly grateful to you.

I also want to thank Dr. Özgür Öztop Çakmak. She helped me to collect all the research data and never ever compliant once even if I call her absurd times. Therefore, I am grateful to Prof. Dr. Yasemin Gürsoy Özdemir and Koç University for the facility and equipment you have provided.

My dear family, who supported me unconditionally, this work cannot be done without you and your insights. You have never stopped since my childhood. You are the superstars.

Finally, the ones who supported me, always being by my side, whenever I felt darkness bringing light to my path. Thank you all. Forever shall I indebted to you.

## TABLE OF CONTENTS

ABSTRACT .....	iv
ÖZ.....	v
DEDICATION .....	vi
ACKNOWLEDGEMENTS .....	vii
TABLE OF CONTENTS .....	viii
LIST OF TABLES .....	xi
LIST OF FIGURES.....	xii
LIST OF ABBREVIATIONS .....	xiv
CHAPTERS	
1 INTRODUCTION.....	1
2 BACKGROUND.....	3
2.1. Parkinson’s Disease.....	3
2.2. UPDRS and Hoehn-Yahr Scale.....	4
2.3. Motor Measurements.....	5
2.3.1. Pinching.....	5
2.3.2. Pronation-Supination.....	6
2.3.3. Face .....	6
2.4. EMG .....	8
2.5. Motivation and Research Question.....	10
3 FEATURE EXTRACTION AND STATISTICAL ANALYSIS OF HAND MOTIONS.....	11
3.1. Pinching Motion .....	11
3.1.1. Method .....	12
3.1.2. Results .....	14
3.1.3. Discussions.....	16
3.2. Pronation and Supination Motion.....	17
3.2.1. Method .....	18
3.2.1.1. Data Collection .....	18
3.2.1.2. Data Sanitization.....	19
3.2.1.3. Feature Extraction.....	22

3.2.1.4.	Statistical Analysis.....	24
3.3.	Results .....	24
3.3.1.	Correlation Analysis.....	24
3.3.2.	Linear Regression Model .....	28
3.3.3.	Discussion .....	29
4	FEATURE EXTRACTION AND STATISTICAL ANALYSIS OF FACIAL EXPRESSIONS COLLECTED BY EMG .....	33
4.1.	Development of Hardware Interface to Collect EMG in Sync with Facial Camera Recordings .....	33
4.1.1.	Detecting Onset From the Trigger Signal .....	35
4.1.1.1.	EMG Data Preprocessing.....	35
4.1.1.2.	Applying CUSUM.....	37
4.2.	Experimental Procedure to Collect Repetitive Facial Expressions .....	40
4.2.1.	Results of Pilot Subject .....	40
4.2.2.	Training Effect and Improving CUSUM .....	41
4.2.3.	Discussions.....	44
4.3.	Experiment with PD Patients .....	44
4.3.1.	Method .....	44
4.3.2.	Results.....	45
4.3.3.	Discussions.....	46
5	FEATURE EXTRACTION AND STATISTICAL ANALYSIS OF FACIAL EXPRESSIONS COLLECTED BY VIDEO CAMERA.....	55
5.1.	Software Development for Facial Image Collection and Analysis .....	55
5.1.1.	Data Collection.....	55
5.1.2.	Data Analysis .....	56
5.1.3.	Still Pictures Experiment.....	57
5.1.3.1.	Method.....	57
5.1.3.2.	Results.....	60
5.1.4.	Video Recording Experiment.....	61
5.1.4.1.	Method.....	61
5.1.4.2.	Results.....	62
5.1.5.	Discussions.....	62
6	DISCUSSION AND FUTURE WORK.....	65
	REFERENCES.....	69

APPENDICES

APPENDIX A ..... 73

    Source Code of Face Registration Routine ..... 73

    Source Code of CUSUM function ..... 77

APPENDIX B ..... 79

APPENDIX C ..... 83

CURRICULUM VITAE ..... 93

## LIST OF TABLES

Table 1: Discarded speed values because of large SD.....	13
Table 2: Demographics of the patients participated.....	18
Table 3: Source code if the trigger device .....	34
Table 4: Whole process starting from preprocessing .....	39
Table 5: Latency calculated from initial subject .....	41
Table 6: UPDRS III scores of the initial subject.....	41
Table 7: Improved onset detection with CUSUM.....	43
Table 8: The average time difference between latencies in control group for original and improved CUSUM .....	44
Table 9: Demographics of the patients participated.....	45
Table 10: Features extracted from EMG for ON/OFF states.....	53
Table 11: Paired t-test between ON/OFF states.....	53
Table 12: Image alignment procedure.....	58
Table 13: Features extracted from Video Frames for ON/OFF states .....	63

## LIST OF FIGURES

Figure 1: (b) shows the changes compared to normal brain in basal ganglia circuitry when substantia nigra stops.....	4
Figure 2: The coil couple generating magnetic response to pinching motion .....	5
Figure 3: The signal recorded from healthy control subject .....	6
Figure 4: Positions of the six infrared markers .....	7
Figure 5: Correlation found in PD patients with facial recordings .....	8
Figure 6: Triphasic pattern showing all the phases .....	8
Figure 7: Photo of clinical EMG in Koç University Hospital.....	9
Figure 8: Photo of ADInstruments Powerlab 16/35 DAQ system.....	9
Figure 9: Photo of ADInstruments Powerlab 26T DAQ system.....	9
Figure 10: The representation of interior design of Leap Motion.....	11
Figure 11: Basic recording setup with laptop and leap controller.....	13
Figure 12: Change of the distance between thumb and index finger .....	13
Figure 13: Distribution of UPDRS III total score and bradykinesia .....	16
Figure 14: Signals after moving average filter was applied.....	20
Figure 15: Frequency spectrum of P/S signals.....	21
Figure 16: Signal after moving average is applied and marked.....	21
Figure 17: Invalid parts of the data was trimmed.....	22
Figure 18: Correlations between features and <b>UPDRS from right hand</b> .....	26
Figure 19: Correlations between features and <b>UPDRS from left hand</b> .....	27
Figure 20: Correlations between features from right hand and <b>UPDRS from left hand</b> .....	28
Figure 21: Significance of the features in top 50 regression models .....	30
Figure 22: List of the features in top 1% (2621) of the regression models with lowest RMSE, ordered with respect to increasing RMSE.....	31
Figure 23: The assembled trigger device used in recording sessions .....	33
Figure 24: Circuit diagram for Trigger Device .....	34
Figure 25: Frequency spectrum of the raw signal recorded from PD subject.....	36
Figure 26: EMG data processing steps.....	37
Figure 27: Onset detected by CUSUM for ON period.....	38
Figure 28: Onset detected by CUSUM for OFF period .....	39
Figure 29: Facial cards for training session .....	40
Figure 30: Two consecutive recording of eyebrow raiser in control subject.....	41
Figure 31: Two consecutive recording of smiling in control subject.....	42
Figure 32: Results of the improved CUSUM.....	43
Figure 33: The data recorded for smiling expression.....	47
Figure 34: The data recorded for eyebrow-lowerer expression .....	48
Figure 35: Processed video recordings for one patient in OFF state .....	49
Figure 36: Processed video recordings for a patient in ON state .....	50
Figure 37: Processed EMG recordings for a patient in OFF state .....	51
Figure 38: Processed EMG recordings for a patient in ON state .....	52

Figure 39: The UI of the software developed for video recording .....	55
Figure 40: Lower face ROI aligned and extracted for the video stream.....	56
Figure 41: The preprocessing steps are face and landmark detection, eyeline detection, registration, and ROI extraction .....	56
Figure 42: Entropy change comparison inside and outside the ROI for smiling .....	57
Figure 43: All the landmarks (in green) automatically found.....	58
Figure 44: The image after alignment is applied .....	59
Figure 45: Three ROIs selected for analysis.....	59
Figure 46: Four ROIs which are upper face, left upper face, right upper face, and bottom face are selected for the analysis.....	60
Figure 47: ANOVA results for upper-face ROI.....	61
Figure 48: ANOVA results for lower-face ROI.....	61

## LIST OF ABBREVIATIONS

<b>ARM</b>	Advanced RISC Machines
<b>COTS</b>	Commercially available off-the-shelf
<b>CPG</b>	Central pattern generator
<b>CUSUM</b>	Cumulative Summation
<b>DAQ</b>	Data Acquisition
<b>DBS</b>	Deep Brain Stimulation
<b>DC</b>	Direct Current
<b>EEG</b>	Electroencephalogram
<b>EMG</b>	Electromyography
<b>GPIO</b>	General Purpose Input/Output
<b>JTAG</b>	Joint Test Action Group
<b>MDS</b>	Movement Disorder Society
<b>PD</b>	Parkinson's Disease
<b>RAM</b>	Rapid Alternating Movement
<b>ROI</b>	Region of Interest
<b>SDK</b>	Software Development Kit
<b>SNR</b>	Signal-to-noise ratio
<b>STM</b>	STMicroelectronics
<b>STN</b>	Subthalamic Nucleus
<b>UPDRS</b>	Unified Parkinson's Disease Rating Scale
<b>USB</b>	Universal Serial Bus

## CHAPTER 1

### INTRODUCTION

Parkinson's disease (PD) is a neurodegenerative disorder characterized by both motor and non-motor symptoms. Symptoms of motor dysfunction comprise tremor (T), rigidity-stiffness (R), bradykinesia-slowness in movement (B), gait-postural instability (GP), and bulbar abnormalities that include difficulties with speech and facial expressions (BA). In Parkinson's disease, the Unified Parkinson's Disease Rating Scale (UPDRS) is the most common tool used in motor symptom assessment.

UPDRS scoring system is based on five-scale scores (0 = normal, 4 = severe) for the severity of the individual tasks and questions targeting different symptoms. Unfortunately, the performance of the patients who are conducting the given tasks are evaluated by the clinicians' observations. Therefore, UPDRS is a subjective scoring system in its nature. UPDRS III (motor subsection) is the main focus of this study and it is extensive enough to addresses all the motor symptoms of PD (Fahn, Marsden, Goldstein, & Calne, 1987).

However, even in two subsequent sessions, it is possible to see discrepancies between the scores if the clinicians are different. In fact, this non-linear and non-repeatable behavior is caused by the lack of quantifiable values in the scoring. Thus, UPDRS scoring cannot be used to track efficiency of a research or treatment.

Physicians can use more than one scoring system to assess the symptoms' stage. The Hoehn and Yahr (HY) scale (Hoehn & Yahr, 1967) is the other most common scale applied during diagnosis and prognosis. However, the scale is superseded by the UPDRS and it is mostly used to target the daily activities rather than the motor symptoms (Goetz, et al., 2004). Therefore, UPDRS is the primary scoring benchmark for this study rather than HY.

In this thesis, a quantifiable value relying on a repeatable method will be developed to measure bradykinesia in PD to address the non-linearity and non-repeatability of UPDRS scoring.

Even though there are several different studies focusing on to measure the bradykinesia level based on rapid alternating movements (RAM) such as finger tapping or wrist pronation/supination (Ji-Won, et al., 2009; Teräväinen & Calne,

1980), the measurement techniques relies on wide variety of devices such as accelerometers (Dunnewold, Jacobi, & van Hilten, 1997), gyroscopes (Salarian, et al., 2007), magnetic devices (Kandori, et al., 2004; Ghassemi, Lemieux, Jog, Edwards, & Duval, 2006), and EMG sensors (de Souza, Dionísio, & Almeida, 2011) and there is no common measurement metric. Especially, relying on a custom device makes them difficult to use in clinical and daily life settings.

To overcome this problem, a stone/mask face aspect of the bradykinesia will be utilized in this study to achieve a quantified measurement method which is in correlation with UPDRS score. The stillness caused by bradykinesia is directly characterized by the loss of facial expressions which called stone/mask face. Therefore, the facial images and EMG recordings of facial muscles will be gathered from PD patients in both ON and OFF medication/treatment cases. Afterwards, these recordings will be analyzed together to develop the method.

The resulting method can be used to evaluate efficiency of the PD treatment studies besides determining state of bradykinesia. This will shorten the research and development times and it can also be adapted into a self-evolutionary product for PD patients.

In this thesis, CHAPTER 2 will describe the medical background and the existing measurement techniques. CHAPTER 3 to 5 contains the different experiments and studies conducted to analyze different methods and modalities. These studies focus on the data gathering, the acquisition device, and the analytical approaches to develop a metric which can be used to assess bradykinesia. Each method and device have its own weaknesses and strengths hence the chapters contain the results and discussions of the approach used. CHAPTER 3 focuses on the data processing and analysis techniques from the hand motion by using COTS device. The correlation results are given under each subchapter. CHAPTER 4 explains the custom hardware device and software developed for EMG data processing and analysis. CHAPTER 5 is the last modality which is the video recording of the facial expressions.

CHAPTER 6 is the final chapter where the results and contributions of the study is summarized. This chapter contains the final remarks and possible future works.

## **CHAPTER 2**

### **BACKGROUND**

#### **2.1. Parkinson's Disease**

Parkinson's Disease (PD) is a neurodegenerative disease caused by the loss of dopamine-generating cells in the substantia nigra pars compacta. Dopamine is a neurotransmitter which is used essentially in the reward circuitry and motor control systems of the brain. Therefore, in the absence of dopamine, the disease progresses gradually and as a result, four major motor symptoms, which are tremor, muscle rigidity, bradykinesia, and posture instability, develop in time besides behavioral dysfunctions. The studies performed in late 1950s revealed that PD is one the most common neurodegenerative disorder of the elderly. Because of the core motor symptoms, the patient might reach to the point where he cannot perform daily routines such as walking, tying shoelaces, and fastening shirt buttons.

Bradykinesia which results in unnatural stillness/slowness in the motions is one of the early symptoms of Parkinson's Disease (PD). Together with tremor, rigidity, and postural instability, they are named as four cardinal symptoms of the disease (Calne, Snow, & Lee, 1992). The main cause of bradykinesia is the dopamine deficiency in basal ganglia from which the inhibitory signals are sent to the motor systems to prevent involuntary actions. Under normal circumstances when the dopamine is present, basal ganglia promotes those motor actions so that the body can act swiftly (Blandini, Nappi, Tassorelli, & Martignoni, 2000). Because of further depletion of dopamine in later stages, bradykinesia follows the progression of the disease and it gets worse. (Figure 1)

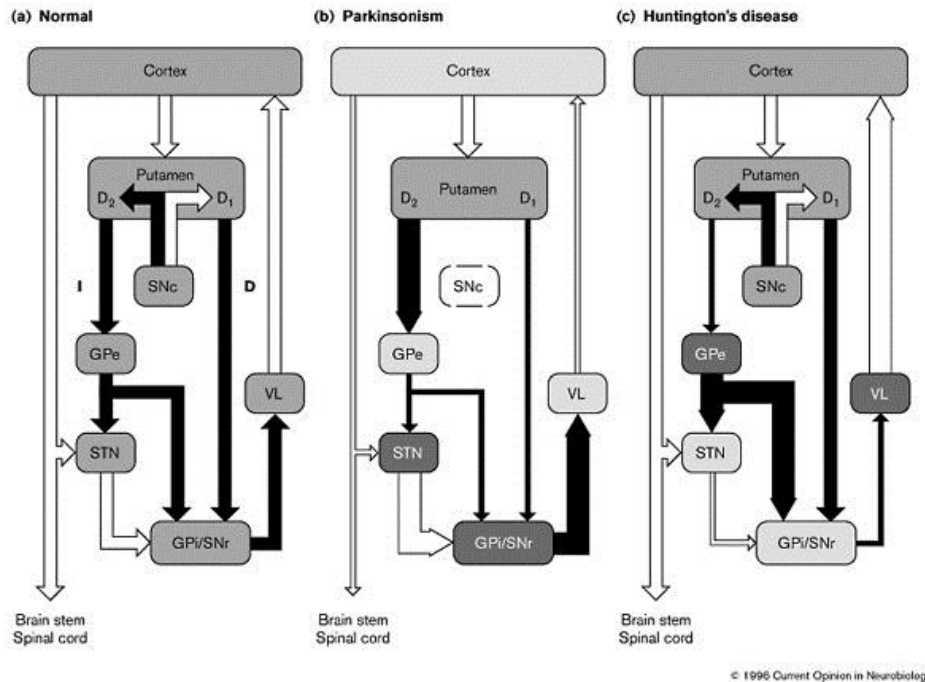


Figure 1: (b) shows the changes compared to normal brain in basal ganglia circuitry when substantia nigra stops (Wichmann & DeLong, 1996)

## 2.2. UPDRS and Hoehn-Yahr Scale

The state of disease and symptoms including bradykinesia is evaluated by Unified Parkinson's Disease Rating Scale (UPDRS). UPDRS was introduced in 1987 and it is composed of different parts assessing different aspects of the disease such as behavior, activities of daily life, motor functions, and complications. In 2007, it is revised by Movement Disorder Society (MDS-UPDRS) in order to create a superior version of the scale specifically addressing motor functions. Both scoring system uses five-scale structure (0 = normal, 4 = severe) which based on clinicians' observations. Even though UPDRS is a method which covers almost all the aspects of PD it is based on the subjective ratings. It is difficult to reach same results if the two scoring sessions are conducted by different clinicians.

Nevertheless, the level of disease and its symptoms are evaluated by Unified Parkinson's Disease Rating Scale (UPDRS). UPDRS scoring is the main clinical approach to diagnose and assess the progression of the disease. Even though UPDRS III (motor subsection) covers almost all the aspects of the motor symptoms (Fahn, Marsden, Goldstein, & Calne, 1987) it depends on the subjective scoring of the physicians. In addition to this inconsistency, the discreet rating scale cannot detect the subtle changes in the symptoms such as bradykinesia.

In summary, this non-linear and non-repeatable behavior is caused by the lack of quantifiable values in the scoring. Thus, UPDRS scoring cannot be used to track efficiency of a research or treatment.

The UPDRS is not the only evaluation method used by the physicians. It is common to assess symptoms' stage by using more than one scale at once. The Hoehn and Yahr (HY) scale (Hoehn & Yahr, 1967) is the other most common scale applied during diagnosis and prognosis. Similar to UPDRS, this scale is based on physicians observations and uses 1-5 scale called stages. However, after its initial release in 1967, the scale is refined and 0.5 steps are added in between the original stages. According to the recent studies, HY scale works best in midranges, in other words, moderate symptom severity. (Goetz, et al., 2004)

## 2.3. Motor Measurements

### 2.3.1. Pinching

The tap rating is one of the popular variables measured during bradykinesia studies. It is known that RAM such as finger tapping, namely, pinching can be used to assess bradykinesia level. In fact, it is already included in UPDRS III which is the motor symptom assessment part of the UPDRS scoring. The pinching task is not only present in scoring schemes but it is also grouped under bradykinesia subgroup. (Postuma, Gagnon, Vendette, Charland, & Montplaisir, 2008; Çakmak, et al., 2017)

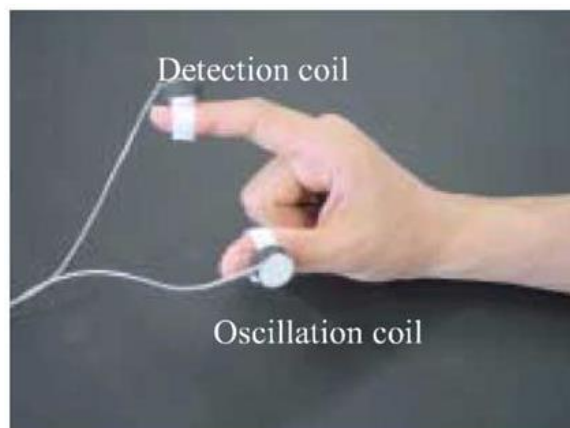


Figure 2: The coil couple generating magnetic response to pinching motion (Kandori, et al., 2004)

For this purpose, Kandori et al. developed a magnetic device composed of two coils to measure it. (Kandori, et al., 2004) The coil couple generating magnetic response is worn on index and thumb fingers as shown in Figure 2. Unlike accelerometers and gyroscopes, the signal generated by the magnetic sensor device is fairly simple. (Figure 3) However, by taking FFT of the signal, the recorded output voltage can only be used to determine the tapping frequency. At this point, Kandori et al. conducted earlier calibration study to figure out the conversion between the output

voltage of the system and the movement distance (D) of the fingers. By using this relation, they converted the recorded waveforms into the movement distance waveforms. This enables them to derive the speed and acceleration of the motion from the movement distance waveform by taking first and second derivatives of it. They couldn't find a strong correlation between the tapping frequency and PD level. However, the main reason of it is the Hoehn and Yahr scale (Hoehn & Yahr, 1967) which is used as comparative PD level in the study. Unlike UPDRS score, HY-scale focuses on the global assessment of the disease rather than its specific disability or symptom. Despite the low granularity of the scale and the results of the tap frequency, the mean values of the motion distance, acceleration, and velocity showed negative correlations with the HY-scale.

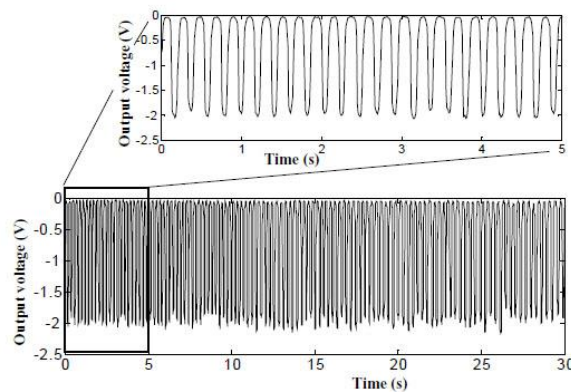


Figure 3: The signal recorded from healthy control subject (Kandori, et al., 2004)

### 2.3.2. *Pronation-Supination*

Like pinching, pronation and supination (PS) is one the motor tasks given to the PD patients to assess their severity level. Furthermore, PS is also classified under bradykinesia group. The researchers such as Ghassemi et al. were decided to use PS in their studies. Ghassemi et al. (Ghassemi, Lemieux, Jog, Edwards, & Duval, 2006) used pronation-supination action to measure bradykinesia. However, in Ghassemi et al.'s work, the pronation-supination action didn't show a significant correlation with the bradykinesia level unlike the tapping and alternating hand movements used in other studies. Nonetheless, Daneault et al. (Daneault, Carignan, Sadikot, & Duval, 2013) clarified those odd findings by showing that the maximal and mean velocity of pronation-supination cycles has significant correlation rather than the cycle duration. Daneault further explained that the maximal and mean velocity does not reflect all the clinical aspects of bradykinesia because the clinical evaluation combines bradykinesia, hypokinesia, and motor coordination. By looking those two studies, it can be said that selection of measurement plays an important role and using more than one measurement might give more clinically correct results.

### 2.3.3. *Face*

It is common to encounter reduced facial expression in PD patients, especially bradykinesia dominant ones. Because of that, the voluntary facial expression

diminishes and even disappears in time. In other words, the abnormalities in movement for facial expressions can be seen in bradykinesia. (Bologna, et al., 2013)

In two different studies, the voluntary facial expression tasks were given and recorded by image recordings. Whereas Marsili et al. (Marsili, et al., 2014) used infrared markers glued onto facial skin, Bowers et al. (Bowers, Miller, Bosch, & Gökçay, 2006) utilized simple camera recordings. The common finding in those studies were the correlation between the measurement and bradykinesia level regardless of the device and measurement technique.

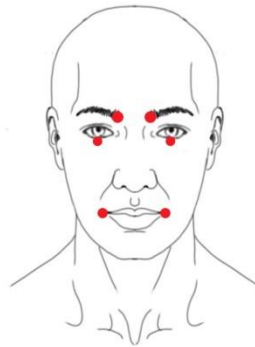


Figure 4: Positions of the six infrared markers (Marsili, et al., 2014)

Marsili et al. (Marsili, et al., 2014) conducted two different recording sessions to find a relation to the bradykinesia level. Firstly, the subjects were asked to imitate Duchenne smile shown on the screen as visual queue. Later, they ask them to grin as much as possible after a simple starting signal. The infrared markers put on 6 different locations as shown in Figure 4. The two markers in the medial eyebrow corners are used only to exclude incongruent emotional activations such as disgust. Namely, the reason of this upper face analysis is to find out if the PD patients can correctly identify the emotion shown by the Duchenne smile. After initial statistical analysis, it was revealed that there is no correlation between the left and right side of the face. Therefore, they combined these two hemi-faces to double their sample size. Unfortunately, the results presented about this claim are not enough to support it. Nevertheless, the striking finding in this study is that the only PD patients showed a correlation between the two sessions with respect to the peak velocity of the labial corner displacement. As seen in Figure 5, while the healthy controls did not show any specific pattern, the correlation in PD patients' case was clearly visible. According to Marsili et al. (Marsili, et al., 2014), this finding might indicate that the PD changes the brain circuitry takes place in these two tasks.

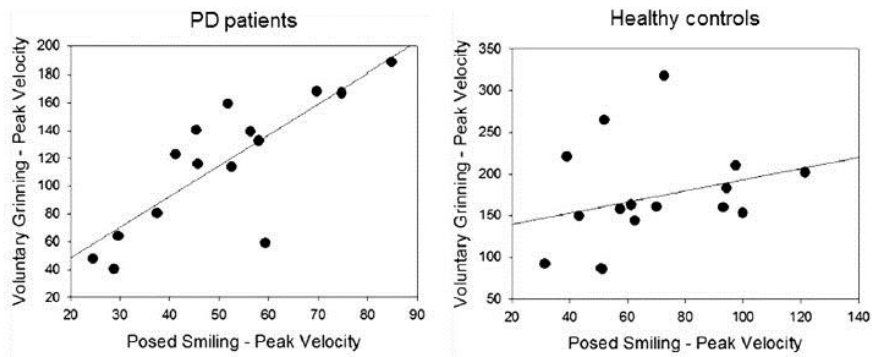


Figure 5: Correlation found in PD patients with facial recordings (Marsili, et al., 2014)

## 2.4. EMG

The previous studies have shown that rapid self-terminated muscle movements show triphasic EMG pattern. (Cheron, Cebolla, Bengoetxea, Leurs, & Danc, 2007) That pattern is composed of three phases following each other. These phases are first agonist burst, quite or antagonist burst, and finally, second agonist burst. (Hannaford, Cheron, & Stark, 1985) Figure 6 shows the basic triphasic EMG pattern both on agonist and antagonist muscles. It is claimed that the source of first agonist burst is the primary motor cortex. However, the involvement of this cortex in other phases is still unknown. (Irlbacher, Voss, Meyer, & Rothwell, 2006) The other property of a typical sEMG signal is its frequency which is above 500Hz.

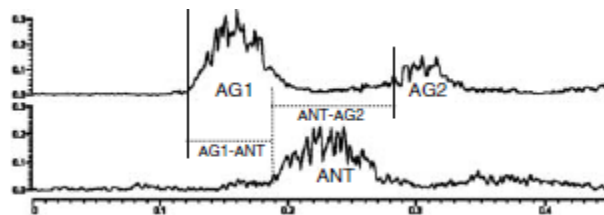


Figure 6: Triphasic pattern showing all the phases, first agonist burst (AG1), quiet phase (ANT), second agonist burst (AG2). (Irlbacher, Voss, Meyer, & Rothwell, 2006)

As seen in Figure 7, the most of the clinical devices have only 2 channels and it is not enough to conduct bilateral. Nonetheless, in neurophysiology labs, the multi-channel research oriented EMG devices can be found. (Figure 8)

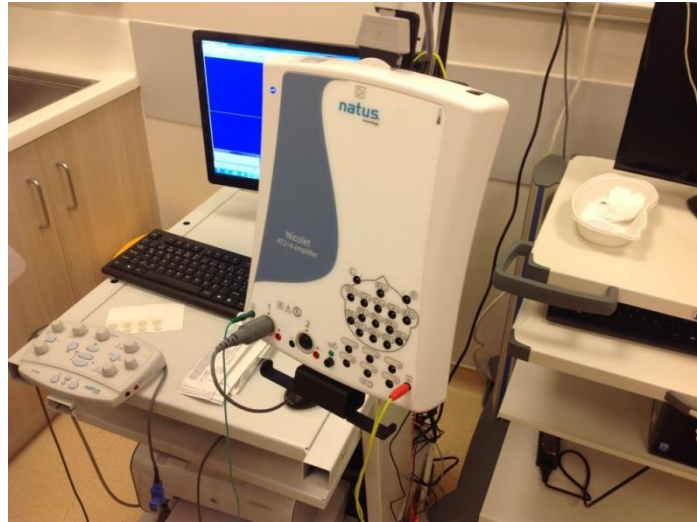


Figure 7: Photo of clinical EMG in Koç University Hospital



Figure 8: Photo of ADInstruments Powerlab 16/35 DAQ system

Under normal circumstances, the research oriented devices don't include bio amplifiers for small signal acquired from surface EMG or any other signal conditioner so that they don't distort the raw signal but they are easy to interface with. For example, even the smallest and cheapest ADInstruments DAQ has trigger input and serial output ports. (Figure 9) By the help of these standard ports, any custom device can be integrated to build a multi-modal data acquisition setup.



Figure 9: Photo of ADInstruments Powerlab 26T DAQ system

## 2.5. Motivation and Research Question

Even though all the studies agree that RAM based task can be used in assessing bradykinesia level, the measurement techniques used in them relies on wide variety of devices such as accelerometers (Dunnewold, Jacobi, & van Hilten, 1997), gyroscopes (Salarian, et al., 2007), magnetic devices (Kandori, et al., 2004; Ghassemi, Lemieux, Jog, Edwards, & Duval, 2006), and EMG sensors (de Souza, Dionísio, & Almeida, 2011).

In summary, the lack of focus on a common measure, which can be used both in clinical and daily life applications, causes every study to implement its own technique and to use time consuming UPDRS scoring. Furthermore, this issue and re-implementation in every new study forces researchers to rely on the variables of one technique. As shown in two conflicting studies (Ghassemi, Lemieux, Jog, Edwards, & Duval, 2006; Daneault, Carignan, Sadikot, & Duval, 2013), the measurement selection is an important issue which is disregarded due to the complexity of the problem. Besides indirect techniques that measure movements, there are also techniques such as EMG and facial recordings. These techniques can perform more thorough analysis. In order to achieve a precise assessment, using more than two techniques and evaluating their data together seems like the only viable solution. Moreover, the recent technical advancements enabled use of handheld and user friendly devices as in Salarian et al.'s study (Salarian, et al., 2007) One example is the software called NeuroRPM (NeuroRPM, 2023). The software that runs on the Apple watch to continuously monitor the cardinal symptoms of the disease is FDA cleared. Therefore, the progression of the symptoms and PD state can be easily monitored both in clinical and research environments. As a result, efficiency of a treatment which is already available or will be developed can be evaluated and improved rapidly.

The research question of this thesis centers on the development of a practical interface to be used in clinical studies. For this purpose, we investigated hand movements as well as facial movements in Parkinson's Disease Patients partnering with Koç University. The clinical data from pinching, pronation and supination hand movements collected by Leap Motion device was analyzed. In terms of the research question, we investigated whether we could predict the UPDRS score automatically. Furthermore, to analyze the facial movements, we developed our own hardware and software interface and investigated if the bradykinesia prediction can be improved with the new data processing techniques.

## CHAPTER 3

### FEATURE EXTRACTION AND STATISTICAL ANALYSIS OF HAND MOTIONS

#### 3.1. Pinching Motion

Various researchers have tried many different assessment techniques to overcome the inadequacy of UPDRS for detecting bradykinesia. All these techniques are mostly focused on rapid alternating movements (RAM) or finger tapping/pinching. Even though all the studies agree that RAM based tasks can be used in assessing bradykinesia level, the measurement techniques are relying on wide variety of devices such as accelerometers (Dunnewold, Jacobi, & van Hilten, 1997), gyroscopes (Salarian, et al., 2007), magnetic devices (Kandori, et al., 2004; Ghassemi, Lemieux, Jog, Edwards, & Duval, 2006), and EMG sensors (Sande de Souza, Dionísio, & Almeida, 2011). The common problem of all these devices is that they are depending on custom designs or setups. In other words, they are not commercially available off-the-shelf (COTS) products.

The objective of this experiment is to develop a new method to measure bradykinesia in PD patients by using COTS product called Leap Motion. Thus, the efficiency of Leap Motion is studied by recording various motor tasks performed by PD patients. The recorded data is analyzed for its various features against the UPDRS scores. The aim is to be able to utilize this easily available and relatively cheap device for daily tracking of patients and their treatments. The study is approved by the local Ethics Committees of Koç University Hospital, İstanbul, Turkey and all participants gave informed consent prior to the study.



Figure 10: The representation of interior design of Leap Motion taken from its product page.

Leap Motion (Leap Motion, Inc., San Francisco, USA) is a motion controller device to capture hand gestures by using pair of cameras and infrared lighting. It is a fairly compact device and very powerful to capture obvious hand motions like pinching and pronation/supination. Figure 10 shows the device interior and its compact design.

Weichert et. al. (Weichert, Bachmann, Rudak, & Fisseler, 2013) analyzed the accuracy of leap motion controller and found that it can achieve 0.7 mm overall average accuracy in all 3 axes. This result is comparable to the average human hand accuracy, 0.4 mm. Besides the accuracy, the controller is able to sample the hand motions around 100 Hz.

### **3.1.1. Method**

Pinching and Pronation-Supination are the two motor tasks given to the subjects. In this study, only the pinching task was used. Other data will be discussed separately. With the software developed on top of Leap Motion SDK, the positions and rotations of the finger joints and wrist are recorded during these tasks. After the recording session, the raw data is processed and several features are extracted. For the pinching, the local minima and maxima of the distances between thumb and index finger are marked. Afterwards, the time difference between the consecutive minimum and maximum is calculated.

By using the time difference and distance obtained from the raw data processing, the speed, acceleration, and frequency of a motion are calculated. In previous studies, it was shown that those three measures can be used to assess bradykinesia. (Daneault, Carignan, Sadikot, & Duval, 2013; Dunnewold, Jacobi, & van Hilten, 1997)

24 patients (7 female, 17 male, mean age  $\pm$  SD = 57.08  $\pm$  8.91) who were diagnosed by neurologist for PD participated in the experiment. All patients were under dopaminergic replacement treatment and their disease duration was 8.04  $\pm$  3.88 years. 20 patients were right-handed whereas 4 patients were left-handed. They came to the hospital in 12-hour OFF state (without medication) and two independent neurologists immediately evaluated UPDRS III (motor section) bilaterally. The average of those two scorings was considered as the final bilateral UPDRS scores ( $\mu_{left} \pm SD_{left} = 11.49 \pm 4.61$ ,  $\mu_{right} \pm SD_{right} = 12.28 \pm 5.15$ ). The patients were not specifically marked as tremor or bradykinesia dominant.

The patients visited hospital multiple times for another ongoing study for the data acquisition. There was at least one week difference between visits. 9 patients came to hospital twice and 15 remaining patients were recorded three times. In every case, the patients were seated against a laptop computer to which the leap motion controller is connected. The controller was laid on the table. To familiarize the patients with the device and to test the setup, they were asked to put their hand above the controller and move their fingers as shown in Figure 11. It was visually verified that the controller was capturing the gestures.

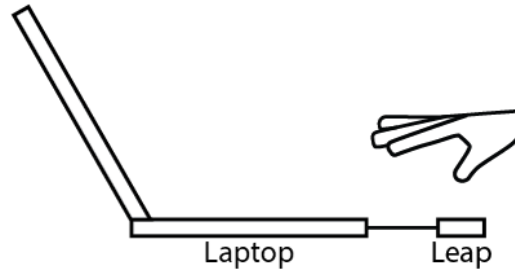


Figure 11: Basic recording setup with laptop and leap controller.

After the initial UPDRS scoring and familiarization was completed, the participant started to experiment. During the study, the motor tasks given to the patients were recorded in 3 successive sessions for both hands. Namely, one patient has total 12 recordings (6 pinching, 6 wrist motion) per hospital visit. At the end of the data acquisition phase, total 378 recordings were taken for pinching. The important part of the study is that before each session, bilateral UPDRS III scoring was evaluated by the same neurologists. The reason for the repeated scoring is to capture the subtle changes in the symptoms between the visits and different sessions. Each motion task was recorded at least 10 seconds for both hands one after another.

Table 1: Discarded speed values because of large SD

Mean Value (mm/s)	SD (mm/s)
216.80	129.36
689.53	543.78

Regardless of the session and action hand, the feature extraction was applied onto all recordings. Because of the fixation problems observed in the data (Figure 12), the first several extracted values of each feature (time difference, distance, and angles) were removed. With remaining features, the mean and standard deviation of speed, acceleration, and frequency were calculated. By comparing the mean and standard deviation of each metric, it was decided if the patient could perform the task correctly or not. Table 1 lists several exemplary values discarded because of having large deviations. In other words, the examples in the table have SD values which are almost comparable to the corresponding mean values.

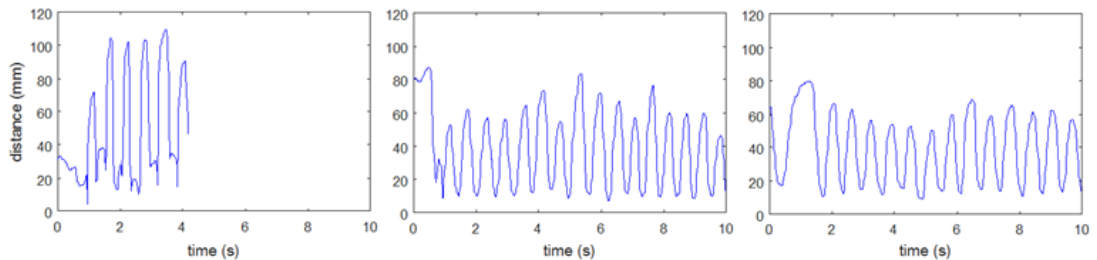


Figure 12: Change of the distance between thumb and index finger, during pinching for 3 different patients. The fixation problem can be seen at the start (before 2 seconds) of signal where the pattern is distorted.

Since the bilateral UPDRS scores were independently taken before each session, the values calculated for both hands were pooled together as Marsili et al. (Marsili, et al., 2014) did. Similarly, the recordings of all the visits and their three distinct sessions were also combined. This data pooling process was done separately for each motor task. After obtaining the two big sets of recordings, the correct metric was selected for pinching and pronation-supination, respectively. Thus, Pearson’s correlation was applied between UPDRS scores and three metrics derived from extracted features.

Later, by using all the metrics of both motor tasks, a linear regression model as in Equation 1 was derived to improve the link between UPDRS III and the data gathered from the controller. The correctness of the model was evaluated by the root-mean-square error defined by Equation 2.

$$U' = a_1f_1 + \dots + a_nf_n + b \quad (1)$$

$$e_{rms} = \sqrt{\frac{\sum_{i=1}^n (U'_i - U_i)^2}{n}} \quad (2)$$

### 3.1.2. Results

Some patients couldn’t complete the tasks given to them. There were 9 such sessions that were excluded from the study. Unrelated to the data content, the data belonging to one patient were discarded because of invalid UPDRS scoring. The features of 43 pinching recordings couldn’t be extracted because of invalid or missing data. As a result, these 43 data were also removed from the data pool.

The investigation of mean and standard deviation of metrics calculated for remaining sessions revealed that almost half of the data for each metric have large deviations ( *speed* = 49%, *acceleration* = 59%, *frequency* = 40% ). Since it is not possible to include these inconsistent values, the correlation study was completed by discarding them.

Firstly, the pinching task was analyzed and it was found that there were very low correlations (  $r_{speed} = -0.222$ ,  $r_{acc} = -0.112$ ,  $r_{freq} = -0.144$  ) between the pinching metrics and their respective contra-lateral UPDRS III scores. However, when the analysis was conducted against the ipsi-lateral scores, a moderate correlation was obtained (  $r_{speed} = -0.512$ ,  $r_{acc} = -0.398$ ,  $r_{freq} = -0.337$ ,  $p < 0.001$  ). UPDRS III motor section contains many items focusing on a specific symptom. Thus, the correlation study was repeated against the bradykinesia subset of UPDRS III because the pinching performance should be mostly affected by bradykinesia. As expected, the results (  $r_{speed} = -0.562$ ,  $r_{acc} = -0.453$ ,  $r_{freq} = -0.388$ ,  $p < 0.001$  ) got better for all three metrics. In the end, the speed is the best metric for the pinching.

Even though the speed was selected as the best metric for pinching, the values were fitted to create linear model from all metrics as in Equation 3 (  $s = speed$ ,  $a = acceleration$ ,  $f = frequency$  ) to estimate UPDRS III score.

$$U' = k_1 s_{pinch} + k_2 a_{pinch} + k_3 f_{pinch} + b \quad (3)$$

$$z_e = \frac{e_{rms}}{\max(UPDRSIII)} \quad (4)$$

The correlation between pinching and bradykinesia was significant so should be the linear model when the features of pinching is selected as sole predictors. The important point is that this model had small root-mean-square error ( $e_{rms} = 4.37$ ) for estimating total UPDRS III score. To better visualize the error, it is normalized ( $z_e = 0.078$ ) by the max value of UPDRS III as in Equation 4.

Because of stronger correlation with bradykinesia subset in pinching, the linear model was also created for UPDRS III bradykinesia score. As expected, the error of this model was similarly small ( $e_{rms} = 2.13$ ,  $z_e = 0.107$ ). Even though the normalized value was slightly bigger than the error in the total score case, it was not significantly different.

Instead of using whole data to create the model, the training procedure was repeated by using randomly selected 75% of the data. After training, the remaining 25% of the data was used for testing the model. This training-testing procedure was repeated 100 times for the different randomly selected training set. After 100 repetitions, the average RMSE values were calculated. The results of trained model were similar to the previous approach for both total UPDRS III ( $e_{rms} = 4.37$ ,  $z_e = 0.078$ ) and bradykinesia subset ( $e_{rms} = 2.12$ ,  $z_e = 0.107$ ) cases. The important finding was that error of estimations was ( $e_{rms} = 5.59$ ,  $z_e = 0.099$ ) and ( $e_{rms} = 2.90$ ,  $z_e = 0.145$ ) respectively.

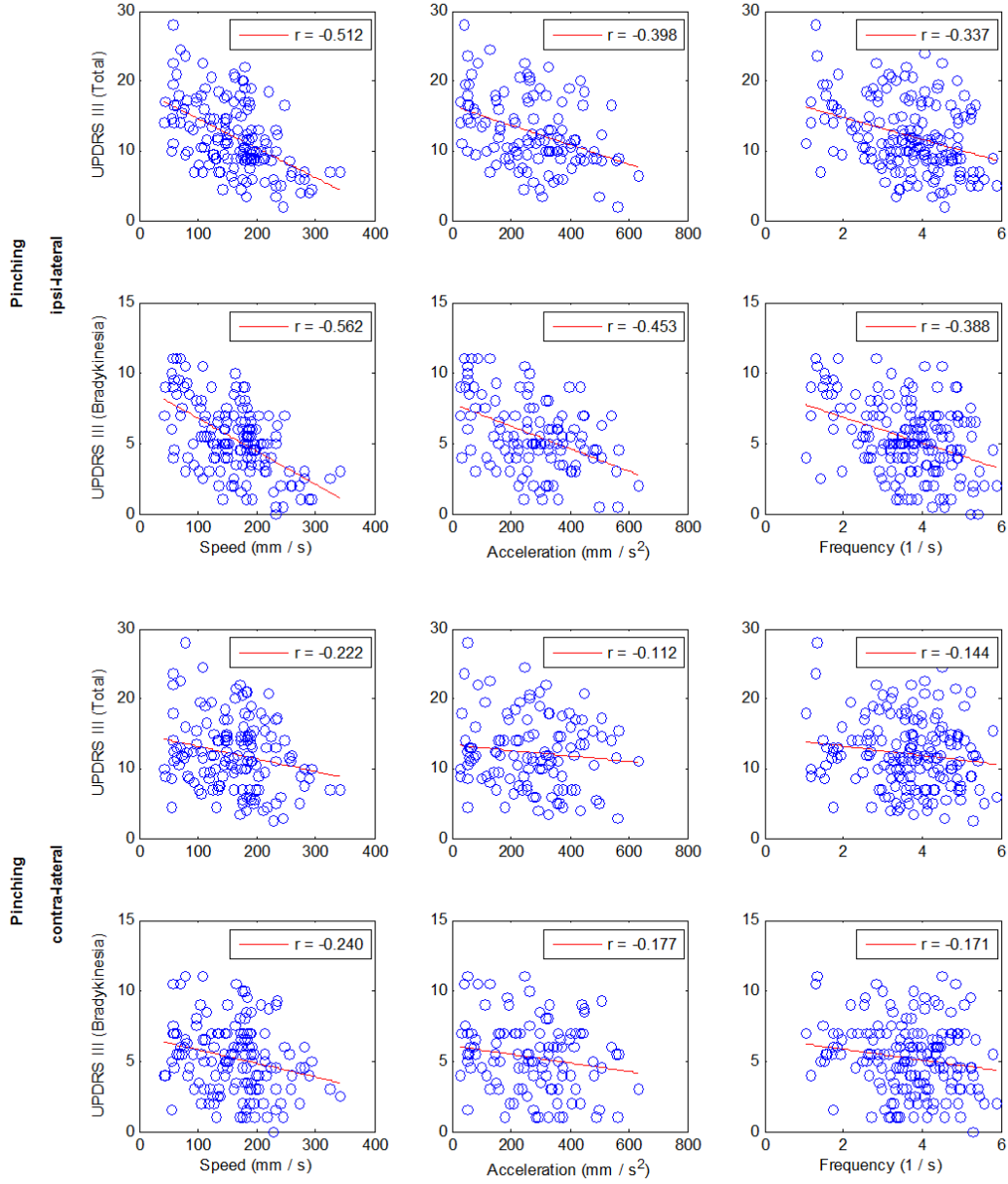


Figure 13: Distribution of UPDRS III total score and bradykinesia subset against the three metrics (speed, acceleration, frequency) extracted from the pinching recordings. The metrics are the combination of data from all the session for both hands. The upper two rows show the ipsi-lateral results while the bottom two rows belong to contra-lateral results. As expected, the speed showed the highest correlation ( $r = -0.512$ ,  $p < 0.001$ ) and the correlation ( $r = -0.562$ ,  $p < 0.001$ ) increases by using bradykinesia subset. Furthermore, the contra-lateral analysis revealed that there was no correlation between the total ( $r = -0.222$ ,  $p < 0.001$ ) and the metrics. Even using bradykinesia subset ( $r = -0.240$ ,  $p < 0.001$ ) scores did not improve it.

### 3.1.3. Discussions

In this study (Çakmak, Ölçek, Özsoy, & Gökçay, 2018), it is showed that a COTS device can be used in simple setup to assess the bradykinesia level of the patient with

PD. Furthermore, it is important that the assessment was done by using a quantitative metric acquired from the device. By comparing the measurements with the UPDRS III scores which are based on the subjective observations of physicians, it was seen that this method can be used as a fast and reliable alternative. The main advantage of this technique is that it helps the physician by keeping the process completely objective, thus, they can better decide on treatment regime. Nevertheless, the number of invalid data suggested that the patients need further familiarization with the task and device. This can be overcome by extending the recording time and the familiarization time. The exclusion of data could be done by using z-scores of the metrics which might give further information why the patients couldn't complete the given task.

UPDRS is a subjective scoring system, although it is widely used in the clinic. Due to its subjectivity, having mild to moderate correlations of UPDRS with an actual physical measure is not surprising. Despite this fact, UPDRS III was chosen for the validation because it is the clinical golden standard for diagnosis and prognosis. The correlation study revealed that the fine movements like pinching expresses bradykinesia well. Further testing of linear model showed that this method is less error-prone than the UPDRS. If a physician makes 1 scale-unit error for each item, the error becomes  $z_e = 0.250$  which is a value much larger than our proposed model's error.

### **3.2. Pronation and Supination Motion**

UPDRS motor scaling, which is the most common assessment modality for the motor symptoms of Parkinson's disease, uses the pronation/supination movement ability to score the bradykinesia/rigidity related sections of the UPDRS but not as a proxy for gait and posture instability. Although the researchers have investigated pronation and supination mechanics (Garza-Rodríguez, Sánchez-Fernández, Sánchez-Pérez, Ornelas-Vences, & Ehrenberg-Inzunza, 2018) the UPDRS motor scaling does not consider the pronation/supination as a proxy for the gait ability. Furthermore, there is no report investigating the potential relationship of the forearm pronation/supination with the gait/posture instability in PD. Numerous biomedical wearables for the forearm including smart watches are in the market to monitor the motor symptoms of PD patients but to our knowledge, none of them were able to provide the gait/posture stability information based on a unilateral forearm/wrist or finger movement. The gait and posture stability info can only be gathered if the multiple wearable sensors are combined and placed on multiple body locations including thorax and limbs but not with the aid of a unilateral, single limb movement based sensor.

As the next step of the previous work done for pinching, the pronation and supination data collected in the same sessions were analyzed to investigate whether the pronation/supination movement data of a single wrist is correlated with the bradykinesia level of PD patients or not. By the help of this work, the forearm

wearables like smart watches that can also be used for continuous monitoring during daily life activities such as walking, standing up, eating, etc.

### 3.2.1. Method

#### 3.2.1.1. Data Collection

The participants of this experiment were exactly same in pinching experiment because this is the continuation of that work. During previous study, two motor tasks were recorded one another, however, only pinching was analyzed for bradykinesia. Nevertheless, in this case, pronation and supination signal recorded during the sessions were processed and evaluated.

In addition to the traditional approach of taking into account the dominant symptom side scores of lateralized subitems (items 20–26) for the UPDRS Part-III motor scale scoring, the scores of lateralized subitems on both sides (ipsilateral and contralateral to the dominant symptoms and to the stimulator) were also documented to demonstrate the potential correlation with B and UPDRS. Moreover, the subscores of UPDRS Part-III were also classified and analyzed as Tremor (items 20–21), Rigidity (item 22), Bradykinesia (items 23–26,31), Gait and Postural Instability (items 27–30) and Bulbar Anomalies (items 18–19), as in previous studies. (Postuma, Gagnon, Vendette, Charland, & Montplaisir, 2008; Çakmak, et al., 2017)

All patients were asked to perform pronation-supination (P/S) motor tasks. The UPDRS III bradykinesia subsection includes pronation-supination task and accordingly patients were observed by the physicians during diagnosis. As seen in Table 2, twenty-four patients with idiopathic PD (17 men, 7 women; mean age  $\pm$  SD = 57.08  $\pm$  8.91 years) participated to this study.

Table 2: Demographics of the patients participated

Age	Gender	Dominant Hand	Affected Side at Onset	PD Duration (year)	H&Y Stage
61	F	R	R	12	3
46	M	R	L	4	3
55	M	R	R	8	2
48	M	R	R	12	2
54	M	R	R	6	2
48	M	R	L	8	2
61	M	R	L	6	2
71	M	R	R	17	2
52	M	R	R	2	2
61	M	R	R	8	3
56	M	R	R	7	2
47	F	R	R	10	2

63	M	R	R	8	2
58	F	R	R	15	2
54	M	R	R	9	3
70	F	R	R	8	3
64	M	R	L	1	2
45	F	R	L	4	2
71	M	R	R	5	2
45	F	R	L	8	2
63	F	R	R	4	2
72	M	R	L	13	2
45	M	L	R	8	2
60	M	R	R	10	2

The raw data belonging to the gestures was recorded by the custom software developed using Leap Motion SDK. The recorded raw data was processed to extract features defining the characteristics of the motions. The wrist rotation on a single axis was processed for pronation-supination and as the task is a rapid repetitive motion, the local minimal and maximal values of the processed data were marked for further extraction. The consecutive markers were used to calculate three final features which relate to speed, acceleration, and frequency. In previous studies (Daneault, Carignan, Sadikot, & Duval, 2013; Dunnewold, Jacobi, & van Hilten, 1997), these three features were also analyzed and were found to be useful in assessing bradykinesia. Figure 14 shows the details of an example raw data collected by the software.

### *3.2.1.2. Data Sanitization*

The occasional glitches and noisy sections of the data that originate from initiation and termination of the movement was excluded from all records. The exclusion procedure was performed with manual marking for these sections with visual control by the same investigator (CO). The full flow of the exclusion process is provided as a supplementary file.

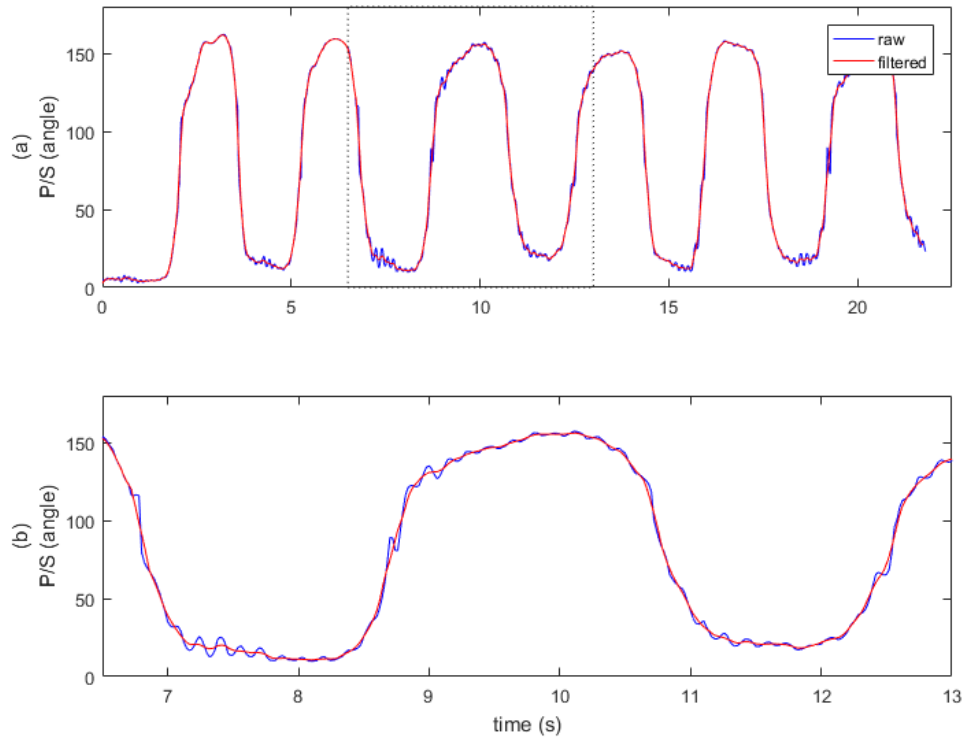


Figure 14: Signals after moving average filter was applied, (a) shows the whole signal and resulting waveform in red after filter. (b) is the zoomed in part where the tremor is clearly visible

If tremor occurs in the middle of the data collection task, it appears as ripples and results in inaccurate minima and maxima detection. To solve this issue, the wave was analyzed by a frequency spectrum and a typical spectrum was observed to contain a significant response below 5 Hz (Figure 15). Taking into account the sampling rate, a moving average filter with window size of 7 was applied to smooth out the signal as shown in Figure 14. At the saddle points, where the motion reaches its extreme points, it was observed that several patients had double peaks which were different to the tremor form. Since our feature selection was based on the difference between time and the angles of the motion, it was possible to use consecutive minima and maxima pairs to calculate the features for pronation and supination. As seen Figure 16, those consecutive points were marked for further feature extraction. As explained in the analysis section, the averaged features derived from several minima and maxima pairs were used. For the analysis any single pronation and supination signals less than 4 consecutive points were excluded from the study. As a result, 3 records are discarded from the entire batch.

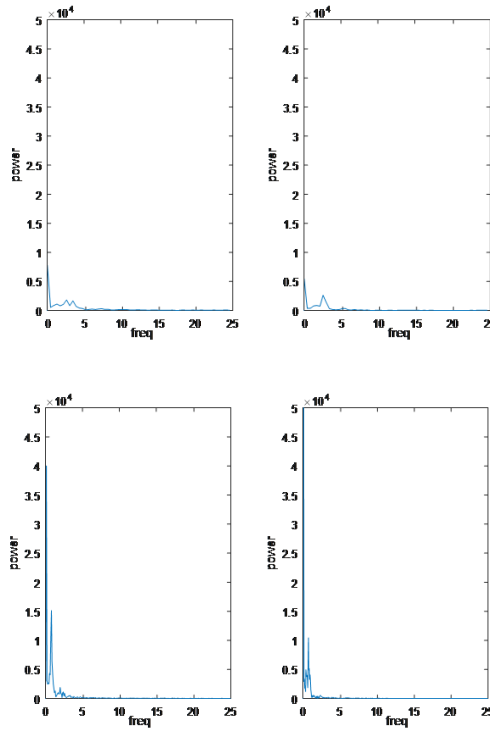


Figure 15: Frequency spectrum of P/S signals. Upper row shows 2 excluded signals after smoothing, while bottom 2 shows the typical frequency spectrum. The proper bottom signals contain powerful response on low frequencies around 2 and 3 which is basically the number of P/S cycles.

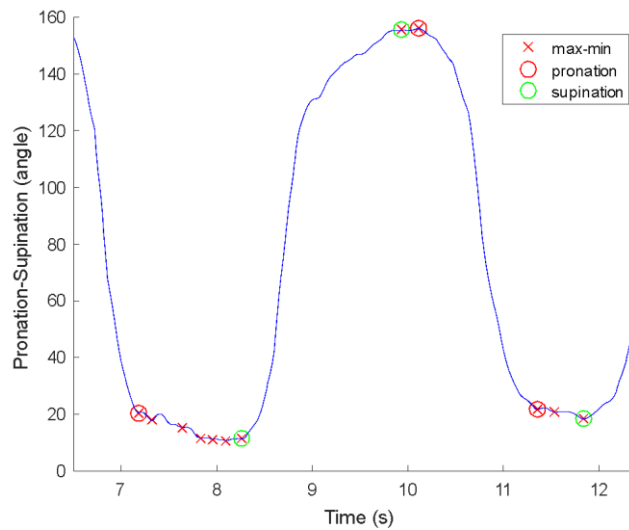


Figure 16: Signal after moving average is applied and marked. The important features of the pronation/supination movement are marked as follows. “x” marks are the extrema points found by the marking process but as seen in the figure not all the markings were accepted. Only if the minima immediately following the maxima or vice versa were accepted as the ones that should be included into feature calculations. Those points are marked by additional circle.

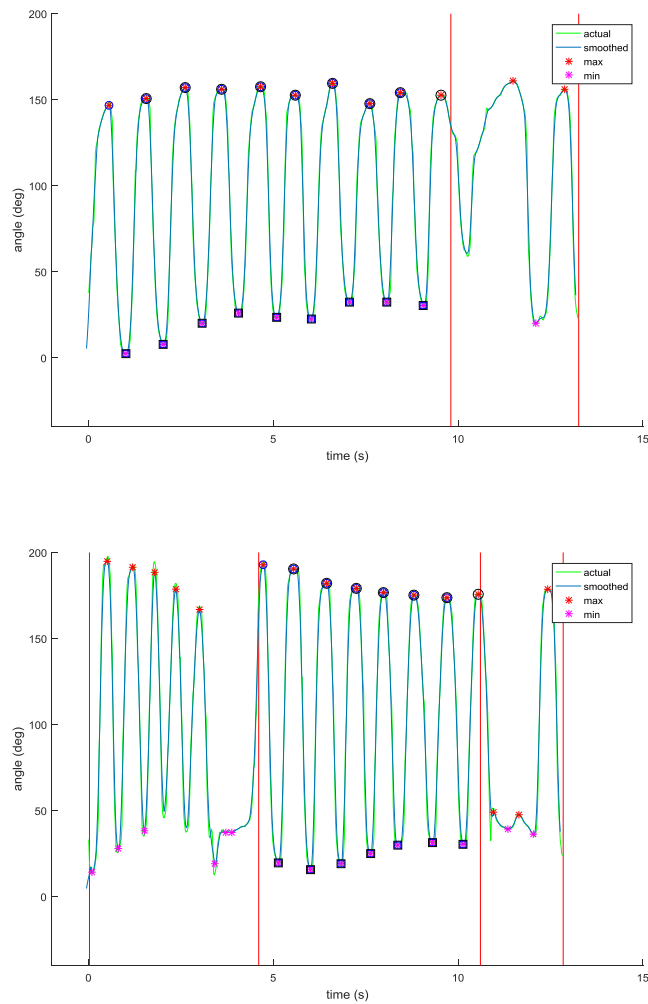


Figure 17: Invalid parts of the data was trimmed. Trimmed parts are the parts inside the red line markers

In total 77 of the 274 recordings must be excluded in the context of incomplete pronation/supination data due to incomplete pronation/supination data (because of the severe rigidity or data collection errors). 197 of the 274 recordings are analyzed. The data analysis algorithm chart can be seen in APPENDIX B.

### 3.2.1.3. Feature Extraction

Following on from the data sanitation phase the remaining datasets (197) were used for feature extraction. In this phase, three specific features were calculated starting from the first minima marker. The mean of the calculated values for each consecutive minima-maxima points in a single record were accepted as the final feature metric (Equation, 7, 8, and 9). Namely,  $f_1$ ,  $f_2$  and  $f_3$  features are influenced by speed, acceleration, and frequency respectively. The marked extrema points

enabled separate metrics for pronation and supination phases. In addition, the features for combined motion were also computed as in Equation 10, 11, and 12.

$$d\phi = |\phi_{min} - \phi_{max}| \quad (5)$$

$$dt = |t_{min} - t_{max}| \quad (6)$$

$$f_1 = \frac{1}{n} \sum d\phi/dt \quad (7)$$

$$f_2 = \frac{1}{n} \sum d\phi/dt^2 \quad (8)$$

$$f_3 = \frac{1}{n} \sum 1/dt \quad (9)$$

$$f_1^{wrist} = \frac{1}{n} \sum (d\phi_{pro} + d\phi_{sup}) / (dt_{pro} + dt_{sup}) \quad (10)$$

$$f_2^{wrist} = \frac{1}{n} \sum (d\phi_{pro} + d\phi_{sup}) / (dt_{pro} + dt_{sup})^2 \quad (11)$$

$$f_3^{wrist} = \frac{1}{n} \sum 1 / (dt_{pro} + dt_{sup}) \quad (12)$$

$\phi$  = wrist angle,  $\phi_{min}$  = angle at local minima,  $\phi_{max}$  = angle at local maxima

$t$  = time,  $t_{min}$  = time at local minima,  $t_{max}$  = time at local maxima

$n$  = number of valid consecutive extrema points

It is important to note that the features shown in Equation 10, 11, and 12, treat the pronation and supination movements altogether as a single sweep, disregarding the pause in between. The angles of pronation and supination are added together, hence the information regarding the turn of the wrist from one direction to the other is not captured in these features because the entire pronation and supination sweep is taken as a single movement.

For each record, there were corresponding independent bilateral UPDRS III scores where right and left side records are considered to be independent records. To keep data set homogeneous, the patients having left hand preference and left hand symptom dominance (4 patients with a total of 47 records) were removed. With final dataset, Pearson's correlation between UPDRS scores and metrics were used to find the highest correlations. Since UPDRS III is composed of 5 subgroups/scores which are tremor (T), rigidity (R), bradykinesia (B), gait and postural instability (GP), and bulbar anomalies (BA), the correlation analysis was not only applied for UPDRS III total score but also for all the possible combinations such as T+R, T+B+BA, summing up to 18 combined UPDRS values ( $n_{combinations} = 18$ ). By adopting this approach, it was aimed to demonstrate the overall pattern of the subgroup contributions and relations.

#### 3.2.1.4. Statistical Analysis

All the statistical analyses were performed in MATLAB (MathWorks R2016a) Statistics and Machine Learning Toolbox. The signal processing phase were also developed in MATLAB (MathWorks R2016a) by using the Fourier Analysis and Filtering functions.

Statistical significance analysis on linear models created in this work required a correction for multiple comparisons because of the difference in the number of correlated features used in each model (i.e. each prediction was correlated with various number of features originating from the same set of measurements). Therefore, a Bonferonni correction (Curtin & Schulz, 1998) was applied for estimating the significance by dividing 0.05 by the number of predictors ( $N_{features}$ ). As a result, the features were classified as significant only when the associated p-value is found to be less than  $0.05/N_{features}$ .

Multi linear regression models with the feature set was constructed to see if B can be predicted from pronation and supination. From 1 feature only models to combinations of multiple features starting from 2 up to 18 features, all the possible combinations of the subsets (more than 200000), were used to create and test linear models. The top 50 models with the minimum root mean square error (RMSE) were used for further regression analysis. Monte Carlo cross validation was applied onto the top 50 models, thus, they were trained and tested against 3 different cases where 90%, 75%, and 50% of data were used in training. Each set was trained 1000 times, wherein the training sets were sampled randomly and the remaining data used to test the accuracy of the models. Both the mean of model RMSE and mean of RMSE between the expected and predicted scores were reported.

### 3.3. Results

#### 3.3.1. Correlation Analysis

The calculated features provide indications of speed, acceleration, and frequency. Namely,  $f_1$ ,  $f_2$ , and  $f_3$  features will be shown respectively as *speed*, *acceleration*, and *frequency* in the figures. Initially to capture the overall picture, a correlation study between subgroups of the UPDRS and the features extracted from the signals was conducted. In order to keep the analysis homogenous, 4 patients whose hand preference was left hand or who had left hand dominant symptoms were excluded. A more generalized work with all patients is intended for future work. In Figure 18, Figure 19, and Figure 20, the correlations are shown through a color map. According to the number of data points in the study, the correlation values that are above 0.2 and below -0.2 qualify to be significant at  $p < 0.05$  level. These correlation values correspond to the shades that range from orange to red (for positive correlations) and from light blue to dark blue (for negative correlations).

The  $f_1$  resembling speed in bradykinesia (B) showed a strong correlation ( $r_{1(B)}^{sup} = -0.60, r_{1(B)}^{pro} = -0.60, r_{1(B)}^{wrist} = -0.62$ ) with large effect size in both pronation and supination components of the motion. Furthermore, the  $f_1$  in rigidity (R) followed the bradykinesia results with similar effect size ( $r_{1(R)}^{sup} = -0.50, r_{1(R)}^{pro} = -0.52, r_{1(R)}^{wrist} = -0.53$ ). Besides bradykinesia and rigidity, gait and postural instability (GP) showed strong correlation in  $f_2$ (acceleration) for supination component ( $r_{2(GP)}^{sup} = -0.51$ ). Although, other features were not as strongly correlated as the  $f_2$  results as seen in *Figure 1*, they had correlations with medium effect sizes. When the combinations were inspected, R+B provided the strongest correlations ( $r_{1(R+B)}^{sup} = -0.62, r_{1(R+B)}^{pro} = -0.63, r_{1(R+B)}^{wrist} = -0.65$ ). R+B was not only the strongest correlated combination to the movements, it also improved the single subgroup correlations.

Among all combinations of the UPDRS scores, those with GP stand out as a third component almost as strong as R and B in correlating with our motion features. By definition, R and B are expected to correlate with speed, acceleration, and frequency of the motion, however, correlation of these features with GP warrants a closer inspection. While R+GP in  $f_2$  ( $r_{2(R+GP)}^{sup} = -0.55$ ) and R+B+GP in  $f_1$  ( $r_{1(R+B+GP)}^{sup} = -0.61$ ) had values close to R+B for supination, pronation had similar R+B+GP ( $r_{1(R+B+GP)}^{pro} = -0.60$ ) and R+B+GP+BA ( $r_{1(R+B+GP+BA)}^{pro} = -0.58$ ) correlation values. Furthermore, the combined  $f_1$ (speed) had slightly better values for B+GP ( $r_{1(B+GP)}^{wrist} = -0.58$ ), R+B+GP ( $r_{1(R+B+GP)}^{wrist} = -0.62$ ), and R+B+GP+BA ( $r_{1(R+B+GP+BA)}^{wrist} = -0.60$ ).

For left hand correlations with ipsilateral UPDRS scores, except a couple of combinations, almost all the combinations had strong correlations (Figure 19) similar to right hand. In addition, the revelation of GP correlation was also strong. Even the single group GP correlations were quite high showing medium effect size in every case. The correlation study served its purpose by giving clues which subgroups are contributing to each other. In fact, GP can be found in many of the moderate and strong correlations.

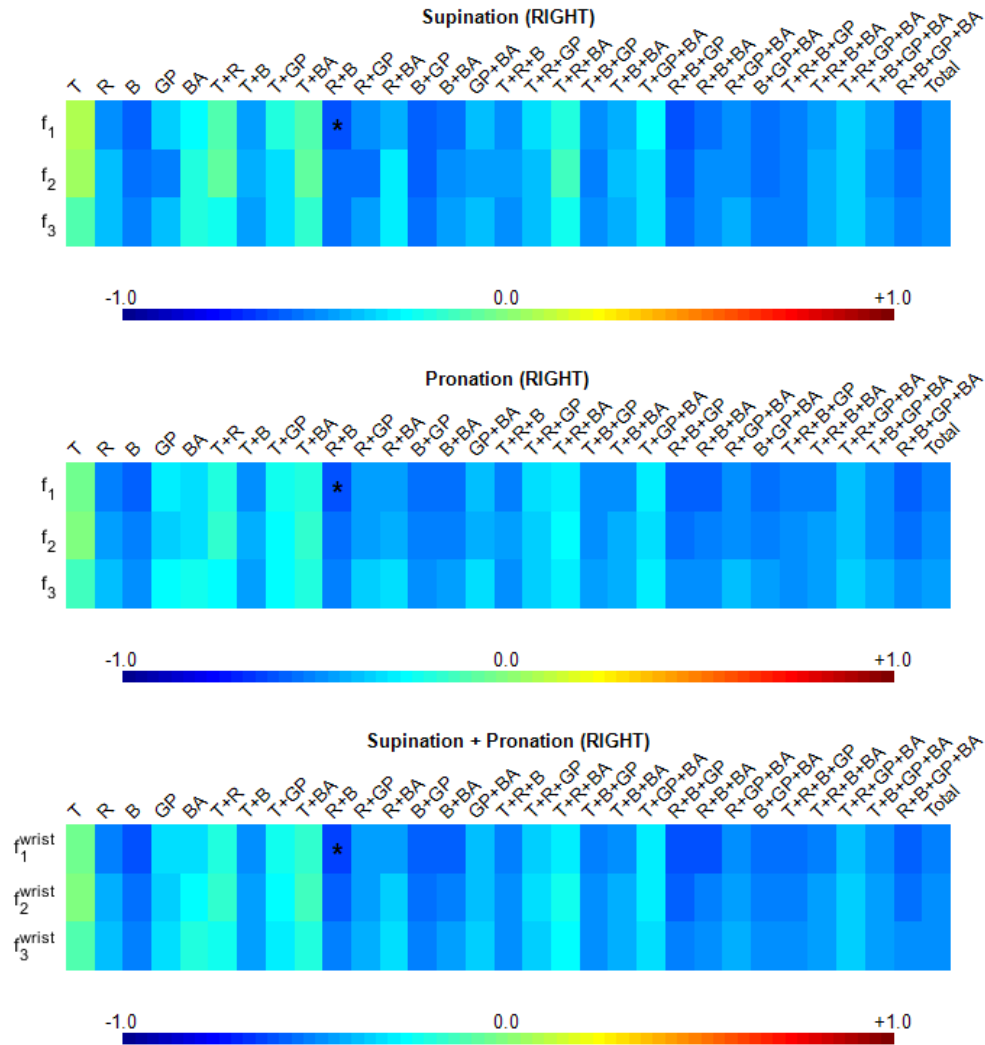


Figure 18: Correlations between features and **UPDRS from right hand** where \* marks the highest correlation. The dataset is composed of only **right hand preferred** and **right hand symptom dominant records**. T=Tremor, R=Rigidity, B=Bradykinesia, GP=Gait and Postural Instability, BA=Bulbar Anomalies. As expected, B and R has powerful correlation with the motion.



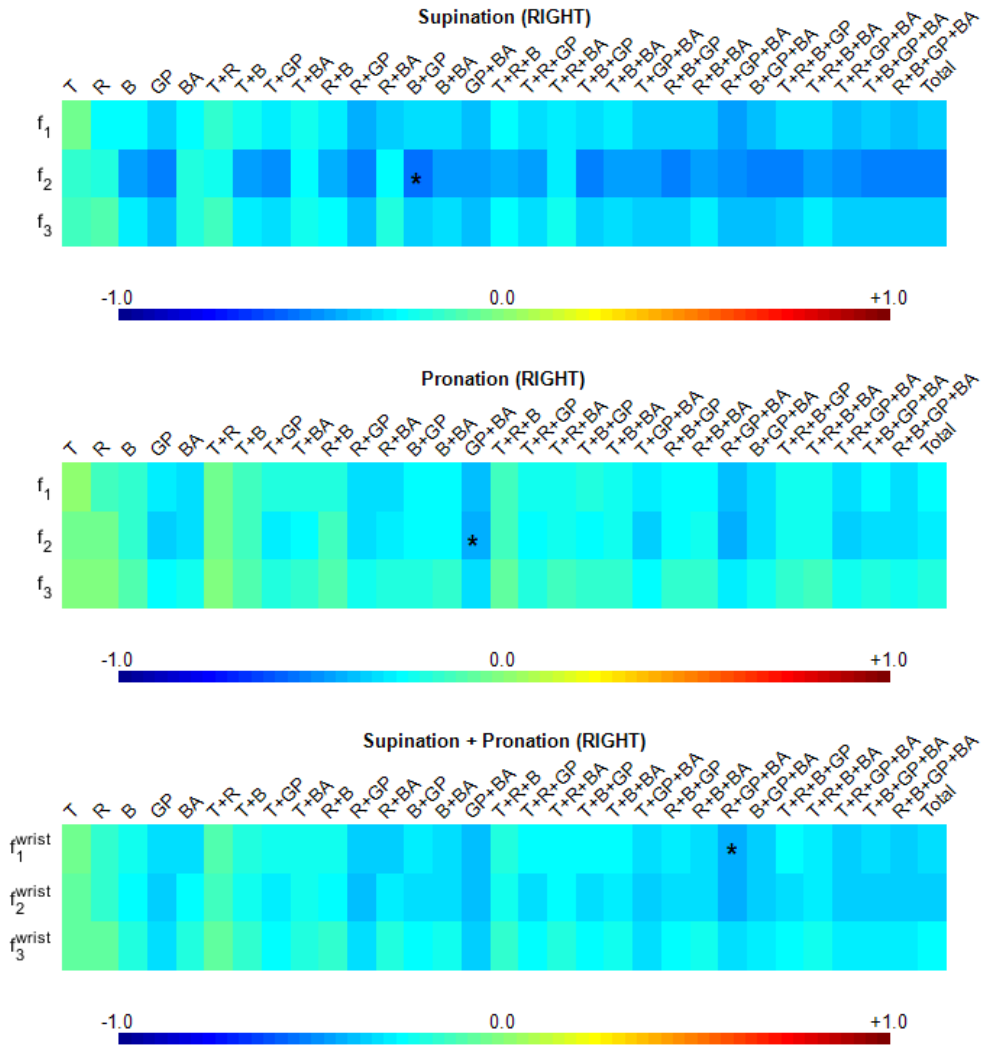


Figure 20: Correlations between features from right hand and **UPDRS from left hand** where \* marks the highest correlation. The dataset is composed of only **right hand preferred and right hand symptom dominant** records. The contralateral correlations are weak except for the acceleration in supination phase. The most interesting outcome is the strong correlation with GP scores which are unilateral.

### 3.3.2. Linear Regression Model

Among all the multiple linear regression model combinations created to predict B score, the top 50 having lowest RMSE were isolated. Figure 21 shows the significance of the factors used in these 50 models and shows that all 50 models show similar patterns with each other. For example, the left hand speed for pronation, and combined were included in almost all the top models. Likewise, right hand acceleration, and frequency of combined motion have also significant contribution to the models. Among these models, the confidence values for the speed components are stronger than the other features. Nevertheless, the results showed

that frequency components follow the speed and are the significant parts of the models.

While the regression models have contributions from the features with large effect sizes it is important to control the model accuracy. Therefore, the prediction accuracy of the selected models were tested by Monte Carlo cross validation with three different training-test percentages. The mean RMSE values of the trained models against the expected results were  $mean(RMSE_{90}) = 1.86 \pm 0.03$ ,  $mean(RMSE_{75}) = 1.96 \pm 0.04$ ,  $mean(RMSE_{50}) = 2.19 \pm 0.07$ , wherein the 50% ratio provided enough accuracy to predict bradykinesia.

### 3.3.3. Discussion

The results demonstrated that B is correlated with the forearm pronation and supination speed on both forearms. Amongst 3 of the P/S movement parameters only the speed component demonstrated a significant correlation with one or more of the 5 subgroups of the UPDRS motor scaling system.

The UPDRS Bradykinesia sub group is composed of 9 measurements where 4 questions repeated bilaterally and 1 question is unilateral. With 9 measurements, the total maximum score can be 45 out of the 5 point scoring system. When the linear models are converted to error percentages, they become 4.14%, 4.35%, and 4.86% respectively. It can be conceptualized that if a physician makes a 1 point error for each measurement, the physician based error can reach up to 20%. In other words, the human error may be much higher in comparison to the errors of the linear regression models. It's worth to note that, there was one case where there was a 12-point difference between the evaluations of two physicians in our data collection. For all the recording sessions, there was a deviation between two physicians ( $mean(dU_B) = 1.95 \pm 2.75$ ). This deviation converted into percentage for total B score is approximately ( $mean(dU_B^{\%}) = 4.33\% \pm 6.12\%$ ). These values show that the theoretical human error assumption is on par with that deviation. In other words, it can be claimed that the linear models have enough accuracy to predict bradykinesia.

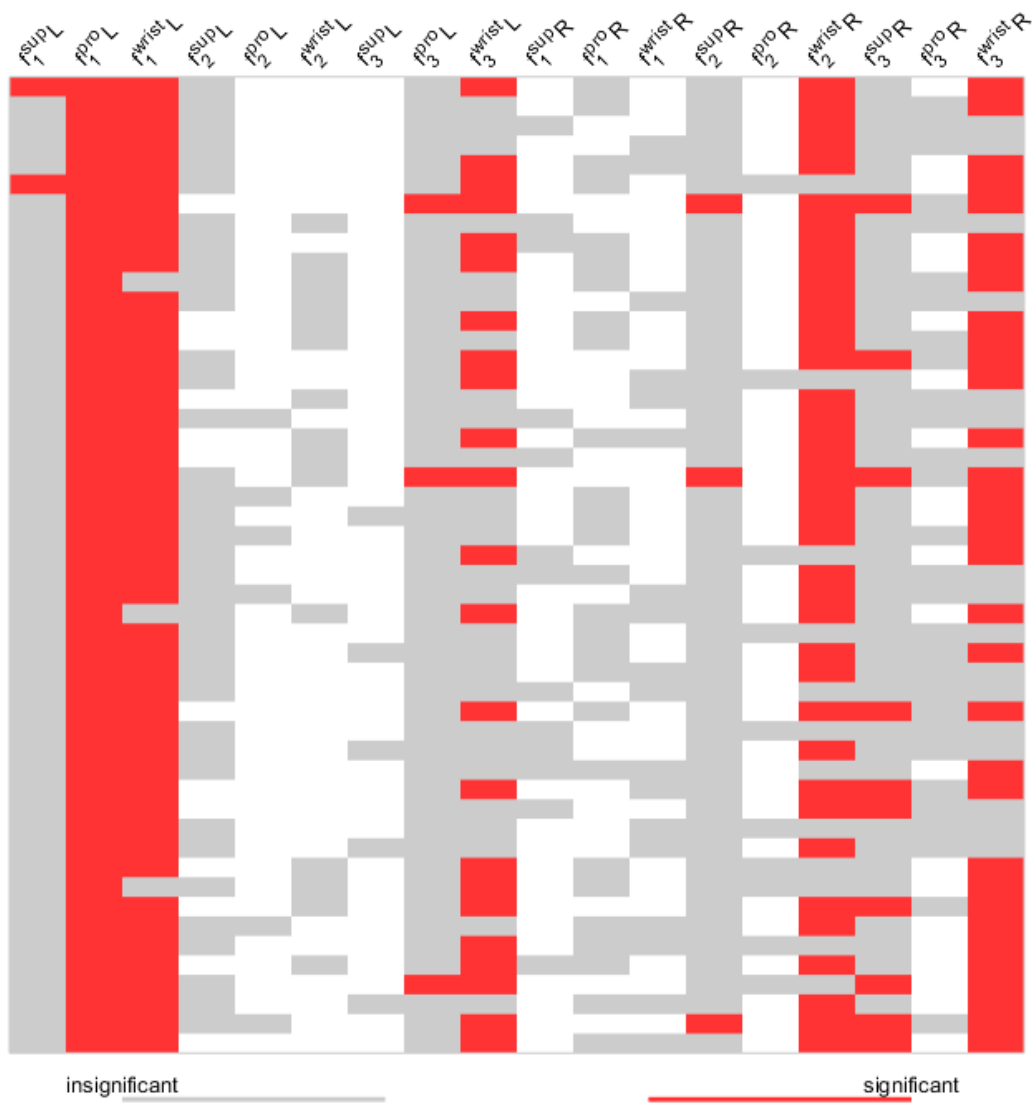


Figure 21: Significance of the features in top 50 regression models having minimum RMSE. Each row shows a single model. Rows are ordered with respect to increasing RMSE (range: 1.73-1.74). Each column identifies a feature in the model. The last character is L=Left and R=Right shows from which hand the feature was extracted. Colors indicate whether the feature is used in the model (white if the feature is absent), whether the feature is significant (red) or not (gray). As expected, the speed component exists in almost all the top models.

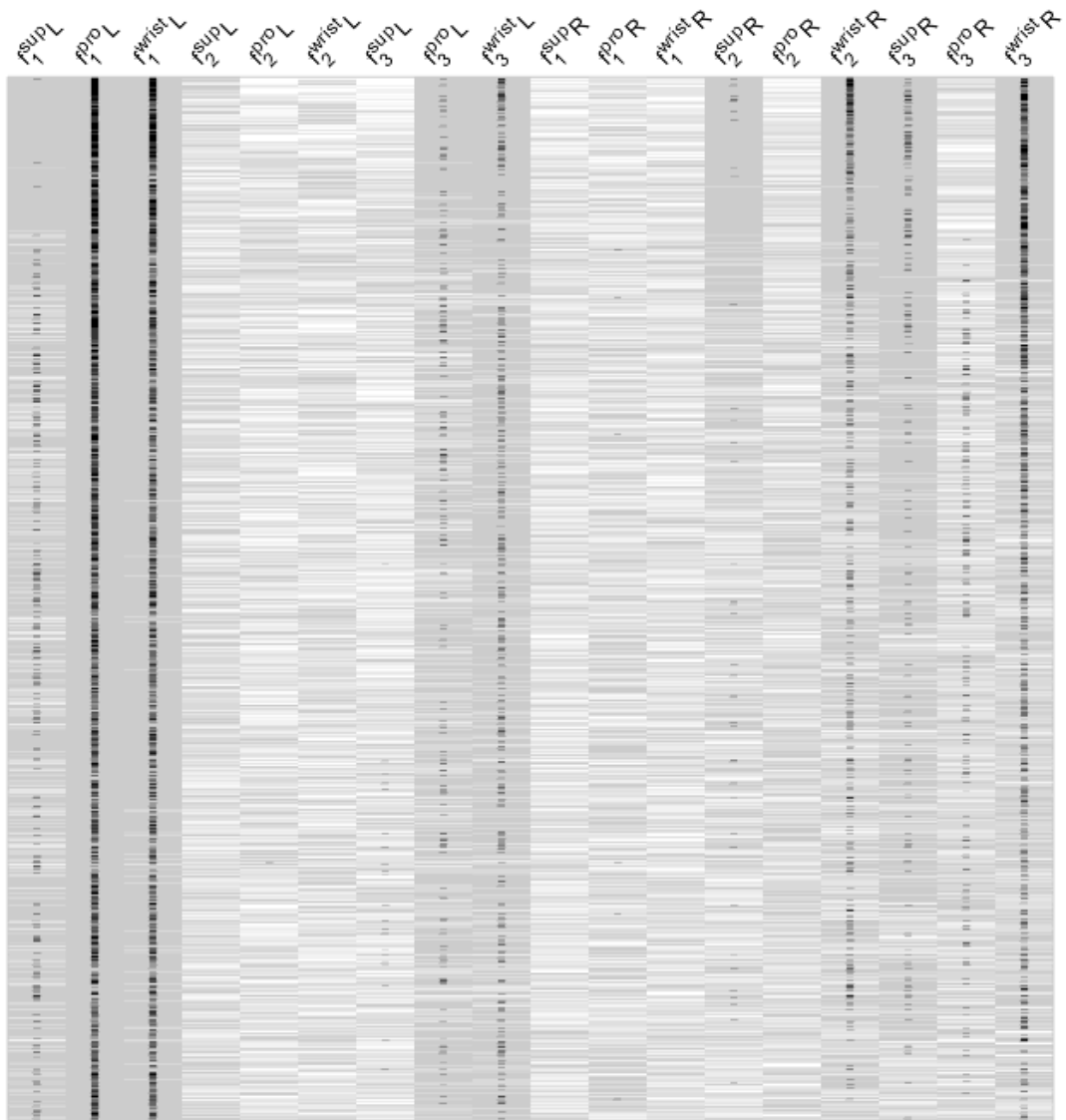


Figure 22: List of the features in top 1% (2621) of the regression models with lowest RMSE, ordered with respect to increasing RMSE (range: 1.73–1.81) (rows: different regression models, columns: model features; L = left hand, R = right hand from which features were extracted; white indicates absent feature, gray indicates contributing feature, black marks the significant features;  $f_1$ ,  $f_2$ , and  $f_3$  are speed, acceleration and frequency). It is clearly visible that the speed component is the most common component, thus the most significant in predicting the UPDRS score.



## CHAPTER 4

### FEATURE EXTRACTION AND STATISTICAL ANALYSIS OF FACIAL EXPRESSIONS COLLECTED BY EMG

#### 4.1. Development of Hardware Interface to Collect EMG in Sync with Facial Camera Recordings

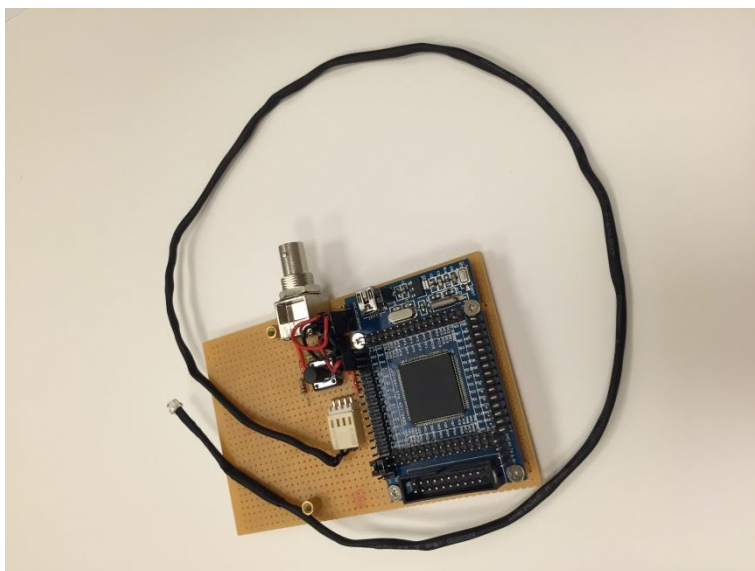


Figure 23: The assembled trigger device used in recording sessions

Synchronization is a major issue when dealing with more than one recording device. Since each device has its own particular sampling rate and interface, it is important to find a reference point in time to synchronize them. In this thesis, the trigger device shown in Figure 23 was designed and developed to create a signal for EMG device and the computer used for video recording. While EMG device has its own trigger input, the software used for video recording captured the trigger sent through USB port. By the push of a button, the device sends signals to both devices and at the same time, it turns the LED light on to give visual cue to synchronize the patient as well. Figure 24 shows the circuit diagram of the device that is based on STM32F103 microcontroller.

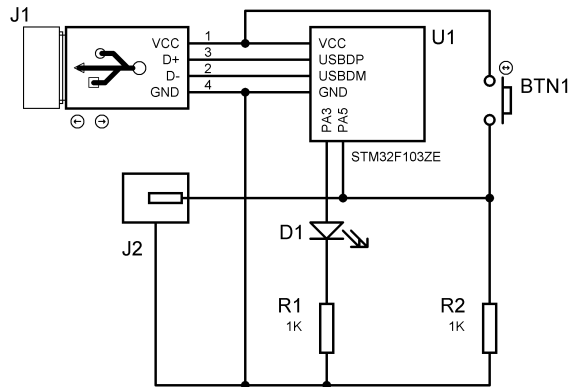


Figure 24: Circuit diagram for Trigger Device

The source code, that can be seen Table 3, was developed in C and kept simple to reduce the possible latency of the data collection when the trigger signal is captured. The developed code is assembled by using arm compiler and STM32 controller is programmed via JTAG interface. Whenever the trigger input is captured on the rising edge of the GPIO pin the code simultaneously writes a message to the USB interface that can be captured by the software on PC side and set another GPIO pin to light the LED lamp. To prevent glitches, the input is debounced for 500 ms so that any false triggers are ignored after the first capture.

Table 3: Source code if the trigger device

```
#include <stm32f10x.h>
#include <stm32f10x_gpio.h>
#include <stm32f10x_tim.h>
#include "USB.h"

int main(int argc, char* argv[])
{
    USB::init();
    RCC_APB2PeriphClockCmd(RCC_APB2Periph_GPIOA, ENABLE);
    GPIO_InitTypeDef gpio;
    gpio.GPIO_Mode = GPIO_Mode_Out_PP;
    gpio.GPIO_Speed = GPIO_Speed_50MHz;
    gpio.GPIO_Pin = GPIO_Pin_3;
    GPIO_Init(GPIOA, &gpio);
    gpio.GPIO_Mode = GPIO_Mode_IN_FLOATING;
    gpio.GPIO_Speed = GPIO_Speed_50MHz;
    gpio.GPIO_Pin = GPIO_Pin_5;
    GPIO_Init(GPIOA, &gpio);
    GPIO_ResetBits(GPIOA, GPIO_Pin_3);

    uint8_t triggerData[] = { 'm', 'k' };
    bool triggered = false;

    while(1)
```

```

    {
        // trigger cleared
        if(triggered && !GPIO_ReadInputDataBit(GPIOA, GPIO_Pin_5))
        {
            GPIO_ResetBits(GPIOA, GPIO_Pin_3);
            triggered = false;
        }

        // trigger at rising edge
        if(!triggered && GPIO_ReadInputDataBit(GPIOA, GPIO_Pin_5))
        {
            GPIO_SetBits(GPIOA, GPIO_Pin_3);

            // send trigger to USB
            USB::write(triggerData, 2);

            // wait 500u
            uint16_t timer = 36000; // 72
            while(timer--);

            triggered = true;
        }
    }
}

```

#### ***4.1.1. Detecting Onset From the Trigger Signal***

##### *4.1.1.1. EMG Data Preprocessing*

Most of the studies start (Cheron, Cebolla, Bengoetxea, Leurs, & Danc, 2007; Hannaford, Cheron, & Stark, 1985; Robichaud, et al., 2009) by applying high pass filter to the raw EMG signal. However, the recorded signal is already conditioned by some of the data acquisition devices. In fact, as seen in Figure 25, the frequency spectrum does not show any low frequency signals with the ADInstruments device. Moreover, the signal-to-noise ratio is large enough for analysis. In summary, it is not necessary to apply any high pass filtering to the raw signal.

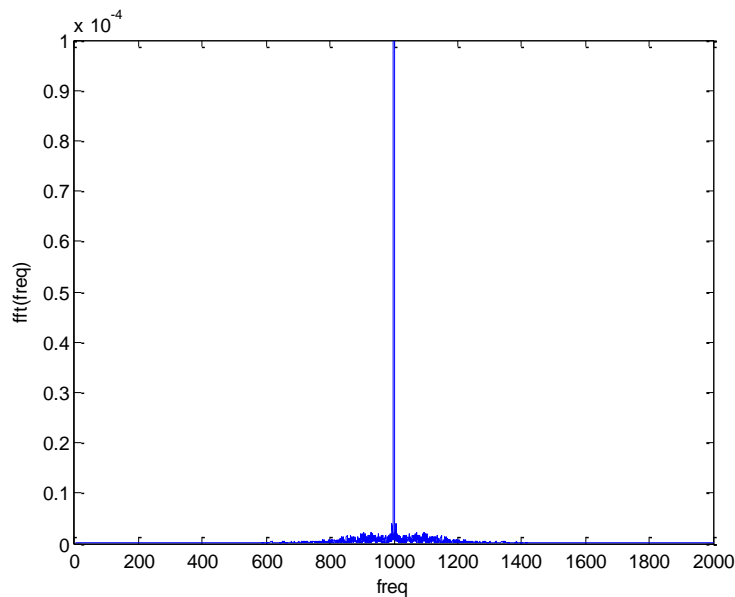


Figure 25: Frequency spectrum of the raw signal recorded from PD subject. The spectrum shows that the signal is already conditioned and filtered the low frequencies. The big spike around 1000 Hz is the small oscillation caused by the data acquisition device. It will be removed during signal smoothing.

The raw signal might contain DC offset which needs to be removed. The red line in Figure 26a marks the DC offset which is the mean value calculated from the first one second of the signal. Since there is no meaningful distinction between negative and positive values, the signal is full-way rectified after its DC offset is removed. Figure 26b shows the signal shape after rectification and the red line is the main signal shape. The EMG signal can have rapid changing local maximas and minimas which might lead to false results during analysis. Therefore, the envelope of the signal is extracted by applying a low-pass Butterworth filter with a cutoff frequency around 10-20 Hz. (Figure 26c) Even though the DC offset is removed, extracting the envelop introduces a slight offset during the fixation period. However, this info doesn't contribute or change of the features used in this study so it is left as is.

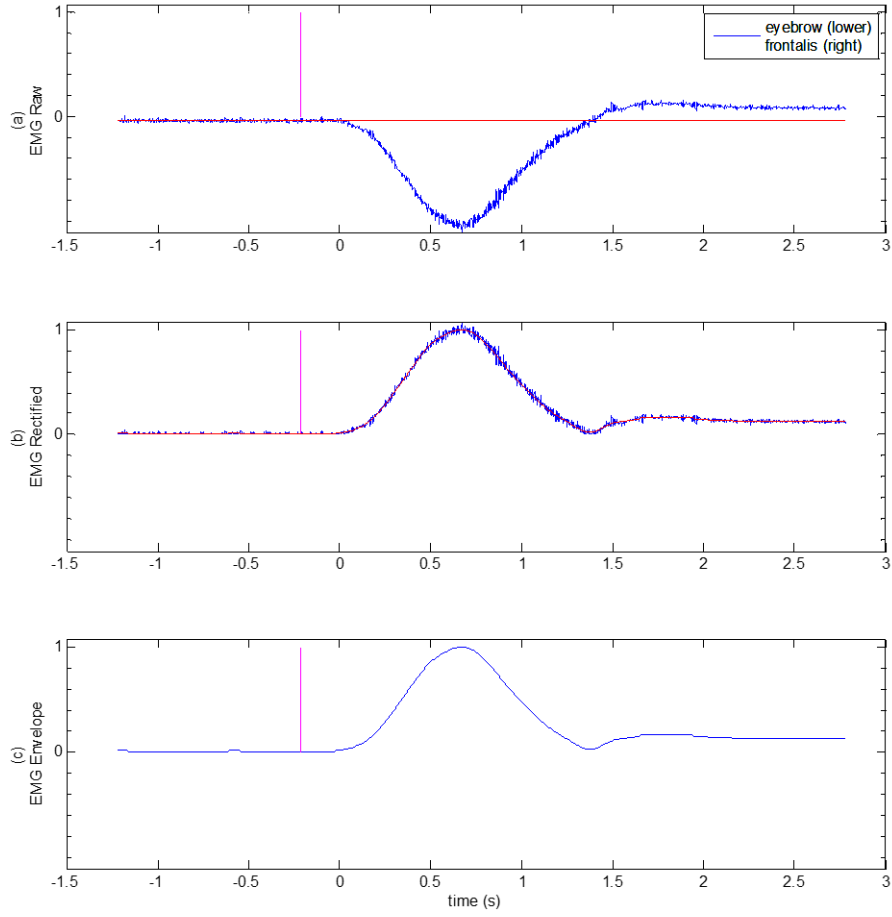


Figure 26: EMG data processing steps. First step (a) is to remove DC offset and signal rectification. (b) shows the signal after the first step. The bottom figure (c) show the signal filter by the low pass Butterworth filter. Red line in the first two figures is the shape in (c).

#### 4.1.1.2. Applying CUSUM

The primary measure decided is the latency of the first burst peak. Therefore, it is required to find the onset time of first agonist burst. CUSUM is the abbreviation of cumulative sum and mostly used in the control engineering for monitoring changes in the signal. (Tam, 2009) As seen in Equation 13 and Equation 14,  $C_i$  represents the cumulative sum of the deviation from the calculated mean ( $\mu$ ) of data ( $x$ ) in positive and negative directions respectively.  $k\sigma$  in these equations is the minimum change that can be detected. Finally, Equation 15 shows how the first two values are used in change detection. If there is  $h\sigma$  change in the signal, the change is detected.

$$C_i^+ = \max [0, x_i - (\mu + k\sigma) + C_{i-1}^+] \quad (13)$$

$$C_i^- = \min [0, x_i - (\mu - k\sigma) + C_{i-1}^-] \quad (14)$$

$$\text{Change Detected} = \begin{cases} C_i^+ > h\sigma & \text{true} \\ C_i^- < -h\sigma & \text{true} \\ \text{else} & \text{false} \end{cases} \quad (15)$$

Nevertheless, to be able to apply CUSUM to the preprocessed EMG signal,  $k$  and  $h$  parameters should be selected. For the signal gathered from Frontalis muscle, 5 and 10 are selected because of the high SNR ratio. However, 3 and 5 are used on the data acquired from Zygomatic Major muscle because of its lower SNR ratio. Figure 27 and Figure 28 shows the auto detected onsets in 3 different actions.

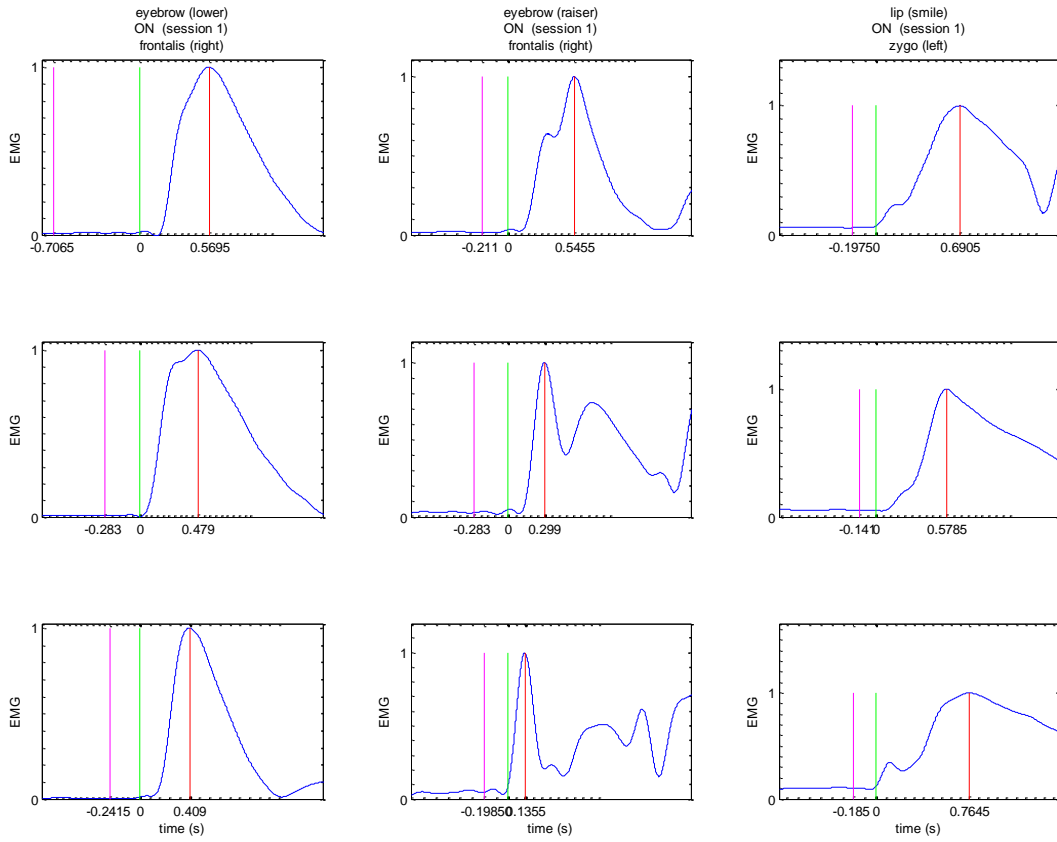


Figure 27: Onset detected by CUSUM for ON period. Purple, green, and red lines are trigger, onset, and maximum locations of the signal collected during pilot study

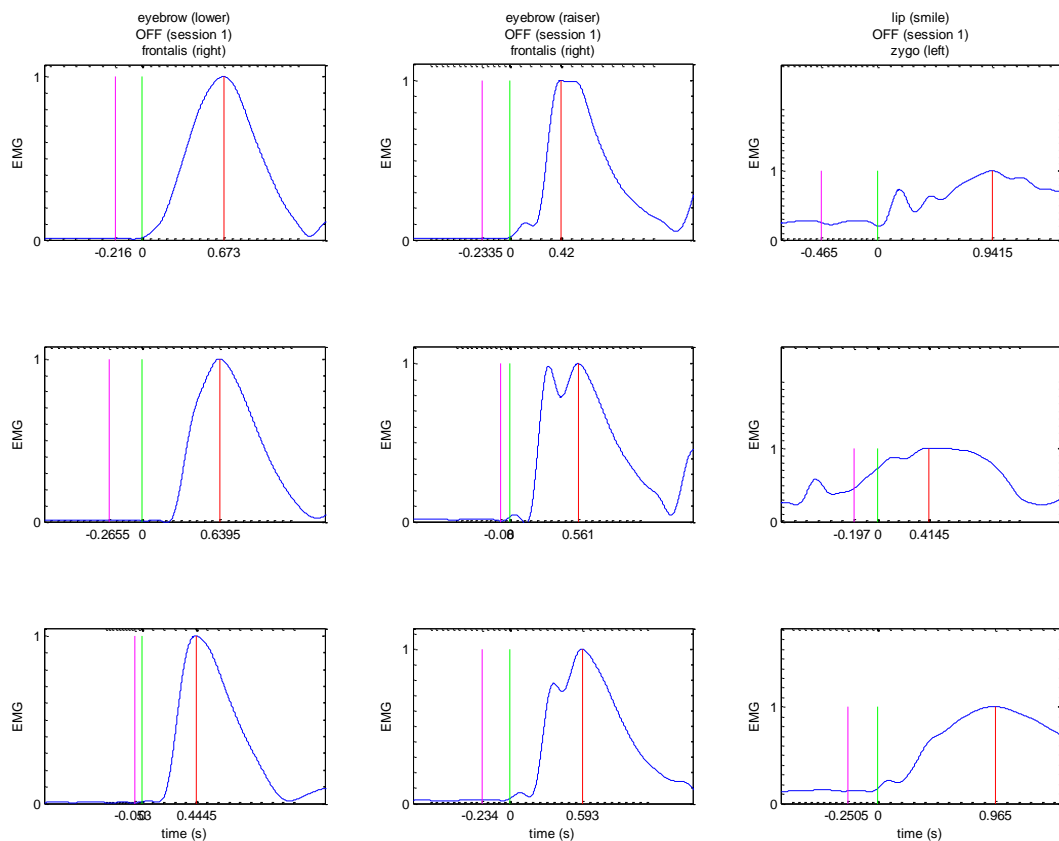


Figure 28: Onset detected by CUSUM for OFF period. Purple, green, and red lines are trigger, onset, and maximum locations of the signal collected during pilot study

Table 4: Whole process starting from preprocessing.

I.	Preprocess
a.	DC Offset Removal: Calculate mean from first second and subtract it from data
b.	Full-wave rectification: Take absolute value of the data
c.	Find Signal Envelope: Apply low pass filter like Butterworth
II.	Analysis
a.	Find Onset: Apply upper CUSUM
b.	Find Max Value in First Agonist Burst: Search for max value in on second after onset

- c. Calculate Latency
- d. Take Average of 2 sessions

#### 4.2. Experimental Procedure to Collect Repetitive Facial Expressions

To collect repetitive facial expressions, the procedure whose detailed steps are given in APPENDIX C was prepared. The procedure is applied to the pilot study at Koç University Hospital. The pilot subject had mild PD symptoms and came to hospital in 12-hour OFF state. The facial cards which can be seen in Figure 29 were shown to the subject during the training session. It was expected that the cards will improve the recognition of the verbal directives.



Figure 29: Facial cards for training session. Images were taken from Du, S. et. al.'s work (Du, Tao, & Martinez, 2014)

The subject was instructed to take medication after the recording session for OFF state completed. Since the medication takes at least 30 minutes to affect, after 45 minutes waiting and the recording session was repeated. Even though the patient has low UPDRS III score for OFF period, it was observed that the symptoms lessen after taking medication. The EMG recordings of the subject can be seen in Figure 27 and Figure 28.

The repetitive nature of the task and the procedure can be susceptible to the training effect. The subjects executing the same tasks repeatedly can start learning it and perform better even though the other factors are constant. Thus, the data become influenced by this phenomenon. The visual inspection of the data taken from first subject showed that the latency decreases almost in every session. This could be the result of training effect.

##### 4.2.1. Results of Pilot Subject

Before and after medication, the subject showed a small change in his UPDRS III score. Nevertheless, as seen Table 5 and Table 6, these changes are detectable in the calculated latency.

Table 5: Latency calculated from initial subject. Latency is the average of the time difference between onset and maximum in seconds of the repetitive tasks.

Facial Task	OFF		ON		
	right	left	right	left	
smile	0.5513	0.9533	0.5455	0.6778	seconds
eyebrow lower	0.5857	0.7410	0.4858	0.5917	seconds
eyebrow raiser	0.5247	0.4352	0.3267	0.4945	seconds

Table 6: UPDRS III scores of the initial subject

UPDRS III	OFF		ON	
	right	left	right	left
	13	12	5	5

#### 4.2.2. Training Effect and Improving CUSUM

The control group composed of 9 healthy subjects whose age is between 20 and 30 was assembled to investigate training effect in repetitive tasks defined in recording protocol. All the subjects were right-hand dominant and 6 of the subjects were female. The recording protocol was applied onto the control group as in initial PD subject.

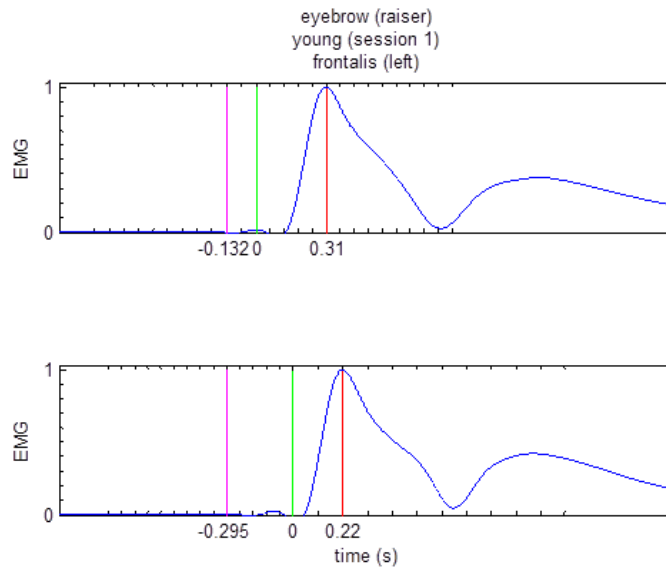


Figure 30: Two consecutive recording of eyebrow raiser in control subject. Purple, green, and red lines are trigger, onset, and maximum locations

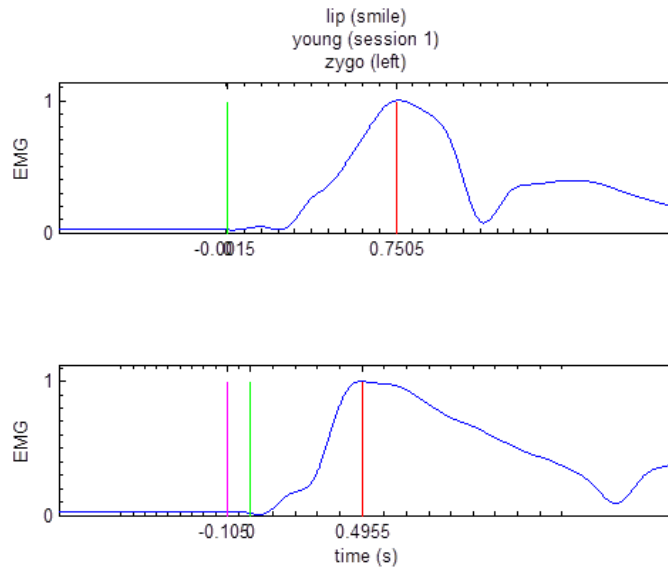


Figure 31: Two consecutive recording of smiling in control subject. Purple, green, and red lines are trigger, onset, and maximum locations

In control group case, the latencies calculated from two consecutive sessions (repetitions) were analyzed by looking the difference of those two. Unfortunately, one smile and one eyebrow raiser was discarded because of noisy EMG. As seen in Figure 30 and Figure 31, the two waveforms belonging to consecutive repetitions taken from one of the subjects are almost identical. However, when the waveforms and automatically extracted onset positions were inspected it is discovered that the CUSUM parameters need further tweaking. In other words, even though the waveforms are almost identical, the auto detected onset locations are not same.

At the end, instead of applying CUSUM directly to find the onset, a better algorithm was developed. Table 7 summarizes the algorithm which salvages the duration of the deviation in the signal to decide if it is an actual onset or not. In the first approach, the onset position was found only by applying upper CUSUM. The first point showing deviation was considered as the onset time. However, this approach showed problems because it did not count if the deviation from fixation is meaningful enough or not. As a result, the positive slopes of small hill like changes were considered as onset. However, the actual action starts later with a longer time span. Therefore, to solve this case, a better heuristic was accompanied. After finding a candidate deviation point by upper CUSUM, the algorithm checks if the deviation has time span longer than 1 second. If the time span is shorter, it continues to search for another candidate starting from the point where previous deviation ends.

Table 7: Improved onset detection with CUSUM

```

t <- 0
loop
  if UPPER_CUSUM(t)
    if deviation_span > 1.0 s
      onset <- candidate_onset
      return
    else
      t <- deviation_time
    end
  end
end
onset <- candidate_onset
return

```

The extracted onset locations shown in Figure 32 are more accurate and closer to each other in the repetitions of the same task. Table 8 also shows that the difference between repetitive tasks get numerically smaller after the improved CUSUM.

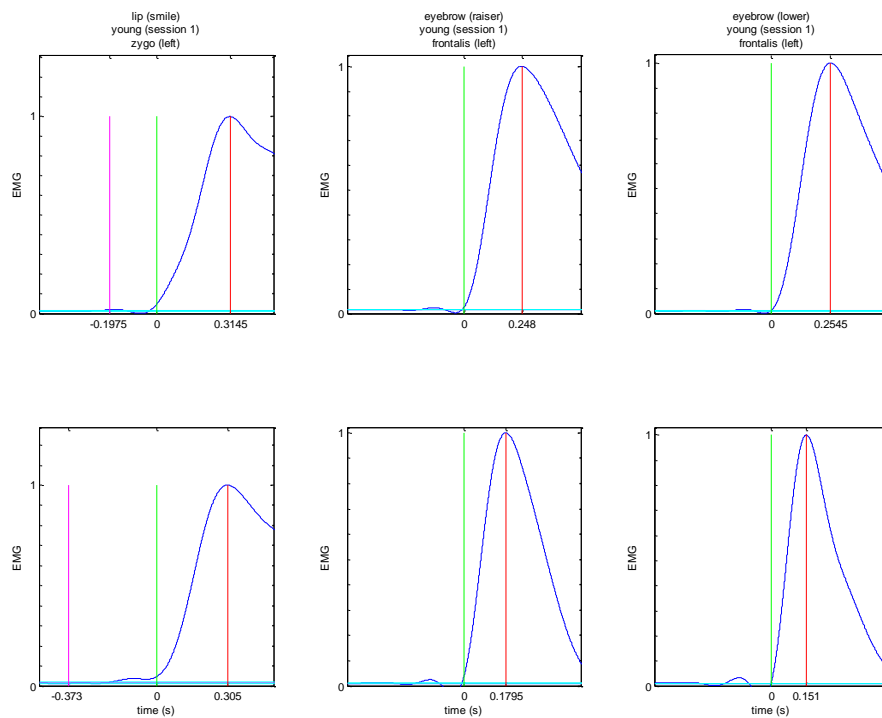


Figure 32: Results of the improved CUSUM. The new onsets locations are correctly detected

Table 8: The average time difference between latencies in control group for original and improved CUSUM

<b>Facial Task</b>	<b><math>\Delta t</math> seconds (original)</b>	<b><math>\Delta t</math> seconds (improved)</b>
smile	0.1161	0.0804
eyebrow lower	0.1443	0.0287
eyebrow raiser	0.0994	0.0662

### 4.2.3. Discussions

As seen in the results, EMG modality shows clean data signals to analyze facial expressions after the preprocessing phase. The numeric results showed that the latency calculated from EMG can be used as a quantitative metric. However, the data set collected also showed that how important the probe positioning is. If the probes are misplaced the SNR gets significantly lower. Hence, the experimenter/physician needs to monitor the signal in real-time to make sure that the data collected has high SNR.

CUSUM can detect the onset location easily, however, it is not enough to build a stable approach to automatize the processing methodology. The initial findings and the ones calculated after improved CUSUM show significant differences. After improved CUSUM was applied, the recalculated average time difference between latencies get lower and the visual inspection also confirmed that the improved approach is working. As seen in Table 8, the initially what was precepted as the training effect isn't the actual problem. In fact, the onset locations were incorrectly detected by the original CUSUM.

## 4.3. Experiment with PD Patients

This part of the thesis is composed of the recordings done by the custom setup prepared in the clinical environment of Koç University Hospital to synchronize EMG and video recordings. The same protocol applied to the pilot study was used with the PD patients.

### 4.3.1. Method

6 PD patients (Table 9) having mild to moderate symptoms (mean  $UPDRSIII_{OFF} \pm SD = 29.6 \pm 6.8$ ) from various age ranges (mean age  $\pm SD = 54.8 \pm 7.6$  years) were participated in the sessions. All the patients received psychological evaluation by psychologist and didn't have depression or dementia. This is important so that it was accepted that the patients can understand the visual and verbal commands given during the experiment.

Table 9: Demographics of the patients participated. Bradykinesia subgroup scores are the sum of the tasks 23, 24, 25, 26, 31 in UPDRSIII

Age	Handedness	OFF				ON			
		UPDRSIII		Bradykinesia		UPDRSIII		Bradykinesia	
		Left	Right	Left	Right	Left	Right	Left	Right
58	R	12	12	6	6	5	5	2	2
51	R	21	13	12	7	11	5	5	1
66	L	7	14	1	6	4	9	1	3
46	R	15	22	7	11	4	10	2	6
53	R	22	10	11	3	11	5	6	2

A recording protocol was prepared as seen in APPENDIX C so that the neurologist can complete all the recording sessions by herself while conducting neurological evaluation as well. Since the patient arrived in OFF state (no medication more than 12 hours), it is crucial that a physician keep observing them. In addition to that, it was necessary to take UPDRS evaluation before each recording session.

When the patients arrived to Koç University Hospital they were asked to sign a consent form before starting to the experiment. Each recording session consisted of 4 repetitions where the first one is for testing the recording setup and train the subject. In each repetition, the patients were asked to do 3 different facial expressions which are smile (lip puller), eyebrow raiser, and eyebrow lowerer. Even though the facial expressions were always given in same order, before the expressions, the patients kept the neutral face for small fixation period around 5 seconds until the visual cue via LED light attached to trigger device was shown. The group of 3 expressions was repeated 3 times at minimum. This session was done again for both OFF and ON state. In addition, before each session, the UPDRSIII scoring was completed by the physician. After OFF session, the patients were instructed to take their medication as usual and wait for at least 45 minutes before starting ON session.

The EMG preprocessing was done as in the previous section. After preprocessing, improved CUSUM was applied to find the onset position of the EMG signals. The results can be seen in the Figure 35-Figure 38

#### 4.3.2. Results

As seen in Figure 33, the data recorded for smile expression has all the features of fake smile. In other words, the upper-face related data do not have any changes in it. For example, the frontalis muscle does not express any action compared to zygomatic-major signal.

Similarly, the eyebrow-lowerer presents significant activity only in the upper part of the face. Figure 34 summarizes all EMG probes and entropy calculations. Nevertheless, the signal strength between zygomatic major (lower) and frontalis (upper) in EMG is visible when Figure 33 and Figure 34 are compared. It is expected

to see different SNR values because of the probe locations. To move the probe out of the video recording's ROI, they were pushed little bit side. Furthermore, there are multiple muscles located in the close proximity of the same location.

The signals recorded for both modalities show similar properties waveforms when they are grouped for channel/ROI and action. This shows that the measurement method is repeatable for the given movement task and recording device. Table 10 shows the extracted numbers from the signals. The onset which is automatically calculated by CUSUM is the time elapsed from the trigger point where the lag is the time elapsed until the signal reaches maximum point.

When the two states are statistically compared to each other, it is difficult to say that the features extracted are enough to detect subtle changes between ON/OFF states. Table 11 lists the p-values of the paired t-test for each feature between two states. Even the combination of the features by taking their difference to calculate the latency ( $dt = t_{lag} - t_{onset}$ ) didn't improve the confidence levels.

### **4.3.3. Discussions**

The signal patterns and acquired data from EMG is enough to analyze the motion tasks given. When the probe positioning is correctly done the SNR values are high enough to preprocess without losing valuable information. As expected, the signals from the upper and lower face expressed the characteristics of the facial expressions.

However, the sample size in this study isn't enough to reach a statistical conclusion. When visually observed, the automatically extracted features shows a difference. Unfortunately, the t-test results do not comply the observation.

Nonetheless, the method has a potential because it is easy to repeat, and an EMG device is available in almost all the clinical settings. Moreover, the data processing can be done automatically by the software. This means that the approach can reveal information missed by the physicians immediately after the data acquisition.

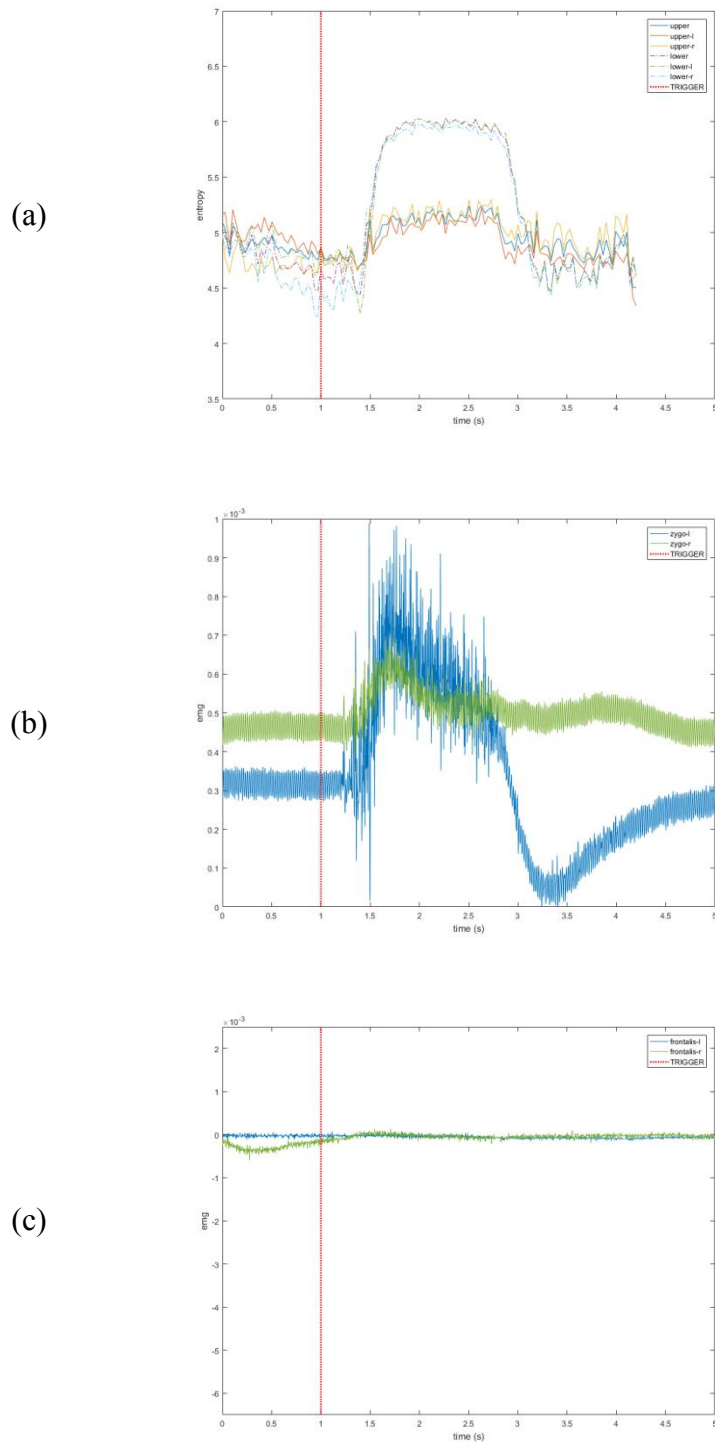


Figure 33: The data recorded for smiling expression. As expected upper regions do not show change while lower regions (lips) show big changes in the signal. (a) top image is the entropy change of the image recordings for the multiple ROIs, (b) zygomatic-major EMG signal, (c) frontalis EMG signal. Red vertical line marks the trigger point

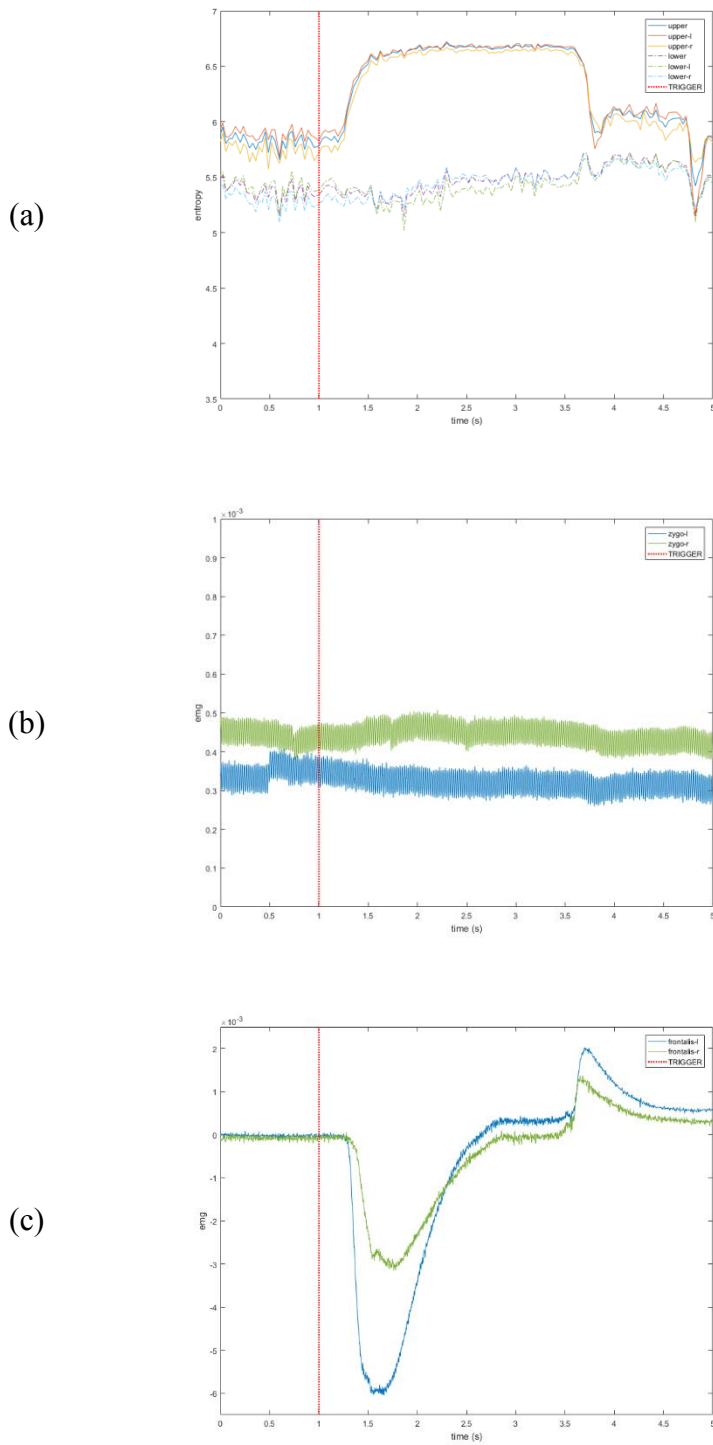


Figure 34: The data recorded for eyebrow-lowerer expression. As expected lower regions do not show change while upper regions (eyebrows) have visible signals. (a) top image is the entropy change of the image recordings for the multiple ROIs, (b) zygomatic-major EMG signal, (c) frontalis EMG signal. Red vertical line marks the trigger point

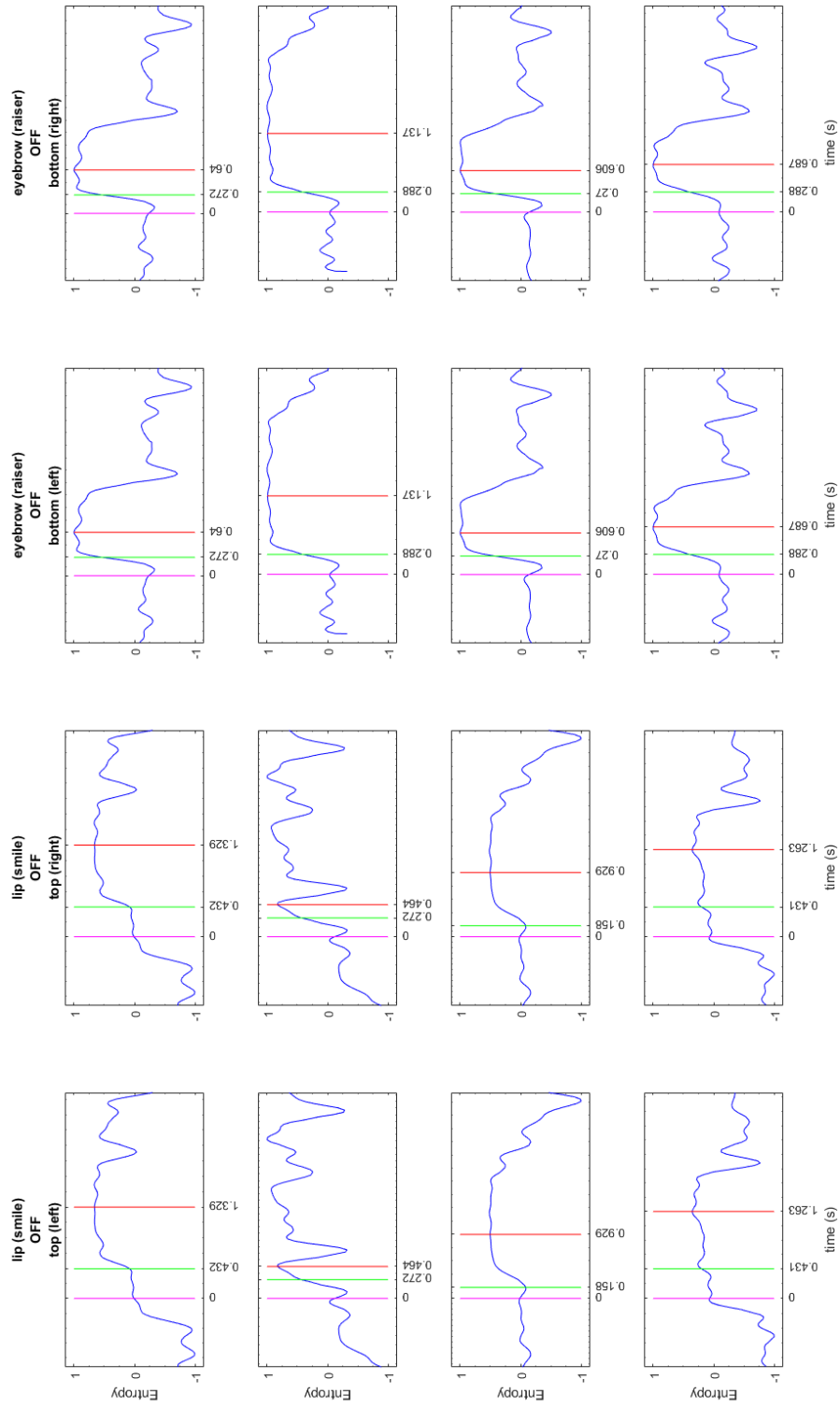


Figure 35: Processed video recordings for one patient in OFF state where the rows are the first, second, third, and fourth repetitions of either smiling or eyebrow raiser tasks and the columns are the respective channels. First marker at 0 seconds is the trigger point where the LED is turned on. Following marker is the auto calculated onset location whereas the final marker is the local maximum where the entropy reaches maximum.

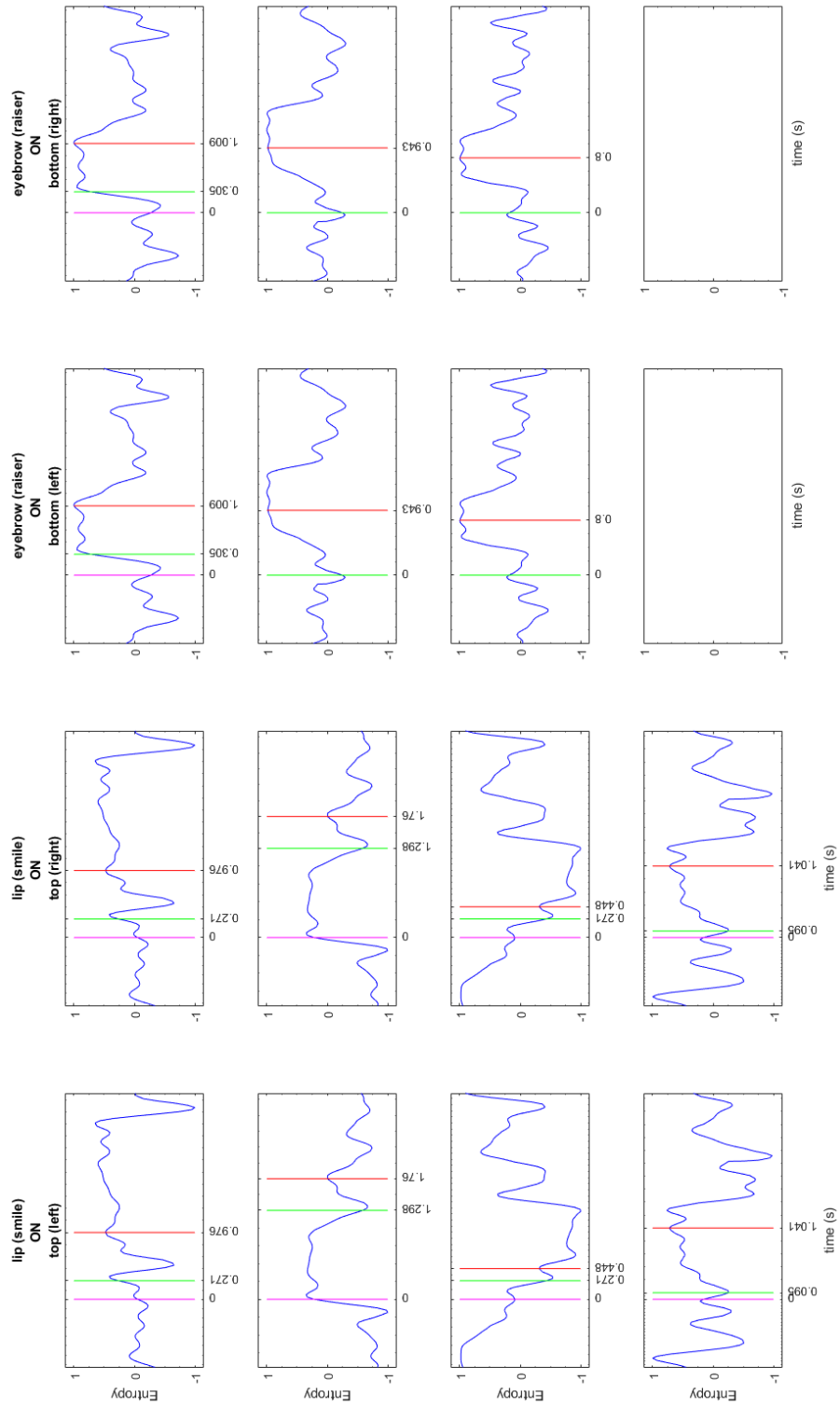


Figure 36: Processed video recordings for a patient in ON state where the rows are the first, second, third, and fourth repetitions of either smiling or eyebrow raiser tasks and the columns are the respective channels. First marker at 0 seconds is the trigger point where the LED is turned on. Following marker is the auto calculated onset location whereas the final marker is the local maximum where the entropy reaches maximum.

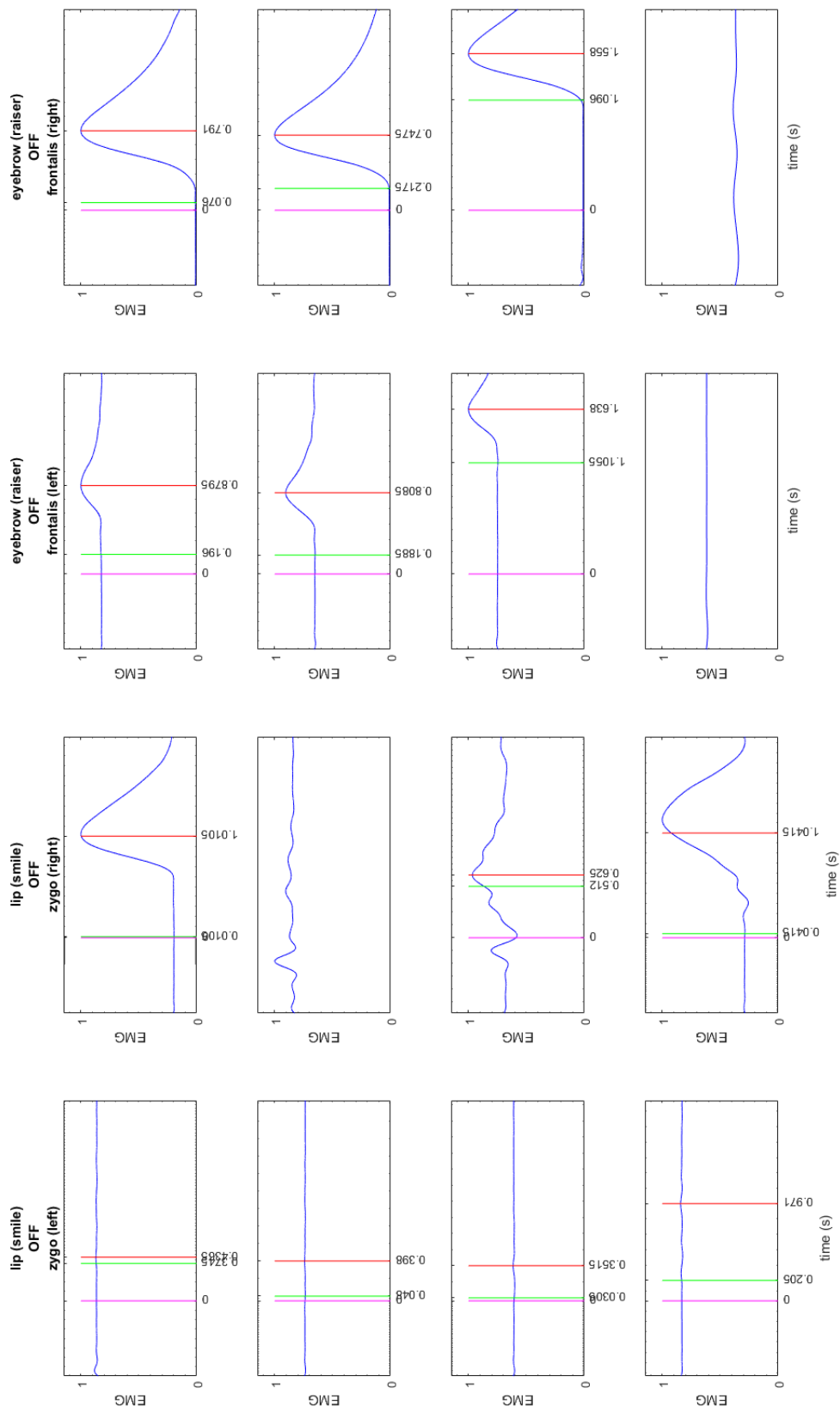


Figure 37: Processed EMG recordings for a patient in OFF state. First marker at 0 seconds is the trigger point where the LED is turned on. Following marker is the auto calculated onset location whereas the final marker is the local maximum where the entropy reaches maximum.

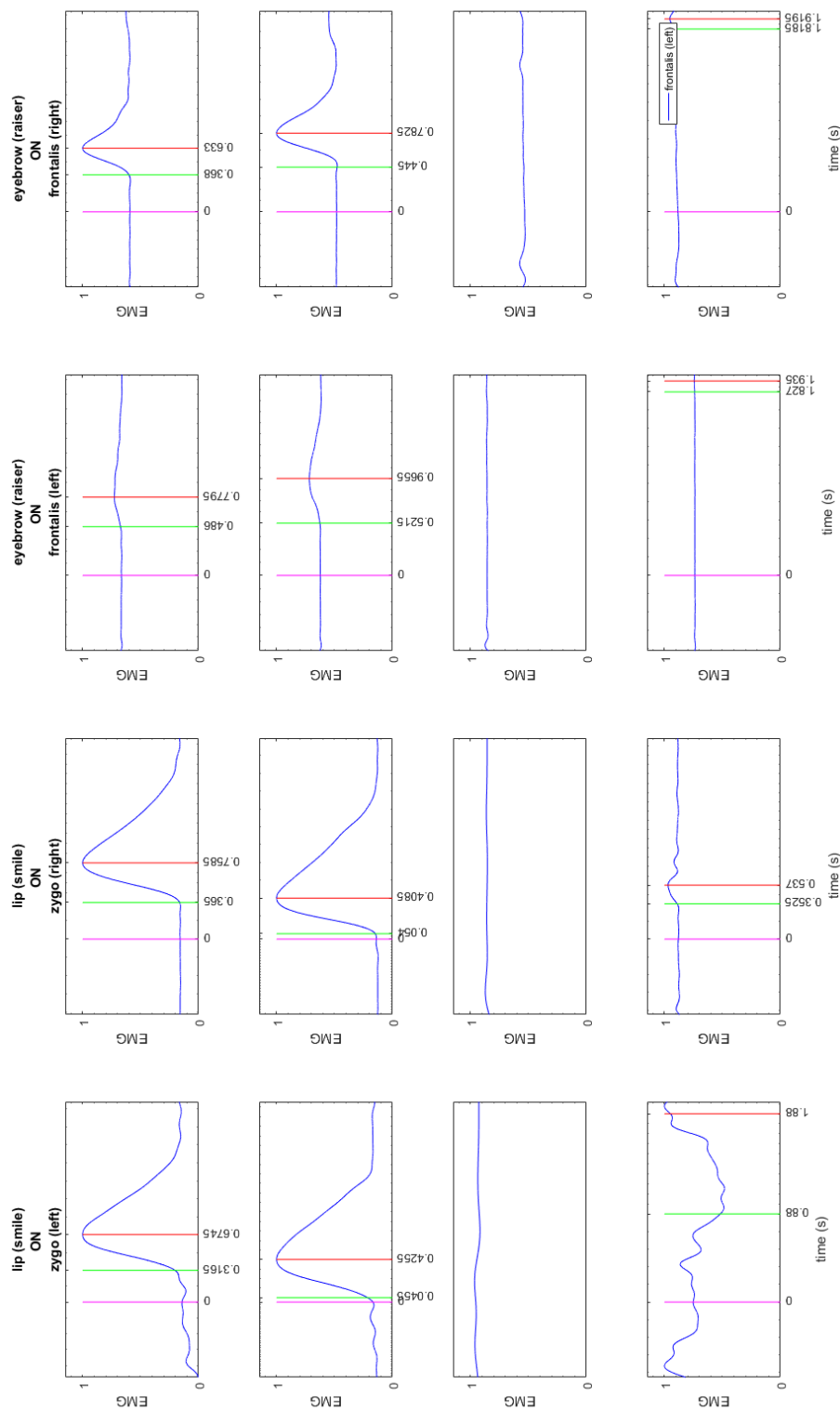


Figure 38: Processed EMG recordings for a patient in ON state where the rows are the first, second, third, and fourth repetitions of either smiling or eyebrow raiser tasks and the columns are the respective channels. First marker at 0 seconds is the trigger point where the LED is turned on. Following marker is the auto calculated onset location whereas the final marker is the local maximum where the entropy reaches maximum.





## CHAPTER 5

### FEATURE EXTRACTION AND STATISTICAL ANALYSIS OF FACIAL EXPRESSIONS COLLECTED BY VIDEO CAMERA

#### 5.1. Software Development for Facial Image Collection and Analysis

##### 5.1.1. Data Collection

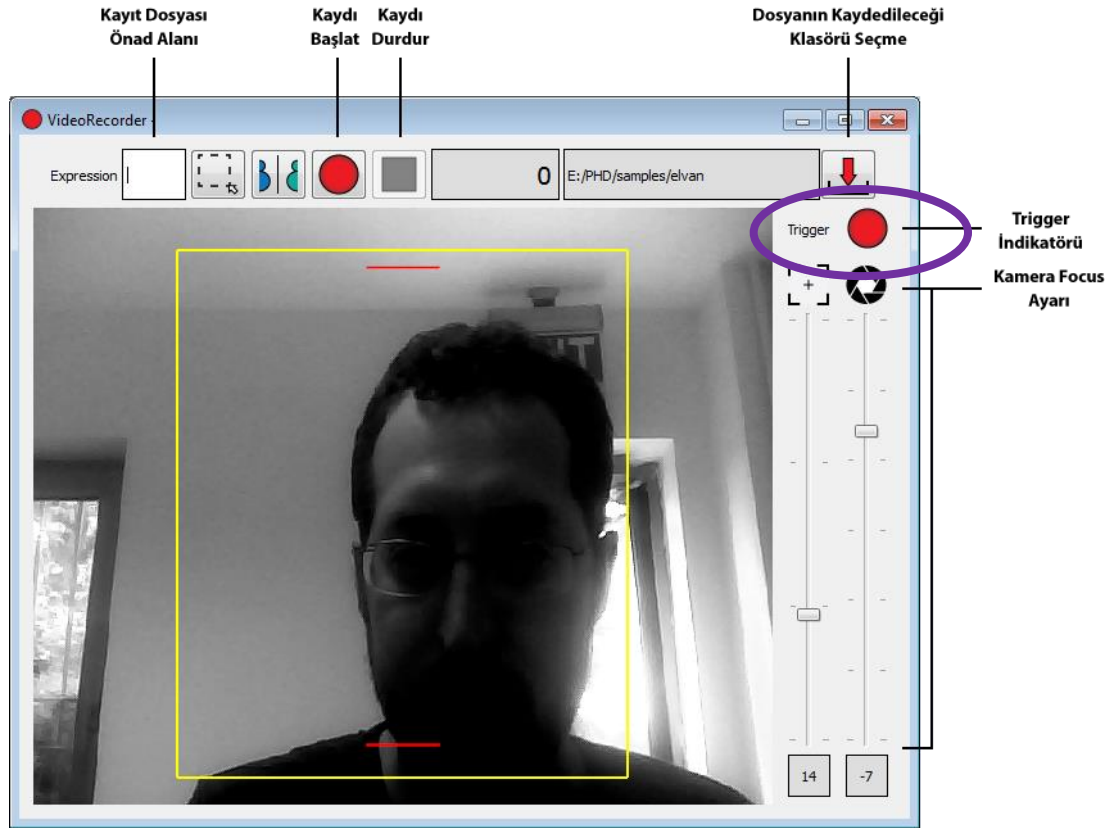


Figure 39: The UI of the software developed for video recording. Like the LED light, an icon to debug if the trigger is received or not is added (marked in purple)

During the multi modal data collection, the video needs to be recorded in sync with the EMG signal without losing the quality of the images. Thus, the available simple video recording applications aren't enough to capture both video data and the trigger signals. The software in Figure 39 was developed to solve this problem. The

application was written in C/C++ and based on the open-source technologies like OpenCV, Eigen, and Qt. Software records the video data which is in RGB format by converting it into Grayscale (Equation 16) (Recommendation ITU-R BT.601-7, 2011) in order to decrease the file size.

$$Y = 0.299 \cdot R + 0.587 \cdot G + 0.114 \cdot B \quad (16)$$

The software is composed of two executables. The first one is to capture the series of images and trigger signal sent from the USB camera and trigger device as fast as possible without losing the quality. The second one is the one processing the recordings automatically extracting ROIs and their entropies for further calculations. Figure 40 shows automatically extracted the lower face ROIs from the frames of the video.

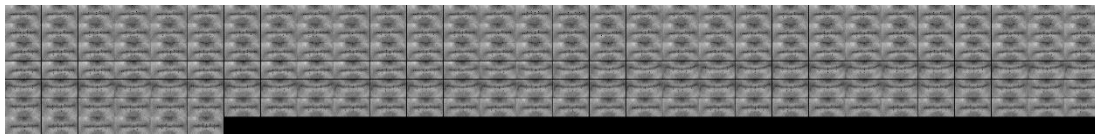


Figure 40: Lower face ROI aligned and extracted for the video stream. Each image belongs to one frame. The first box is the frame 0 and the frames go from 0 to n in left to right direction. The first frame in the new line is the next from the end of the previous line.

### 5.1.2. Data Analysis



Figure 41: The preprocessing steps are face and landmark detection, eyeline detection, registration, and ROI extraction

The facial expression frames need processing procedure as in EMG. The processing step is done by the second part of custom software developed. The second part composes of various steps as shown in Figure 41.

Bowers et al.'s work states various emotional states such as happy, disgust, and angry can be discriminated from the video recordings of the facial expression. (Bowers, Miller, Bosch, & Gökçay, 2006) In the same study, they claim that Equation 17 which is the entropy of the intensity change of the pixels is a good measure to capture the expression. It is expected to see a change only in the lower region of the face when involuntary smile is considered. (Ekman & Friesen, 1982)

Therefore, the lower region of interest is usually extracted from the images before applying the analysis.

$$E = -\sum_{p \in ROI} (p_t - p_{t-1}) \log_2(p_t - p_{t-1}) \quad (17)$$

As seen in Figure 42, the entropy is indeed a good measure; namely, the transition from neutral to the expression can easily be captured. This proves that the facial video recording is the suitable as a second modality next to EMG. Why the ROI selection is important can also be seen in the same figure. Only significant change happens inside the ROI which agrees with the lower face statement. The DC offset observed in both signal is caused by the natural noise coming from the sensory device. In other words, the intensity of a pixel does not stay same even for a still image. Therefore, the intensity of the expression should be calculated by subtracting the average of the signal observed in the neutral state.

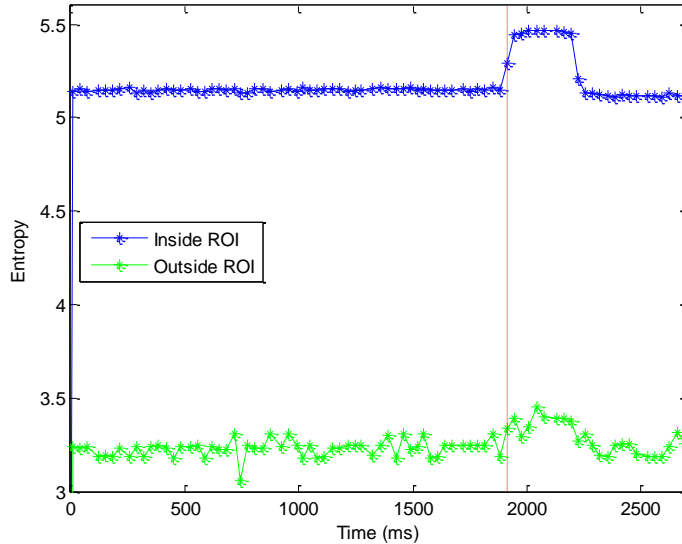


Figure 42: Entropy change comparison inside and outside the ROI for smiling

When dealing with a one patient and a short video recording, it is easy to do the ROI selection and data processing. It is even possible to do it manually. For this study, an automatic method was necessary, therefore, during a joint research, the data processing method and the software for facial video recordings was created and refined.

### 5.1.3. Still Pictures Experiment

#### 5.1.3.1. Method

As a part of the joint study with Assoc. Prof. Atilla YILMAZ from Mustafa Kemal University, Hatay, Turkey, 25 PD patients under STN DBS were recorded while they are on stimulation and medication. They were asked to pose neutral and three different emotional expressions which are happy, sad and angry. When they are

holding the expression a still picture was taken by Canon 350 D camera. This process was repeated for 5 different DBS frequencies (while 5<sup>th</sup> is the DBS OFF) to find which one is more effective to ease the symptoms. When the frequency changed before commencing to the photo shoots, 15 minutes of gap was forced to let the patient reach steady-state.

To make the data processing autonomous, a face recognition algorithm was applied to each image. The algorithm provided the important landmarks such as bottom of nose, outer labia, inner eye, and outer eye locations. (Figure 43)



Figure 43: All the landmarks (in green) automatically found

Because of the tremor, it was necessary to align the images of different expressions. Therefore, the neutral image was used as the base and all the other images are aligned to it. The alignment process given in Table 12 was basically applies an affine transform to the images. After the transformation (Figure 44), all the images have equal inner eye distance and orientation. Thus, the ROIs selected from neutral image should map to the same regions in all the images.

Table 12: Image alignment procedure

```

lm_base <- landmarks of neutral image
l_base <- lm_base[leftInnerEye]
r_base <- lm_base[rightInnerEye]

for each img in images
    lm_base <- landmarks of neutral image

    l <- lm[leftInnerEye]
    r <- lm[rightInnerEye]
    dx <- l - l_base
    sx <- (r_base - l_base) / (r - l)

    img <- translate(img, dx)
    img <- rotate(img, sx)
end

```



Figure 44: The image after alignment is applied where left is the original and right is the transformed image

When the images are aligned and registered to each other the selection of ROI becomes a trivial task. The regions selected in neutral image can be easily used in the images of the expressions. Since the expressions used in the study consists of actions involving both upper and lower face, lower face, left upper face, and right upper face visible in Figure 45 were defined as the ROIs.

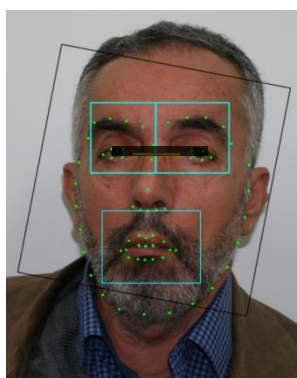


Figure 45: Three ROIs selected for analysis

To make the ROI selection automatic, the landmarks and certain multipliers were used. For example, left and right edges of the lower face region were taken as the middle of the outer jaw and labia. The height was calculated as the two times of the distance between labia and bottom of the nose. On the other hand, the upper face region needed a special attention because of the expected eyebrow movement. In details, the top edge was found by adding %6.25 of the facial bounding box height (shown black in Figure 46) to the eyebrow landmark which is located at the top.

After the alignment, and ROI extraction the entropies of the intensity difference in expression images with respect to the neutral image were calculated. As seen in Figure 46, the aligned images gave proper ROIs that do not suffer from tremor or camera movement side effects.

The main purpose of this study was to select the best DBS frequency which eases the symptoms, namely, bradykinesia and rigidity on facial expressions. Accordingly, one

way ANOVA was applied to the entropies to find which frequency show significantly expression, in other words, movement in it.



Figure 46: Four ROIs which are upper face, left upper face, right upper face, and bottom face are selected for the analysis

#### 5.1.3.2. Results

As a part of the analysis, it was initially investigated if the left and right sides of the face have significant difference among them. However, any significant difference couldn't be found, consequently, the further analysis were conducted as upper and lower regions.

**Statistical Analysis:** To measure the influence of stimulation frequency and facial expressions on facial expressivity (i.e., the entropy value), a 5x3 repeated measures ANOVA was carried-out using the Data Analysis Toolkit of Excel with 'Two-factor with replication' setting. The two independent factors were adjusted to 5 levels of stimulation frequency (no stimulation, f1, f2, f3, f4), and 3 levels of facial expressions (Happy: 1, Sad: 2, Angry: 3).

The results indicated that at the 0.05 significance level, for the upper face ROI, the main effect of stimulation frequency was significant with  $p = 0.005$  and the main effect of facial expression was significant ( $p = 0.00002$ ). For the lower face, similar results are obtained: the main effect of stimulation frequency was significant with  $p = 0.003$  and the main effect of facial expression was significant ( $p = 0.003$ ). The interaction between stimulation frequency and facial expressions was not significant. An illustration of the effects of DBS frequencies is provided in the figure below.

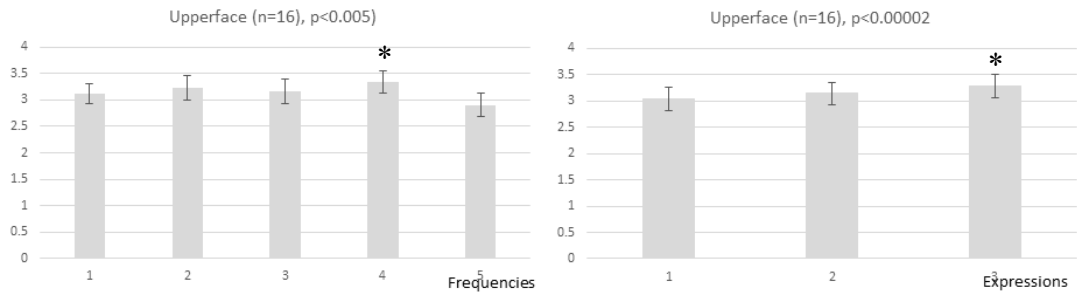


Figure 47: ANOVA results for upper-face ROI where \* marks the significant frequency and expression

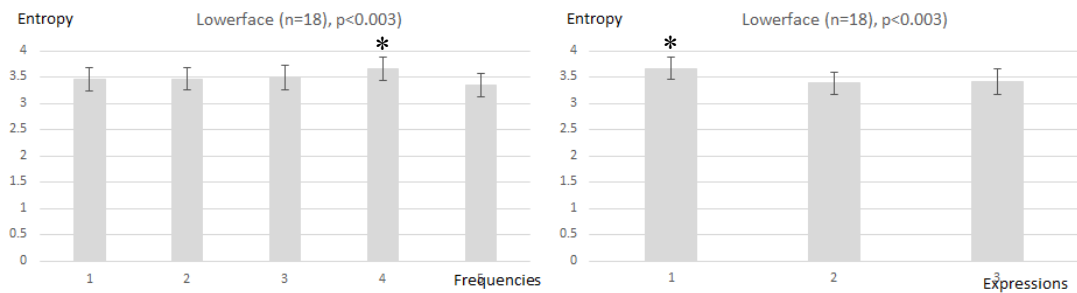


Figure 48: ANOVA results for lower-face ROI where \* marks the significant frequency and expression

As seen in Figure 47 and Figure 48, 4<sup>th</sup> frequency (the value of the frequency was kept hidden on purpose because of the on-going study) was found as the most significant one. However, because of the nature of the approach, it was necessary to validate the results. Thus, another significance analysis based on surveys was also completed in Hatay. In conclusion, both results were same and this states that entropy approach is validated. Furthermore, the autonomous approach was worked as intended and can be used in next steps of the study.

#### 5.1.4. Video Recording Experiment

##### 5.1.4.1. Method

The recording protocol is explained in the EMG chapter and the video images are recorded simultaneously for both modalities. The video recordings are collected in sync with EMG by the custom setup used in previous chapter.

The autonomous image processing technique was extended for video recordings, namely, for series of frames. In practice, the first frame is accepted as the neutral image and any images following that are aligned and registered to that the first frame. The resulting image stream can be seen in Figure 40 where each extracted region is appended next to each other. Afterwards, the entropy of the intensity difference was calculated for each frame by using this stream.

The similar preprocessing used for EMG and the improved CUSUM is applied to entropy signals generated from the video frames to find the onset positions. The results can be seen on the Figure 35-Figure 38 with the EMG signals together.

#### *5.1.4.2. Results*

Video analysis of the smile-expression shows similar features like the EMG recording. As seen in Figure 33 (a), the clear change in entropy visible for upper regions.

The entropy of eyebrow-lowerer seen in Figure 34 (a) has significant activity in the upper part of the face compared to the lower part. Table 13 lists the onset points which are automatically calculated by CUSUM. The lag feature is the time elapsed until the signal reaches maximum point like in the EMG signals.

#### *5.1.5. Discussions*

As expected, the video frame modality contains almost same patterns as in the EMG modality. It can be claimed that both modalities can be used interchangeably to predict bradykinesia and to detect subtle changes in the symptoms.

However, the frame rate is far inferior to the EMG signal. It is possible to double the frame rate to 60 Hz by using commercially available cameras or mobile phones. If the data will be collected simultaneously the computer needs to be powerful to not miss any frame during the recording session.

Table 13: Features extracted from Video Frames for ON/OFF states. All the numbers are in seconds

OFF												ON											
Smile (Lower)						Eyebrow Raiser (Upper)						Smile (Lower)						Eyebrow Raiser (Upper)					
Left			Right			Left			Right			Left			Right			Left			Right		
Onset	Lag		Onset	Lag		Onset	Lag		Onset	Lag		Onset	Lag		Onset	Lag		Onset	Lag		Onset	Lag	
0.289	0.816		0.274	1.202		0.280	1.216		0.391	1.016		0.390	1.099		0.274	1.233		0.288	1.050		0.309	1.227	
0.287	1.136		0.400	1.109		0.367	1.119		0.335	1.174		0.416	1.242		0.389	1.179		0.282	0.992		0.335	1.179	
0.417	1.244		0.336	1.407		0.432	1.426					0.408	1.353		0.328	1.168		0.352	1.296		0.328	1.201	
0.258	0.976		0.478	1.230		0.320	1.200		0.421	1.077		0.270	0.948		0.351	1.225		0.288	1.033		0.389	1.056	
0.325	1.045		0.368	1.232					0.394	1.257		0.280	1.160		0.315	1.190		0.316	1.031		0.385	1.114	



## CHAPTER 6

### DISCUSSION AND FUTURE WORK

While UPDRSIII motor scaling is an observational method that is commonly used by neurologists to assess motor functions of the PD patients, the observational aspect of the UPDRS includes lack of objectivity and it is limited by human perception. Hence numerous motion capture systems have been proposed for the objective assessment of the motor function of the PD patients. To overcome the objectivity and improve the quality, the UPDRS data can be assessed by 2 different neurologists (instead of only one neurologist's UPDRS scoring as a regular clinical approach) and obtained the UPDRS data bilaterally (instead of regular unilateral-dominant symptom side-UPDRS approach). In the sub-studies covered in this work, this method is adapted while developing the statistical methods. Unfortunately, even though UPDRS is one of the clinical standards the problem of being a discreet scale still hinders the PD studies. Any device or methodology which obtains its data in a continuous manner such as EMG or video signals needs to extract heuristic features from the data.

This problem reveals two main problems, the sample size, and data quality. To be able to devise meaningful values for a heuristic feature, the sample size must be big and the data variance, in other words, the quality must be good. As seen in the experiment described in CHAPTER 5.1.3, the high quality and high resolution still images resulted in stable values. However, the still images are not enough to capture all the aspects of the motion because of the sampling rate. However, the EMG recordings on PD patients in CHAPTER 4.3 is affected by the small sample size. In addition, even when the patterns of one patient is examined, it is easy to see that the waveforms are changing significantly. Compared to the other modalities and devices, the leap motion overcame the sample size issue. The easy to setup device is also compact thus the recording sessions can be conducted anywhere rapidly.

Nevertheless, it is also visible on the same signals that if the task given to the patient is conducted properly the methods generate similar waveforms. In other words, the researcher conducting the recording session should keep an eye on the outputs and don't rush the sessions. Even one of the recordings becomes invalid because of displaced probe or setup issues it means that the data set shrinks further.

Unfortunately, increasing the sample size isn't easy for PD studies. During the recording sessions, it is observed that when the patients are in OFF state (off

medication for the last 12 hours) their symptoms worsen significantly, and they cannot even travel to the hospital by public transportation. This can also be seen by the scores in demographics (Table 9) where the difference between ON and OFF states is large.

These are the reasons why this study is important. In other words, finding a method which is easy to repeat can solve the repeatability and reliability issues. If the data acquisition step can be completed at home alone by a patient, the sample size can be increased freely and the disease severity can be tracked by the long-term works.

The video capturing used in this study revealed that camera is an easy modality to use. However, the problem is the data resolution. When the recording session started for this study, hi-resolution video cameras wasn't common. However, in past 3 years, the video cameras embed in our mobile devices are already surpassed the professional cameras used for photography. In CHAPTER 5.1.4, the low-resolution camera generated satisfactory and repeatable outputs if the recording environment is carefully controlled. As seen in the recent studies (Liua, et al., 2023; Lua, et al., 2021), the video sequences can be used to predict UPDRS scores. Even though the studies are focused on the tremor and GP, they contain various preprocessing steps with CNN. Both studies required heavy CUDA enabled computers. In comparison, the entropy extraction approach in this study is much simpler and easier to implement on a portable device, because the entropy approach was completed on a regular laptop. In summary, it can be claimed that the facial recording and the entropy feature generated in this thesis is confirmed by the studies of Liua, et. al (Liua, et al., 2023) and Lua, et. al. (Lua, et al., 2021).

Even though EMG isn't common and available for home use, it is common for the clinical environments. In the recent years, the wearable sensors have been evolving and have improved considerably. The smart watches are started to collect many physiological signals. For example, Isaacsona, et al. used wearable device called Kinesia to monitor patients at their home to assess various motor symptoms. (Isaacsona, et al., 2019) Their results show that the small wearable devices can support the decision making during the long-term treatment. Moreover, portable wireless EMG systems such as the one available in Biometrics Ltd. can be used outside the clinical settings are being sold. During this study, all the EMG recordings showed good quality data if the probes are properly placed. Even the SNR is enough if the probes are off location but not loose. Therefore, this second modality is also acceptable to build a quantitative measure.

Nevertheless, the statistical analysis on the EMG recordings was highly affected by the sample size and the results seen in previous substudies cannot be clearly observed. Although CUSUM approach to find onset location and data preprocessing steps worked the dirty data skewed the extracted features. Research focusing solely on the data gathering from a larger sample size should be done to improve the results.

The most important outcomes of this study are the improvement of the CUSUM and the development of the hardware and software interfaces to collect multiple modalities in an autonomous way. The emerging technologies such as NeuroRPM (NeuroRPM, 2023) show that the mobile applications can be used for long-term continuous monitoring. The hardware and software developed in this study is based on the underlying mobile technologies such as ARM based processor and the multi-platform software kit OpenCV. In other words, it is possible to adapt the software to a mobile device as a future work to increase the sample size.

In terms of future work, it was aimed to develop a measure which is non-linear and repeatable to improve the objectivity of the traditional UPDRS part III scoring system to assess bradykinesia. However, the results of this study should also be validated with data that will be obtained by other modalities.



## REFERENCES

- Çakmak, Y. Ö., Ölçek, S. C., Özsoy, B., & Gökçay, D. (2018). Quantitative Measurement of Bradykinesia in Parkinson's Disease using Commercially Available Leap Motion. *11th International Conference on Bio-inspired Systems and Signal Processing*, 3, pp. 227-232. BIOSIGNALS.
- Çakmak, Y. O., Apaydın, H., Kızıltan, G., Gündüz, A., Özsoy, B., Ölçer, S., . . . Ertan, F. (2017). Rapid Alleviation of Parkinson's Disease Symptoms via Electrostimulation of Intrinsic Auricular Muscle Zones. *Frontiers in Human Neuroscience*, 11.
- Association, E. P. (n.d.). *Unified Parkinson's Disease Rating Scale (UPDRS)*.
- Blandini, F., Nappi, G., Tassorelli, C., & Martignoni, E. (2000). Functional changes of the basal ganglia circuitry in Parkinson's disease. *Progress in Neurobiology*, 62(1), 63-88.
- Bologna, M., Fabbrini, G., Marsili, L., Defazio, G., Thompson, P. D., & Berardelli, A. (2013). Facial bradykinesia. *Journal of Neurology, Neurosurgery & Psychiatry*, 84, 681-685.
- Bowers, D., Miller, K., Bosch, W., & Gökçay, D. (2006). Faces of emotion in Parkinson's disease: Micro-expressivity and bradykinesia during voluntary facial expressions. *Journal of the International Neuropsychological Society*, 12, 765-773.
- Calne, D., Snow, B., & Lee, C. (1992). Criteria for diagnosing Parkinson's disease. *Annals of Neurology*, 32(S1), S125-S127.
- Cheron, G., Cebolla, A. M., Bengoetxea, A., Leurs, F., & Danc, B. (2007). Recognition of the physiological actions of the triphasic EMG pattern by a

- dynamic recurrent neural network. *Neuroscience Letters*, 414(2007), 192–196.
- Curtin, F., & Schulz, P. (1998). Multiple Correlations and Bonferroni's Correction. *Society of Biological Psychiatry*, 44, 775–777.
- Daneault, J., Carignan, B., Sadikot, A., & Duval, C. (2013). Are quantitative and clinical measures of bradykinesia related in advanced Parkinson's disease? *Journal of Neuroscience Methods*, 219(2), 220-223.
- de Souza, L., Dionísio, V., & Almeida, G. (2011). Multi-joint movements with reversal in Parkinson's disease: Kinematics and electromyography. *Journal of Electromyography and Kinesiology*, 21(2), 376-383.
- Dietz, V., & Sinkjaer, T. (2012). Spasticity. *Handb Clin Neurol.*, 109, 197-211.
- Du, S., Tao, Y., & Martinez, A. M. (2014). Compound facial expressions of emotion. *Proceedings of the National Academy of Sciences*, 111(15), E1454-62.
- Dunnewold, R., Jacobi, C., & van Hilten, J. (1997). Quantitative assessment of bradykinesia in patients with parkinson's disease. *Journal of Neuroscience Methods*, 74(1), 107-112.
- Ekman, P., & Friesen, W. V. (1982). Felt, false, and miserable smiles. *Journal of Nonverbal Behavior*, 6, 238-252.
- Ertekin, C., Tarlacı, S., Aydoğdu, İ., Kiylioglu, N., Yüceyar, N., Turman, B. A., . . . Esmeli, F. (2002). Electrophysiological evaluation of pharyngeal phase of swallowing in patients with Parkinson's disease. *Movement Disorders*, 17(5), 942-949.
- Fahn, S., Marsden, C., Goldstein, M., & Calne, D. (1987). Recent developments in Parkinson's disease. *Annals of Neurology*, 22(5), 153–163.
- Fedirchuk, B., Nielsen, J., Petersen, N., & Hultborn, H. (1998). Pharmacologically evoked fictive motor patterns in the acutely spinalized marmoset monkey (*Callithrix jacchus*). *Experimental Brain Research*, 122(3), 351–361.
- Garza-Rodríguez, A., Sánchez-Fernández, L. P., Sánchez-Pérez, L. A., Ornelas-Vences, C., & Ehrenberg-Inzunza, M. (2018). Pronation and supination analysis based on biomechanical signals from Parkinson's disease patients. *Artif. Intell. Med.*, 84, 7–22.
- Ghassemi, M., Lemieux, S., Jog, M., Edwards, R., & Duval, C. (2006). Bradykinesia in patients with Parkinson's disease having levodopa-induced dyskinesias. *Brain Research Bulletin*, 69(5), 512-518.

- Goetz, C. G., Poewe, W., Rascol, O., Sampaio, C., Stebbins, G. T., Counsell, C., . . . Seidl, L. (2004). Movement Disorder Society Task Force report on the Hoehn and Yahr staging scale: Status and recommendations. *Movement Disorders, 19*(9), 1020-1028.
- Hannaford, B., Cheron, G., & Stark, L. (1985). Effects of Applied Vibration on Triphasic Electromyographic Patterns in Neurologically Ballistic Head Movements. *Experimental Neurology, 88*(2), 447-60.
- Hoehn, M. M., & Yahr, M. D. (1967). Parkinsonism: onset, progression, and mortality. *Neurology, 17*(5), 427.
- Irlbacher, K., Voss, M., Meyer, B., & Rothwell, J. C. (2006). Influence of ipsilateral transcranial magnetic stimulation on the triphasic EMG pattern accompanying fast ballistic movements in humans. *The Journal of Physiology, 574*(Pt 3):917.
- Isaacson, S. H., Boroojerdi, B., Walnc, O., McGrawd, M., Kreitzmane, D. L., Klosf, K., . . . D, T. (2019). Effect of using a wearable device on clinical decision-making and motor symptoms in patients with Parkinson's disease starting transdermal rotigotine patch: A pilot study. *Parkinsonism and Related Disorders, 132-137*.
- Ji-Won, K., Joseph, L., Jin-Young, S., Jae-Ho, L., Do-Young, K., Kun-Woo, P., . . . Gwang-Moon, E. (2009). Measurement of Angular Velocity of Forearm Pronation-Supination Movement for the Quantification of the Bradykinesia in Idiopathic Parkinson's Disease Patients. *J. Biomed. Eng. Res., 30*, 142–146.
- Kandori, A., Yokoe, M., Sakoda, S., Abe, K., Miyashita, T., Oe, H., . . . Tsukada, K. (2004). Quantitative magnetic detection of finger movements in patients with Parkinson's disease. *Neuroscience Research, 49*(2), 253-260.
- Liua, W., Linb, X., Chena, X., Wangc, Q., Wangd, X., Yanga, B., . . . Lin, Y. (2023). Vision-based estimation of MDS-UPDRS scores for quantifying Parkinson's disease tremor severity. *Medical Image Analysis, 85*.
- Lua, M., Zhaob, Q., Postonc, K. L., Sullivanb, E. V., Pfefferbaumb, A., Shahide, M., . . . Adelia, E. (2021). Quantifying Parkinson's disease motor severity under uncertainty using MDS-UPDRS videos. *Medical Image Analysis, 73*.
- Marsili, L., Agostino, R., Bologna, M., Belvisi, D., Palma, A., Fabbrini, G., & Berardelli, A. (2014). Bradykinesia of posed smiling and voluntary movement of the lower face in Parkinson's disease. *Parkinsonism & Related Disorders, 20*(4), 370-375.
- NeuroRPM*. (2023). Retrieved from [www.neurorpm.com](http://www.neurorpm.com)

- Oh, E., Seo, J., & Kang, H. (2016). Assessment of Oropharyngeal Dysphagia in Patients With Parkinson Disease: Use of Ultrasonography. *Annals of Rehabilitation Medicine*, 40, 190.
- Postuma, R. B., Gagnon, J. F., Vendette, M., Charland, K., & Montplaisir, J. (2008). Research paper REM sleep behaviour disorder in Parkinson's disease is associated with specific motor features. *J. Neurol. Neurosurg., Psychiatry* 79, 1117–1121.
- (2011). *Recommendation ITU-R BT.601-7*. International Telecommunication Union.
- Robichaud, J. A., Pfann, K. D., Leurgans, S., Vaillancourt, D. E., Comella, C. L., & Corcos, D. M. (2009). Variability of EMG patterns: A potential neurophysiological marker of Parkinson's disease? *Clinical Neurophysiology*, 120(2009), 390–3.
- Salarian, A., Russmann, H., Wider, C., Burkhard, P., Vingerhoets, F., & Aminian, K. (2007). Quantification of Tremor and Bradykinesia in Parkinson's Disease Using a Novel Ambulatory Monitoring System. *IEEE Transactions on Biomedical Engineering*, 54(2), 313-322.
- Sande de Souza, L., Dionísio, V., & Almeida, G. (2011). Multi-joint movements with reversal in Parkinson's disease: Kinematics and electromyography. *Journal of Electromyography and Kinesiology*, 21(2), 376-383.
- Tam, D. (2009). A Theoretical Analysis of Cumulative Sum Slope (CUSUM-Slope) Statistic for Detecting Signal Onset (begin) and Offset (end) Trends from Background Noise Level. *The Open Statistics and Probability Journal*, 1, 43-51.
- Teräväinen, H., & Calne, D. B. (1980). Action tremor in Parkinson's disease. *J. Neurol. Neurosurg. Psychiatry*, 43, 257–263.
- Weichert, F., Bachmann, D., Rudak, B., & Fisseler, D. (2013). Analysis of the Accuracy and Robustness of the Leap Motion Controller. *Sensors*, 13(5), 6380-6393.
- Wichmann, T., & DeLong, M. R. (1996). Functional and pathophysiological models of the basal ganglia. *Current Opinion in Neurobiology*, 6(6), 751-758.

## APPENDICES

### APPENDIX A

#### Source Code of Face Registration Routine

```
void Face::transform(const cv::Mat& m)
{
    cv::warpAffine(image, image, m, image.size());
    for(auto&& p : landmarks)
    {
        cv::Mat v = (cv::Mat_<double>(3, 1) << p.x, p.y, 1);
        cv::Mat r = m * v;
        p.x = r.at<double>(0);
        p.y = r.at<double>(1);
    }
}

void Face::align()
{
    cv::Vec2f center = landmarks[Constants::noseBottom];

#ifdef _FACE_DEBUG
    cv::Line(image, landmarks[Constants::leftInnerEye],
landmarks[Constants::rightInnerEye], cv::Scalar(0, 255, 255), 2);
#endif

    cv::Vec2f innerEyeline = landmarks[Constants::rightInnerEye] -
landmarks[Constants::leftInnerEye];
    innerEyeline = cv::normalize(innerEyeline);

    float d = atan2(innerEyeline[1], innerEyeline[0]) - atan2(0, 1);
    cv::Mat R = cv::getRotationMatrix2D(center, d * 180.0 / M_PI, 1);

    transform(R);
}

void Face::registerTo(const Face& other)
{
    const auto& targetLeft = other.landmarks[Constants::leftInnerEye];
```

```

const auto& targetRight = other.landmarks[Constants::rightInnerEye];

const auto& left = landmarks[Constants::leftInnerEye];
const auto& right = landmarks[Constants::rightInnerEye];

const auto dx = targetLeft - left;
const auto sx = (targetRight.x - targetLeft.x) / (right.x - left.x);

cv::Mat T = (cv::Mat_<double>(2, 3) <<
            1, 0, dx.x,
            0, 1, dx.y);
transform(T);

//cv::Mat S = cv::getRotationMatrix2D(targetLeft, 0, sx);
cv::Mat S = cv::getRotationMatrix2D(targetLeft, 0, 1);
transform(S);

crop(other);
}

void Face::select()
{
    // select upper face
    {
        const auto& leftFace = landmarks[Constants::leftFace];
        const auto& leftOuterEye = landmarks[Constants::leftOuterEye];
        const auto& rightFace = landmarks[Constants::rightFace];
        const auto& rightOuterEye = landmarks[Constants::rightOuterEye];
        const auto eyebrowsRect =
cv::boundingRect(Landmarks(&landmarks[Constants::eyebrowsStart],
&landmarks[Constants::eyebrowsEnd + 1]));

        const auto l = leftFace.x + (leftOuterEye.x - leftFace.x) / 2;
        const auto r = rightFace.x + (rightOuterEye.x - rightFace.x) /
2;

        const auto t = eyebrowsRect.tl().y - exterior.height * 0.0625;
        const auto b = landmarks[Constants::noseMiddle].y;

        const auto center = landmarks[Constants::leftInnerEye] +
(landmarks[Constants::rightInnerEye] - landmarks[Constants::leftInnerEye]) /
2;

        regions.push_back(Region{ cv::Rect(l, t, r - l, b - t) });
        regions.push_back(Region{ cv::Rect(l, t, center.x - l, b - t)
});
        regions.push_back(Region{ cv::Rect(center.x, t, r - center.x, b
- t) });
    }

    // select bottom face
    {
        const auto& noseBottom = landmarks[Constants::noseBottom];
        const auto& leftFace = landmarks[Constants::leftBottomFace];
        const auto& rightFace = landmarks[Constants::rightBottomFace];

```

```

        const auto lipsRect =
cv::boundingRect(Landmarks(&landmarks[Constants::lipsStart],
&landmarks[Constants::lipsEnd + 1]));

        const auto l = leftFace.x + (lipsRect.tl().x - leftFace.x) / 2;
        const auto r = rightFace.x + (lipsRect.br().x - rightFace.x) /
2;

        const auto t = noseBottom.y;
        const auto b = lipsRect.br().y + (lipsRect.tl().y -
noseBottom.y);

        regions.push_back(Region{ cv::Rect(l, t, r - l, b - t) });
        regions.push_back(Region{ cv::Rect(l, t, noseBottom.x - l, b -
t) });
        regions.push_back(Region{ cv::Rect(noseBottom.x, t, r -
noseBottom.x, b - t) });
    }

#ifdef _EQU_HIST
    cv::equalizeHist(image, image);
#endif

    for(auto&& r : regions)
    {
        r.data = image(r.roi);
    }
}

void Face::crop(const Face& other)
{
    regions = other.regions;

#ifdef _EQU_HIST
    cv::equalizeHist(image, image);
#endif

    for(Face::Regions::size_type i = 0; i < regions.size(); ++i)
    {
        auto&& r = regions[i];
        r.data = image(r.roi);

        cv::absdiff(r.data, other.regions[i].data, r.diff);
        r.entropy = entropy(r.diff);
    }
}

bool Face::fit()
{
    typedef std::vector<cv::Rect> Faces;

    for(int t = 0; t < 2; ++t)
    {
        if(t % 2 != 0)
        {
            std::cout << "    Trying with equalizeHist!!!" <<
std::endl;
            equalizeHist(image, image);

```

```

    }

    Faces faces;
    faceCascade().detectMultiScale(image, faces, 1.1, 3, 0,
cv::Size(30, 30));

    std::vector<std::vector<cv::Point2f>> shapes;
    if(facemark().fit(image, faces, shapes))
    {
        int fid = -1;
        for(Faces::size_type i = 0; i < faces.size(); i++)
        {
            exterior = faces[i];
            if(exterior.area() < 6000)
            {
                std::cout << "Too small skipping... " <<
exterior.area() << std::endl;
                continue;
            }

            fid = i;
            break;
        }

        if(fid >= 0)
        {
            landmarks.swap(shapes[fid]);
            return true;
        }
    }

    return false;
}

```

## Source Code of CUSUM function

```
function [ res, range ] = cusum(data, h, k, varargin)
    range = 0;
    options = struct(...
        'up', 1, ...
        'down', 1, ...
        'samples', 30, ...
        'tm', NaN, ...
        'td', NaN, ...
        'after', NaN);

    optionNames = fieldnames(options);

    for pair = reshape(varargin,2,[]) %# pair is
    {propName;propValue}
        inpName = lower(pair{1}); %# make case insensitive

        if any(strcmp(inpName,optionNames))
            %# overwrite options. If you want you can test for the
            right class here
            %# Also, if you find out that there is an option you keep
            getting wrong,
            %# you can use "if
            strcmp(inpName,'problemOption'),testMore,end"-statements
            options.(inpName) = pair{2};
        else
            error('%s is not a recognized parameter name',inpName)
        end
    end

    c = options.samples;
    if isnan(options.tm)
        tmean = mean(data(1:c));
    else
        tmean = options.tm;
    end

    if isnan(options.td)
        tdev = std(data(1:c));
    else
        tdev = options.td;
    end

    h = h * tdev;
    k = k * tdev;
    d_u = (data - tmean) - k;
    d_l = (data - tmean) + k;
    csu = 0;
    cs1 = 0;
    res = -1;
    range = 0;

    for x = c:length(d_u)
```

```

    if(options.up == 1)
        csu = max(0, d_u(x) + csu);
        if res > 0 && csu == 0
            range = x - res;
            break;
        elseif res == -1 && (isnan(options.after) || x >
options.after) && csu > h
            res = x;
        end
    end

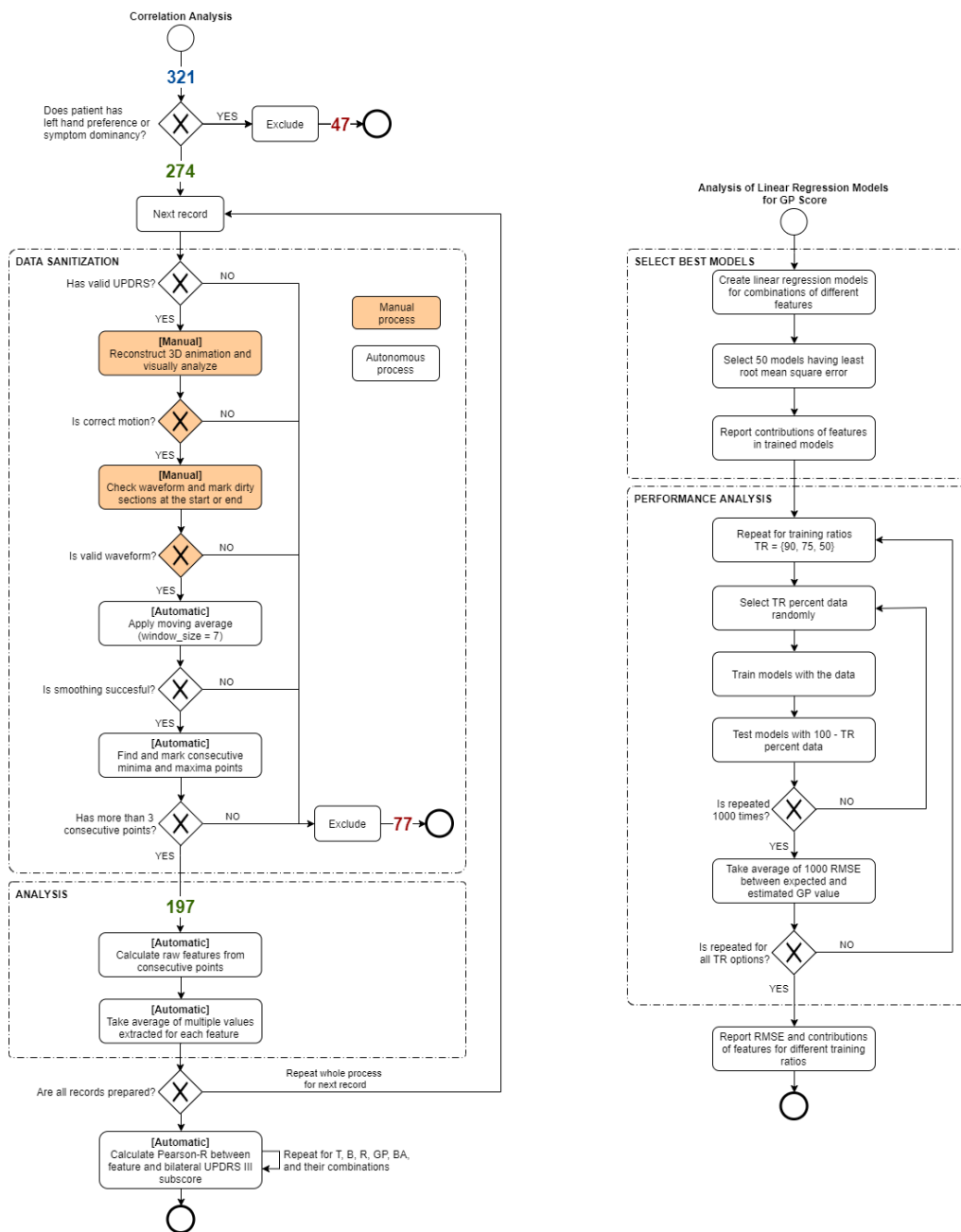
    if(options.down == 1)
        csl = min(0, d_l(x) + csl);
        if res > 0 && csl == 0
            range = x - res;
            break;
        elseif res == -1 && (isnan(options.after) || x >
options.after) && csl < -h
            res = x;
        end
    end

    if range == 0 && res > 0
        range = x - res;
    end
end

```

# APPENDIX B

## Data Sanitization Flow







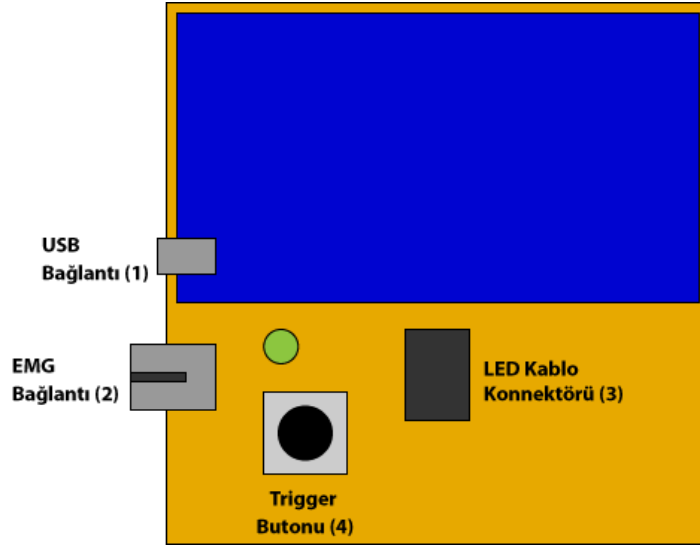


**APPENDIX C**

**Parkinson'da Bradykinesia Deneyi  
Kayıt Protokolü**

**KOÇ ÜNİ. HASTANESİ – ODTÜ  
Temmuz, 2016**

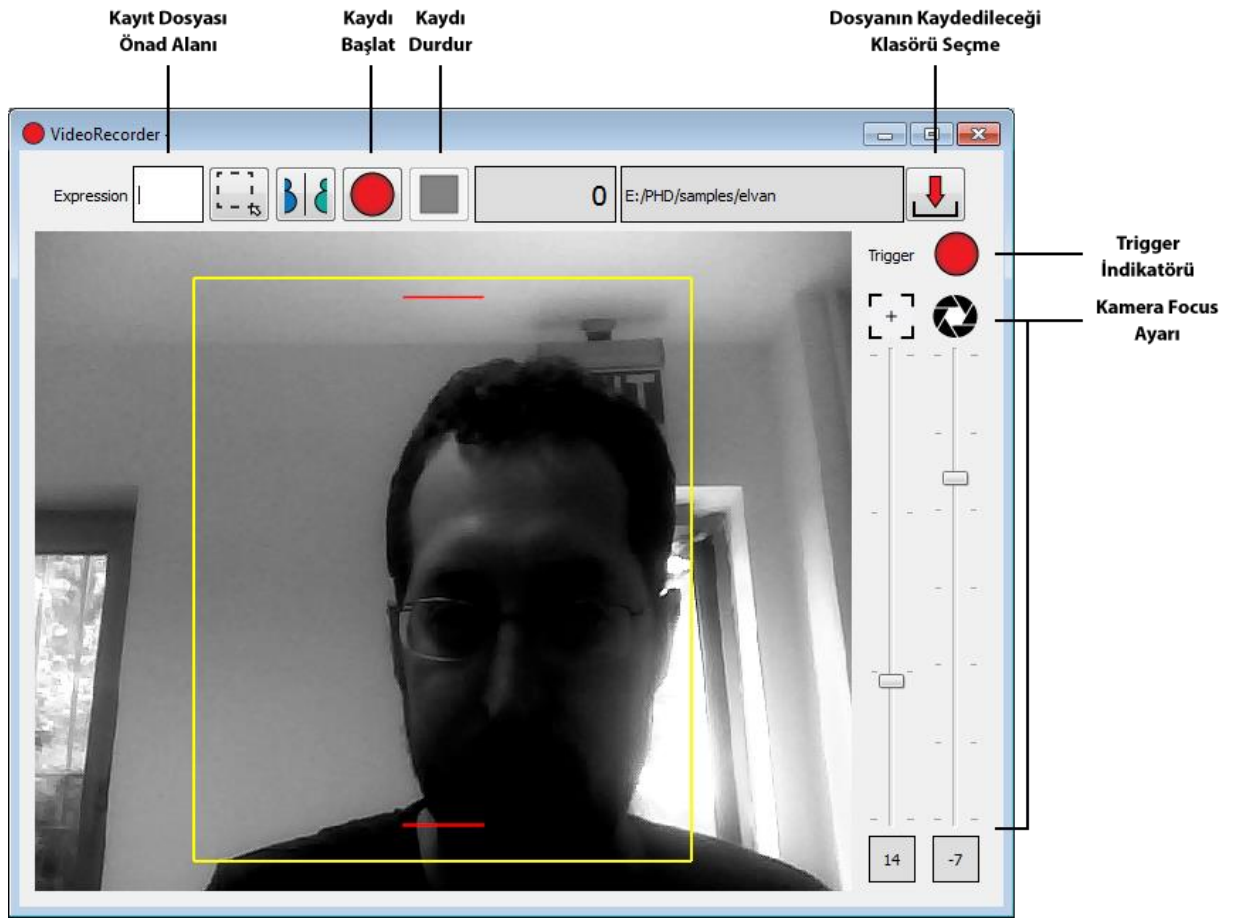
## KURULUM



Şekil 1 - Trigger Kartı Bağlantı Şeması



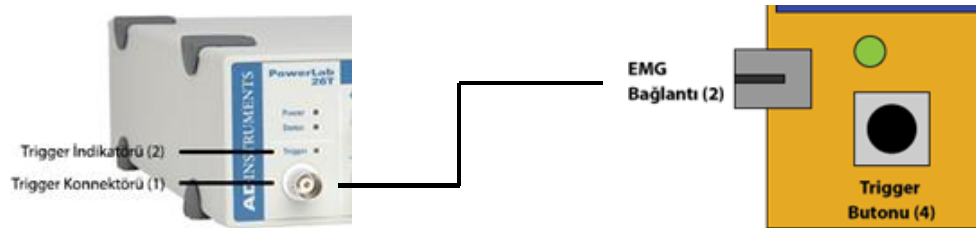
Şekil 2 - EMG Cihazı Bağlantı Şeması



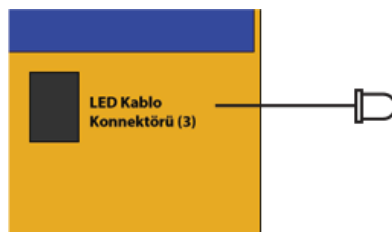
Şekil 3 - VideoRecorder yazılım arayüzü

### Cihazların ve Yazılımın Birbirine Bağlanması

- 1- EMG cihazı *Trigger Konnektörü (1)* ile **Trigger** kartı *EMG Bağlantı (2)*'yi coaxial (anten kablosu ucu gibi olan) kablo ile bağlayınız.



- 2- **Trigger** kartı üzerine **LED kabl**osunu *LED Kablo Konnektörü (3)*'e bağlayınız



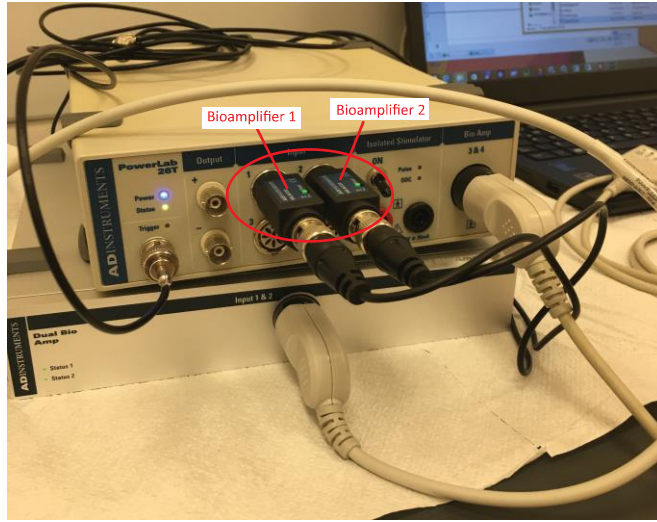
- 3- **Trigger** cihazını *USB bağlantısını (1)* Laptop'un **SOL** tarafındaki USB'ye takıp, bilgisayarın cihazı tanması için bekleyiniz.
- 4- **EMG** cihazını Laptop'ın **SAĞ** tarafındaki USB konnektörlerinden birine bağlayınız.
- 5- **USB kamerayı** da **EMG** ile aynı taraftaki (**SAĞ**) USB girişine takınız.
- 6- Kamerayı aşağıdaki resimdeki gibi **tripoda** tutturunuz.



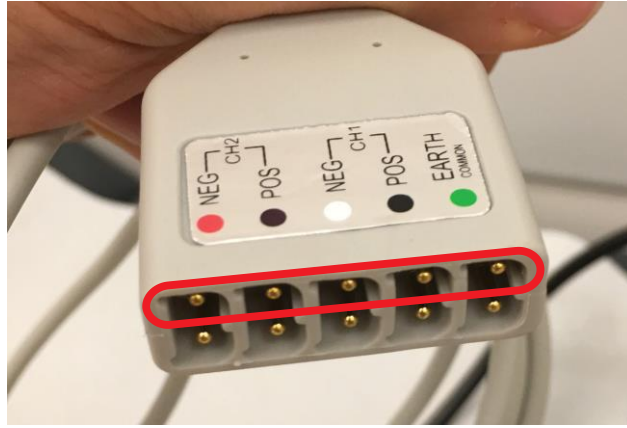
- 7- Ucunda **LED olan kabloyu**, kameranın yanına veya hastanın görebileceği ama kamera da gözükmeyecek bir yere tutturunuz. (bant ile kameranın kenarına bantlanabilir)
- 8- **VideoRecorder** yazılımının bulunduğu klasörde varsa settings veya settings.ini dosyasını siliniz
- 9- Eğer bağlantılar doğru ise **VideoRecorder** uygulaması çalıştırıldığında hata vermeden açılacaktır.
- 10- **VideoRecorder** yazılımında kamera görüntüsünü gördüğünüzden emin olunuz.

### **EMG ve Bioamplifierın Bağlanması**

- 1- **Bioamplifier** modülünden gelen iki kabloyu aşağıdaki resimde görüldüğü gibi **EMG** cihazının **1 ve 2** nolu kanallarına bağlayınız.
- 2- **Bioamplifier**'ın **1 nolu** kanalından gelenin **1, 2 nolu** kanalından gelen kablunun **2'ye** girdiğine emin olun



3- **Probe**'ları her iki sokette **üst sırasına**, aşağıdaki düzene uygun şekilde takınız.

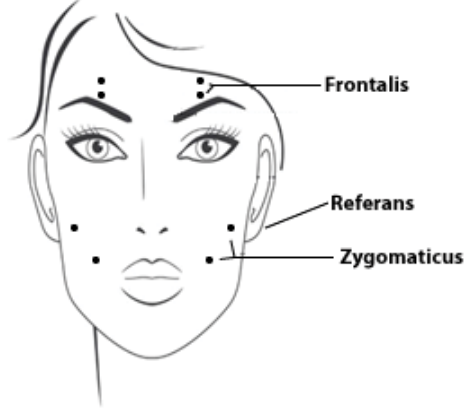


Bioamplifier CH1	Sağ Zygomaticus
Bioamplifier CH2	Sol Zygomaticus
EMG CH1	Sağ Frontalis
EMG CH2	Sol Frontalis

## DENEY

### Deneye Başlama

- 1- Deneğe **Onam Formunu** imzalayıp bir kopyasını saklayınız.
- 2- Eğer denek ilk kez geliyorsa denek için yeni bir **klasör** yaratınız (Örneğin, PD\_Denek1 )
- 3- Deneğin **ilaç durumuna** göre 2. Adımdaki klasör içerisine **ON veya OFF** diye bir klasör daha yaratınız
- 4- Denek bilgi formunu doldurup 2. *adımdaki* klasöre kaydediniz.  
([DenekBilgiFormu.xlsx](#))
- 5- Deneğin **her iki tarafı** için ayrı ayrı **UPDRS III** skorlaması yapıp, UPDRS formunu **ilaç durum** bilgisini not ederek saklayınız.
- 6- **VideoRecorder** da  *Dosyanın Kaydedileceği Klasörü Seçme* butonu 3. *adımdaki* seçiniz.
- 7- *Kamera Focus Ayarını*,  için +12 ve  için -6'ya aralayıp hastanın kamera görüntüsünde net olduğuna emin olunuz.
- 8- **LabChart** yazılımını için 4 kanal için önceden ayarlanmış olan **setup.adicht 3**. *adımdaki* klasöre kopyalayınız.
- 9- **LabChart** yazılımını 7. adımda kopyalanan dosyayı açınız. Bu dosya açılınca trigger ayarı yapılmış ve 4 kanal için kayda hazır bir kayıt ortamı gelmelidir.
- 10- **Trigger** kartı üzerindeki, Trigger butonuna basınca hem **VideoRecorder**  hem de **EMG** cihazı üzerindeki *Trigger İndikatörlerinin* yandığına emin olunuz.
- 11- Eğer **EMG** cihazı üzerinde Trigger ışığı yanmıyorsa, LabChart yazılımda Setup menüsünden *External Trigger*'ı açınız ve *Voltage Level* modunu ve *Channel 1*'i seçiniz ve 6. adımı tekrarlayınız.
- 12- Deneğin yüzünün her iki tarafına EMG probe'larını yerleştiriniz.
  - a. Bir probe çiftini kaşın ortasına dik şekilde frontalis kasına,
  - b. Diğer probe çiftinden bir ucu zygomaticus kasının ortasına diğer ucunu ise kasın başlangıç noktası olan elmacık kemiğinin dış kısmına,
  - c. Referans probe'unu kulak arkasına yerleştiriniz.



### Deneğin Hazırlanması

- 1- Deneç, ilaç ON ve OFF olmak üzere iki oturumda, deneme ve 2 adet gerçek kayıt olmak üzere 3 adımda gerçekleştirilecektir.
- 2- Deneçe “Sizden sırayla **dört** adet yüz mimięi yapmanız istenecek. Komutum ile gözünüzü kapatıp yüzünüzü serbest bırakacaksınız. Bir süre sonra ben size, yapmanızı istediğim mimięi söyleyeğim, örneğın, gülümseme. Bu komuttan sonra gözlerinizi açıp uyarıcı ışığı bekleyeceksiniz. Işığı görür görmez en güçlü şekilde istenen hareketi yapıp bir iki saniye bekledikten sonra, yüzünüzü tekrar serbest bırakıp gözlerinizi kapatacaksınız.

Bu işlemi dört mimik için de tekrarlayacağız.” şeklinde açıklama yapınız.

- 3- Deneğın direktifleri anladığı görmek ve düzeneğın çalıştığına emin olmak için ilk olarak deneme kaydını alınız.

### Deneme Kaydı

- 1- Deneçe, “İlk olarak deneme kaydı alacağız, komutlarımızı takip ediniz” komutunu veriniz
- 2- **LabChart** yazılımından mevcut durumu, *File > Save As...* menüsünden **deneme.adicht** adıyla kaydedin.
- 3- **LabChart** yazılımından kaydı başlatınız.
- 4- **VideoRecorder**'da  Kayıt Dosyası Önad Alanına **deneme\_gul** yazınız. Daha sonraki tekrarlarda yapılacak olan mimięe uygun olarak **deneme\_catma**, **deneme\_kaldirma** ve **deneme\_dudak** yazınız.

- 5- Deneğe, gülümseme mimiğini gösteren kartı gösterip, “Bu gülümseme, komut verdiğimde gözlerinizi açıp uyarı ışığını görür görmez en güçlü şekilde gülümseyiniz. Şimdi gözlerinizi kapatınız ve yüzünüzü serbest bırakınız” komutunu verin.



- 6- **LabChart**'da, *Add Comment* diyip **gulumseme** yazın.
- 7- Deneğe “Gözlerinizi açıp bekleyiniz, ışığı gördüğünüzde hemen en güçlü şekilde **gülümseyip/kaş çatıp/kaş kaldırıp/dudak büküp** ve biraz bekledikten sonra yüzünüzü serbest bırakınız” komutunu verin
- 8- Denek gözünü açtıktan sonra, **VideoRecorder**'da  *Kaydı Başlat* tuşuna basınız
- 9- Ardından kısa bir süre içinde **Trigger** cihazından *Trigger Butonuna* basınız ve Deneğin komutları doğru anlayıp uyguladığından emin olunuz.
- 10- Denek mimiği yapıp yüzünü serbest bıraktığında **VideoRecorder** uygulamasında  *Kaydı Durdur* tuşuna basınız
- 11- Eğer denek uygulamada zorlanırsa veya kayıt cihazlarında/programlarında bir hata olursa bu mimiği bir kez daha tekrarlayınız.
- 12- Bu bölümü 4. adımdan itibaren **kaş çatma, kaş kaldırma** ve **dudak bükme** için tekrarlayınız, her mimik arasında **en az 30 saniye** beklediğinize emin olun
- 13- **LabChart** yazılımından kaydı durdurup kaydediniz.

### Gerçek Kayıt

- 1- Deneğe, “Asıl deney kaydına başlıyoruz, komutlarımı takip ediniz” komutunu veriniz
- 2- **LabChart**'tan Deneğin klasörüne kaydedilmiş olan **setup.adicht** dosyasını açarak sıfır bir kayıt ortamı oluşturun.
- 3- **LabChart** yazılımından mevcut durumu, *File > Save As...* menüsünden **1\_session.adicht** adıyla kaydedin. İkinci seansta **2\_session.adicht** olarak kaydedin.
- 4- **LabChart** yazılımından kaydı başlatınız.
- 5- **VideoRecorder**'da  *Kayıt Dosyası Önad Alanına* **1\_gul** yazınız. Daha sonraki tekrarlar da yapılacak olan mimiğe uygun olarak **1\_catma, 1\_kaldirma** ve **1\_dudak** yazınız. İkinci seansta **2\_gul, 2\_catma, 2\_kaldirma** ve **2\_dudak** şeklinde giriniz.
- 6- **LabChart**'da, *Add Comment* diyip **gulumseme** yazın.

- 7- Deneęe, “Gözlerinizi kapatınız ve yüzünüzü serbest bırakınız” komutunu verin
- 8- Deneęe “Gözlerinizi açıp bekleyiniz, ışığı gördüğünüzde hemen en güçlü şekilde **gülümseyip/kaş çatıp/kaş kaldırıp/dudak büküp** ve biraz bekledikten sonra yüzünüzü serbest bırakınız” komutunu verin
- 9- Denek gözünü açtıktan sonra, **VideoRecorder**'da  *Kaydı Başlat* tuşuna basınız
- 10- Ardından kısa bir süre içinde **Trigger** cihazından *Trigger* Butonuna basınız.
- 11- Denek mimięi yapıp yüzünü serbest bıraktığında **VideoRecorder** uygulamasında  *Kaydı Durdur* tuşuna basınız.
- 12- Bu bölümü *4. adımdan* itibaren **kaş çatma, kaş kaldırma** ve **dudak bükme** için tekrarlayınız, her mimik arasında **en az 30 saniye** beklediğimize emin olun
- 13- LabChart yazılımında kaydı durdurunuz.
- 14- Bütün işlemleri bir kere daha tekrarlayıp ikinci bir kez daha kayıtları alınız



## CURRICULUM VITAE

### Personal Information

---

**Sabri Can Ölçek**

Nationality T.C. / TR e-mail e129272@metu.edu.tr

### Education

---

2010-... Middle East Technical University (METU), Informatics Institute  
**Medical Informatics – PHD**

2006-2010 METU, Institute of Natural and Applied Sciences  
**Computer Engineering – MS**

2002-2006 METU, Faculty of Engineering  
**Electrical and Electronics Engineering – Bs. Major**

2003-2005 METU, Faculty of Arts and Science  
**Department of Physics – Bs. Minor**

2001-2002 METU, School of Foreign Languages  
**Department of Basic English**

1994-2001 Ankara Anadolu High School, German Language Department  
**Mathematics - Science Branch**

### Work Experience

---

Apr, 2021 – ... MeikoSoft, Ankara  
**Founder, Software Architect**

Jul, 2019 – ... Farm-Hand, Edinburgh  
**Consultant, Senior Expert Software Architect**

Oct, 2018 – Jan, 2022 Ekodenge, Ankara  
**Consultant, Product Manager**

Aug, 2017 – Apr, 2020 Zibumi, Ankara  
**Consultant, Technical Lead**

May, 2016 – Aug, 2017 Argedor, Ankara  
**Senior Expert Software Engineer, Technical Lead**

Dec, 2012 – May, 2016 Space and Defence Technologies (SDT), Ankara  
**Senior Expert Software Engineer, Technical Lead**

Jul. 2010 – Dec, 2012 Sobee Studios, Ankara  
**Full-Time Software Engineer, Technical Lead**

Apr., 2007 – Jun., 2010 Siemens Enterprise Communications (*iSEC*), Ankara  
**Full-Time Software Engineer,**

Jul., 2006 – Apr., 2007 Siemens, *Program and System Engineering (PSE)*, Ankara  
**Full-Time Software Engineer,**

Oct., 2004 – Apr., 2007 Siemens, *Program and System Engineering (PSE)*, Ankara  
**Part-Time Software Engineer,**

Agu., 2004 Havelsan, *Avionics Department*, Ankara  
**Summer Practice at Depot Level Maintenance**

## Languages

---

Turkish (**Native**), English (**Fluent**), German (**Intermediate**),  
Japanese (**Intermediate – N3**)

## Certificates

---

- 2009 Microsoft Certified Professional Developer (**MCPD**)
- 2009 Amateur Sailor Certificate (*Amateur Maritime Federation, Turkey*)
- 2009 VHF Radio Operator Certificate (*Amateur Maritime Federation, Turkey*)
- 2007 **ITIL** Foundation Certificate

## Trainings and Events

---

- 2018 BIOSTEC 2018, *Madeira, Portugal*, **Paper Author**
- 2015 I/ITSEC, Modelling and Simulation Conference, *Orlando, USA*, **Participant**
- 2013 I/ITSEC, Modelling and Simulation Conference, *Orlando, USA*, **Participant**
- 2012 IEEE Signal Processing Society Summer School on Game Audio, *Ankara*,  
**Participant**
- 2009 Microsoft 2310C – Developing Web Applications Using Microsoft Visual Studio 2008,  
*InfoPark, Ankara*, **Trainee**
- 2009 Microsoft 2541 – Core Data Access with Microsoft Visual Studio 2005,  
*InfoPark, Ankara*, **Trainee**
- 2009 Microsoft 2124 – Programming with C#, *InfoPark, Ankara*, **Trainee**
- 2009 Creative Thinking and Problem Solving Techniques, *HRM, Ankara*, **Trainee**
- 2008 Conflict Management, *Linkage Turkey, İstanbul*, **Trainee**
- 2007 ITIL Foundation Education, *Infratec, Ankara*, **Trainee**
- 2007 Cost-based Optimization by Jonathan Lewis, *ORACLE University, İstanbul*, **Trainee**
- 2006 stdSEM Engineering Methodologies, *Siemens, Ankara*, **Trainee**
- 2001 AutoCAD 2000 - 3D Course, *TMMOB Society of Civil Engineers, Ankara*, **Trainee**
- 2001 AutoCAD 2000 - 2D Course, *TMMOB Society of Civil Engineers, Ankara*, **Trainee**